Faculty of Engineering and Physical Sciences

School of Engineering

Monitoring macronutrient dynamics in soil and water with droplet microfluidic sensors

by

James Lunn

ORCID: 0000-0003-1961-3336

A thesis for the degree of Doctor of Philosophy

10th October 2025

University of Southampton

Abstract

Faculty of Engineering and Physical Sciences

School of Engineering

Doctor of Philosophy

Monitoring macronutrient dynamics in soil and water with advanced microfluidic sensors

by

James Steven Ralph Lunn

Inorganic nitrogen soil is a key indicator of soil health and its analysis still mainly relies on time and labour-intensive grab sampling; with sample degradation being a major source of error in these studies it is imperative that sensors are developed that can monitor this area; with the advent of different microsampling techniques such as microdialysis and ultrafiltration this is becoming possible.

In this work, a droplet microfluidic analyser using microdialysis and ultrafiltration was developed and field-tested to monitor nitrate in soil. This colorimetric sensor was calibrated using both solutions and spiked soil samples (0.8 to 20 mM NO_3^-) of varying moisture contents (30 to 100% of maximum water holding capacity), showing good linearity across the ranges tested. From this, the sensor was used to detect changes in soil amended with glucose, from which significant nitrate consumption was monitored, showing its potential in recording changing nitrate levels. 4 measurements per day were taken over a period of 12 days with low reagent consumption per measurement (0.198 mL), showing the ability for this sensor to be used in field deployment.

Analysers were then deployed at both Highfield Campus (Southampton, UK) and the Writtle Forest (Essex, UK), with a deployment length of two weeks and a year respectively, using only 96 µL of reagent per measurement whilst producing high quality data through two sampling methods, with small error (2-3% for ultrafiltration, 10% for microdialysis) whilst only requiring monthly maintenance. Further from this, a combined analyser was developed to monitor nitrate, nitrite, and ammonium simultaneously, showing potential to monitor inorganic nitrogen in multiple forms from a single source in-situ. Variations of the analyser were made to either run intermittently or continuously, allowing for many areas of potential deployment ranging from agricultural to bacterial analysis. This analyser was deployed to analyse total inorganic nitrogen in soil (measuring NH_4^+ and NO_3^-) and then in conjunction with a bioreactor (measuring NH_4^+, NO_2^- and NO_3^-), showing changes in inorganic N makeup throughout both deployments.

With further development and technology maturation, this multinutrient analyser can be revolutionary in monitoring inorganic N change forms allowing for the development of automated feedback loops for more efficient growth periods.

Table of Contents

Table of Figures

List of Abbreviations

Abbreviation	Definition
ABTS	2,2′-azino-bis(3- ethylbenzothiazoline-6-sulfonic acid
ADC	Analog to Digital Conversion
ADC_{air}	ADC value given by the sensor when in air
ADC_{Soil}	ADC value given by the sensor when in soil
AOD	Acute Oak Decline
AWG30	American Wire Gauge 30
CAN	Calcium Ammonium Nitrate fertiliser
COD	Chronic Oak Decline
DIC	Dichloroisocyanurate
DGT	Diffusive Gradients in Thin Films
ESI-MS/MS	Electrospray ionisation-tandem mass spectrometry
FDM	Fused Deposition Modeling
HPLC-UV	High Performance Liquid Chromatography coupled to UV-Vis Spectroscopy
HRP	Horseradish Peroxidase
IC	Ion Chromatography
ID	Inner diameter
ISE	Ion-selective Electrode
ISFET	ion-sensitive field-effect transistor

LC-MS	Liquid chromatography mass spectrometry
LED	Light-emitting dIode
LIG	Laser induced graphene
LOD	Limit of Detection
MD	Microdialysis
M_r	Molecular weight
MWCO	Molecular weight cut-off
NEDD	N-(1-Napthyl)ethylenediamine dihydrochloride
NPK	Nitrogen, Phosphorus, and Potassium
NTC	Negative Temperature Coefficient thermistor
OCP	Open Circuit Potential
PCR	Polymerase Chain Reaction
PD	Photodiode
PDMS	Poly(dimethylsiloxane)
PEEK	Polyether ether ketone
PLA	Polylactic acid
PMMA	poly(methylmethacrylate)
PTFE	Polytetrafluoroethylene
PVC	Polyvinyl Chloride
RAS	Return Activated Sludge
RPM	Revolutions per Minute
R_{soil}	Soil moisture dependent recovery

RTIL	Room-Temperature Ionic Liquid
SC-ISE	Solid-contact ion-selective electrode
SOC	Soil Organic Carbon
SERS	Surface-enhanced Raman Spectroscopy/Scattering
SRP	Soluble reactive phosphorus
STW	Sewage Treatment Works
UF	Ultrafiltration
WHC	Water Holding Capacity
W_{soil}	Moisture content of soil
ΣNO_x^-	Combined nitrate and nitrite

Research Thesis: Declaration of Authorship

Print name: James Steven Ralph Lunn

Title of thesis: Monitoring chemical dynamics in soil and water with advanced microfluidic sensors

I declare that this thesis and the work presented in it are my own and has been generated by me as the result of my own original research.

I confirm that:

1. This work was done wholly or mainly while in candidature for a research degree at this University;

2. Where any part of this thesis has previously been submitted for a degree or any other qualification at this University or any other institution, this has been clearly stated;

3. Where I have consulted the published work of others, this is always clearly attributed;

4. Where I have quoted from the work of others, the source is always given. With the exception of such quotations, this thesis is entirely my own work;

5. I have acknowledged all main sources of help;

6. Where the thesis is based on work done by myself jointly with others, I have made clear exactly what was done by others and what I have contributed myself;

7. Parts of this work have been published as:-

Lu, B.; Lunn, J.; Yeung, K.; Dhandapani, S.; Carter, L.; Roose, T.; Shaw, L.; Nightingale, A.; Niu, X., Droplet Microfluidic-Based *In Situ* Analyzer for Monitoring Free Nitrate in Soil. *Environmental Science & Technology* **2024,** *58* (6), 2956-2965.

Contributions: *Experimental planning and preparation, including preparing reagents, soil samples for analysis and calibration of the analyser. Also with the maintenance of the sensor in the Writtle forest deployment, as well as with data analysis for soil WHC calibrations, the Glucose addition test and the Writtle deployment.*

Lu, B.; Lunn, J.; Nightingale, A. M.; Niu, X., Highly sensitive absorbance measurement using droplet microfluidics integrated with an oil extraction and long pathlength detection flow cell. Frontiers in Chemistry **2024**, 12.

Contributions: *Fabrication of the paired oil extraction and flow cell units, preparation of reagents and experimental running for calibration for the flow cell units of different path lengths and helping with data analysis of these calibrations.*

Signature: ..... Date: ……

Acknowledgments

We thank the UK's Natural Environment Research Council for funding (NE/R013578/1, NE/S013458/1, NE/T010584/1).

First, I thank Xize Niu and Adrian Nightingale for giving me the opportunity to join the Mechatronics group, for supervising me during the production of this thesis, and for their sage advice throughout.

Thanks to Bingyuan Lu, Liam Carter, Ken Yeung, Jose Morales, Gregory Slavik, Sherif Attia, Pinar Ayas and Jelena Milinovic for their help in both developing and troubleshooting the analysers. It was a team effort and I am grateful for each of your valuable inputs.

Thanks to Molly Philips and Jayshree Bunge for their support during my PhD, providing much-needed morale boosts and advice throughout.

I thank Yongqiang Liu for providing advice on fabricating and running the bioreactor system.

From the University of Reading, I thank Selva Dandaphani and Liz Shaw for help during the Writtle Forest deployment, giving key insights into soil dynamics, and Ellie Barbrook for providing the organic amendment experiment to which I could join.

Thanks to my family and friends for their wonderful support over the years. I am forever grateful for the encouragement you've provided.

Chapter 1 Introduction

Soil impacts us through most areas of life. The science of agriculture has allowed for humans to flourish, and in doing so we must take care of the science of agriculture. With the growing worldwide population, land dedicated to crops now accounts for around 10% of all landmass[1]. Average soil macronutrient (Nitrogen, Phosphorus and Potassium (NPK)) concentration has depleted in lower-income countries[2], leading to lower crop output, whilst over-addition of nutrients has led to an oversupply in higher-income countries. The oversupply has been linked to contributing to the pollution of waterways through leaching and to global warming through the off-gassing of compounds such as N_2O[3].

To keep up with agricultural demand, more efficient farming techniques must be used. Incorporating macronutrient sensors into crop systems would allow farmers to monitor how much of a nutrient gets taken up by the crop and make informed decisions of how/what type of fertiliser to add, either increasing yield or reducing greenhouse gas emissions. This would contribute to a much more sustainable fertilisation strategy, which will be essential for our growing population.

These macronutrients are often analysed using lab-based techniques, requiring periodical destruction of soil to obtain slurries, which can then be filtered and analysed. In-situ techniques have been developed to measure soil macronutrient levels, such as microdialysis, which have allowed for less invasive sample collection, yet these methods have not yet been coupled to sensing systems for use in soil. Through development of an in-situ analyser in soil, we will be able to avoid sample degradation that has been common in soil analysis, providing a minimally invasive method of analysing soil macronutrient levels.

1.1 Methodology

In this thesis, droplet microfluidic systems for macronutrient analysis will be developed for use in both soil and water systems. This will first be through the development of a nitrate analyser for soil environments using microdialysis, then development of a system to increase sensitivity of phosphate analysis for droplet microfluidic systems, followed by the development of a multinutrient analyser for

simultaneous analysis of NH_4^+, NO_3^- and NO_2^-, allowing for the analysis of inorganic N in different states, common in wastewater treatment.

Droplet microfluidics allow for microliter samples to be taken and analysed in a much more efficient manner than regular microfluidics, requiring much less bespoke architecture allowing for more robust systems that require less power to run.

For the nitrate analyser in soil, microdialysis was used to take advantage of its passive sampling nature, providing a nutrient extraction method that would not deplete the moisture content of the surrounding soil. This method was compared to an ultrafiltration probe to analyse the microdialysis probe's recovery in soil under the different sampling techniques. It has been shown in my group's previous work on biomarker assays that microdialysis pairs well with droplet microfluidic architecture and as some soil studies currently use microdialysis for soil sampling these two methods should combine well for soil analysis, preventing sample degradation whilst still giving continuous data. This will allow for deeper insights into rhizosphere nitrogen dynamics, allowing for fertilisation methods to be more deeply studied in their effect on these dynamics, potentially allowing for more efficient fertilisation strategies to be developed.

After developing the analyser, solution-based nitrate calibrations will be performed using both microdialysis and ultrafiltration, with the ultrafiltration method giving a baseline to calculate the recovery of the microdialysis method in solution. This will then allow for soil-based calibrations, analysing how the concentration of nitrate in the microdialysis probe changes with the water content of the soil. From this, a correction factor can be used to calculate the amount of nitrate per gram of soil independent of the moisture content of the soil as long as the moisture content is monitored, allowing the results to be compared to other soil studies in the field which commonly use g NO_3^--N per g dried soil. This analyser will then be deployed in two locations; one preliminary study to make sure of the robustness of the analyser in a campus garden and a second, longer study in the Writtle forest, in which the analyser response will be compared to soil grab samples.

One drawback of droplet microfluidic colorimetric devices is the confinement of the path length to the size of tubing used, creating issues in analysing low concentration substances or those with a small extinction coefficient. In the second part of this thesis, an oil extraction method will be paired to a droplet microfluidic pumping system to benefit from the inherent increase of mixing droplet microfluidics provides whilst also allowing for the long pathlengths that continuous microfluidics can benefit from.

For the oil extraction and extended path length sections, we will first monitor the robustness of the oil extraction system through testing the extraction efficiency at a higher flow rate than we are planning to run the system at for an extended period of time. After this, the extended path length flow cells will be validated through a comparison in absorbance of these flow cells of different lengths to that of a UV-Vis spectrophotometer first using a dye, then using the molybdate blue assay for phosphate. After the calibration of these flow cells, the system will be tested using real samples to compare the oil extraction and flow cell's results to a typical droplet microfluidic system and a UV-Vis spectrophotometer.

Through development of a multinutrient analyser for inorganic N, fluxes from one form of N to another can be studied. In riverine systems and wastewater treatment, this will allow for a greater insight into nutrient dynamics, which are currently analysed mainly using grab samples which can change in composition with time before analysis. By analysing multiple analytes immediately, less information is lost. Using this analyser in a bioreactor environment could allow for control systems can be implemented to allow for more efficient bacterial growth cycles.

In the development of this multinutrient analyser, a combined heater and flow cell system will be developed to monitor three droplet microfluidic lines simultaneously, in which three LED-flow cells will be attached to a heater capable of heating multiple lines of tubing simultaneously. This system will allow for the separate nutrients to be monitored simultaneously from a single source, giving greater insight into inter-nutrient dynamics. This device will first be developed for the monitoring of the effect of different types of organic amendment in the nutrient profile in soil during baby spinach cultivation. For this, the device will be calibrated using nitrate and ammonium samples in solution as an ultrafiltration probe will be used for sample collection. After calibration, this analyser will be connected to a plant pot of a type of amendment added (either glycerol, straw or a control), with 3 total analysers being deployed for this study. The analysers will collect one sample per day, giving a concentration of nitrate and ammonium, which will then be converted from mM to g N per g dry soil (with the soil having a consistent moisture content of 85% throughout the experiment) and the results from the analysers will be compared to grab samples collected in similar pots throughout the deployment.

The device will then will be calibrated for measuring nitrate, nitrite and ammonium in a bioreactor scenario, observing the process of denitrifying bacteria converting ammonium into nitrite and then nitrate. These two scenarios require different monitoring rates, with the soil experiment being

measured once a day through intermittent running and the bioreactor experiment being measured continuously (one sample per minute), so the system will be modified to run at a much slower rate continuously. Calibrations of a wider range will be performed reflecting the higher nutrient concentration present in bioreactor environments than in soil. In the bioreactor, a feedstock of ammonium chloride will be made, which will be added to a small volume of denitrifying sludge. The multinutrient analyser will be connected through the side of the bioreactor, monitoring the nutrient concentrations present in the solution. After a 12-hour cycle, half of the bioreactor solution will be removed (excluding sludge) and fresh ammonium feedstock will be added to allow for the monitoring of several cycles. Grab samples will be taken during specific cycles for comparison with the analyser.

1.2 Aims

The aims of this thesis are:

- Develop a droplet microfluidic analyser using microdialysis to analyse nitrate in soil, allowing for long-term in-situ analysis, which will allow for better agricultural fertilisation schemes
- Improve the state of microfluidic phosphate analysis through incorporating droplet microfluidics, reducing system complexity by avoiding washing stages
- Develop a multinutrient analysis platform, capable of tracking multiple droplet microfluidic colorimetric systems simultaneously sampling from a single source, allowing for the analysis of multiple forms of N simultaneously, with the potential to develop control systems for aquaponic and wastewater environments.

The work will be divided into 7 chapters:

Chapter 1: An overview of the aims of the thesis.

Chapter 2: A review of the literature, discussing N and P dynamics in water and soil systems, soil sampling and analysis methods, microsample analysis and multinutrient analysis

Chapter 3: Development of an analyser for nitrate in soil using microdialysis and ultrafiltration coupled with a droplet microfluidic wet chemistry analyser, using the Griess+ colorimetric assay, with in-lab tests followed by deployments.

Chapter 4: Development of an oil extraction system for droplet microfluidics paired with a long path length flow cell for the analysis of Phosphate in riverine systems

Chapter 5: Development of multinutrient analysers for intermittent and continuous analysis of inorganic N species (NO_3^-, NO_2^- and NH_4^+) for use in water and soil environments.

Chapter 6: Deployment of these multinutrient analysers with a soil experiment (Measuring NO_3^- and NH_4^+ intermittently) and a bioreactor experiment (Measuring NO_3^-, NO_2^- and NH_4^+ continuously)

Chapter 7: Summary of the work in the thesis and outlines future developments and applications

Chapter 2 Literature Review

In this literature review, the critical roles of nitrogen (N) and phosphorus (P) in soil and water systems will first be discussed. This will be followed by an overview of current soil-water sampling methods, including both laboratory-based and in-situ approaches, with a particular focus on microdialysis as a promising technique. Potential analytical methods that can be coupled with microdialysis will then be explored. Subsequently, other methods of nutrient analysis will be reviewed, with attention given to the detection of key macronutrients- nitrate/nitrite, ammonium and Phosphate, in both soil and water. Finally, the review will examine the current state of multinutrient analysers, their implementation across different sectors, and the areas where further development is needed..

2.1 Macronutrients in Water and Soil

Firstly, we need to consider the nutrients commonly used to monitor soil and aquatic health. Monitoring of N and P in soil is of vital importance to our agricultural system, with fluctuations in these levels leading to drastic effects from limitations of growth to crop failure, whilst measurements of riverine N and P allow us to understand key health outcomes for river habitats, which can be impacted by anthropogenic sources such as fertiliser or sewage systems.

Macronutrients are the building blocks for the marine food web, enabling growth for phytoplankton in both freshwater and seawater[4] environments, which in turn provide food for zooplankton and other aquatic organisms. However, through anthropogenic sources such as fertilisers, nutrient availability in freshwater ecosystems has significantly increased, which then flow into coastal waters. This heightened availability has led to environmental problems, such as algal blooms and loss of habitats, leading to drastic changes in fish populations through fish kills[5, 6].

One common indicator of soil health is through monitoring levels of nitrogen (N) in the soil. Being one of the fundamental building blocks for proteins, low nitrogen could lead to low growth rates both in microbes[7] and in plants[8]. In soil, N is normally found in the form of inorganic N such as Nitrate (NO_3^-) and Ammonium (NH_4^+), both from natural sources in the soil, such as animal and plant residue, and from anthropogenic sources such as fertiliser.

2.1.1 Soil N Cycle and Nitrogen Transformations

2.1.1.1 Introduction to Soil Nitrogen

Nitrogen is a primary nutrient on which all living organisms depend on. It is present in our DNA, the chlorophyll in plants and all proteins. Figure 1 shows a typical overview of the natural nitrogen cycle, excluding anthropogenic sources into the soil, outlining the typical pools of N and their sources and sinks.

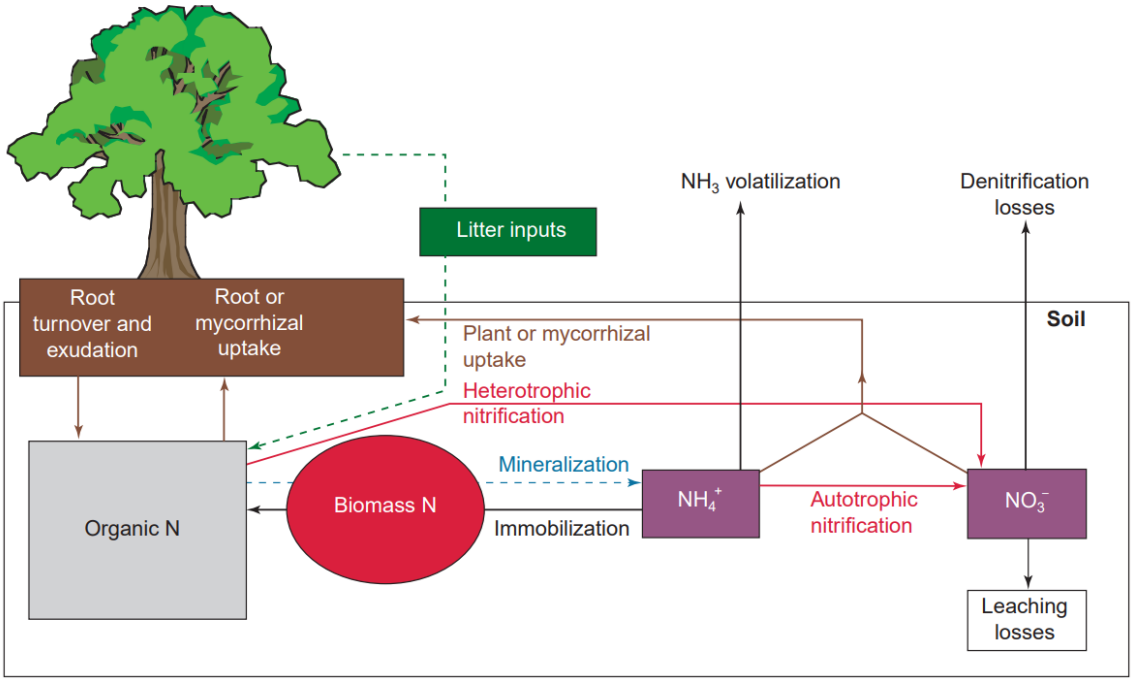

Figure 1 Diagram of the Nitrogen cycle in soil. Pools of N are represented by boxes and arrows represent the flux between pools, excluding animal inputs and N fixation. This figure was adapted from ref. [9] with permission from Elsevier, copyright July 2000

Nitrate (NO_3^-) is a key nitrogen source for plants, needed for essential processes such as photosynthesis and carbon fixation. The major anthropogenic input of nitrate into soil ecosystems is through the use of nitrate-based fertilisers[10] such as Ammonium Nitrate. The use of N-based fertilisers contributed heavily to a doubling of N loads since the start of the 20th century[11]. In high levels, the soluble nature of NO_3^- allows it to leach out of soil with precipitation and collect into waterways, leading to eutrophication which leads to the destruction of natural riverine habitats. Nitrite (NO_2^-) in

drinking water has also been linked to methemoglobinemia in infants, in which haemoglobin is converted into methemoglobin, leading to low oxygen flow into cells[12]. The increased input of N into soils has also increased the emission of NO_x from the soil surface, contributing to the greenhouse effect[13].

Ammonium (NH_4^+) also plays a significant part in N uptake[14] in plants, with excess ammonium being toxic. Its analysis is often carried out alongside nitrate, using both forms of N to give an estimation of total inorganic Nitrogen in soil.

Natural sources of N into the soil include N fixation, decomposition of animal matter and litter inputs from plants and microbial decomposition.

2.1.1.2 Nitrogen Fixation

Nitrogen in its most abundant form, N_2, has too stable a bond to be used directly by plants, so it first needs to be processed into forms of N that are more biologically available. N fixation is a process in which N_2 is converted to NH_3 mainly through nitrogen-fixing bacteria[15], a diverse range of bacteria including both aerobic[16] and anaerobic[17, 18] species, all containing the nitrogenase enzyme complex.. A small amount of N is fixed in abiotic processes through lightning[19], converting N_2 into NO_x species, which can then be dissolved and converted into nitrates in rainwater and can be transported into the soil. Anthropogenic N fixation takes place through the combustion of fossil fuels, through the generation of NO_x.

2.1.1.3 Litter Input

Plant litter provides N to soil through several steps, first through leaching soluble material, then through microbial decomposition of components, mainly proteins[20], to amino acids. Root systems also return N to the soils through turnover, in which old root systems decompose into organic N whilst newer root systems take their place, and through root exudation, in which organic N is directly released into the soil from the roots to stimulate root growth, microbial activity and to respond to external stimuli such as drought[21]. The contribution of root turnover to overall biomass litter varies wildly from species to species of plant[22]. The decomposition of microbial matter also accounts for a significant portion of N in soils, with microbial necromass accounting for >60% of soil organic nitrogen[23], mainly in the form of poly-amino compounds such as proteins yet also as amino sugar polymers, which are released from the decomposition of bacterial and archaeal cell walls.

2.1.1.4 Mineralisation and Immobilisation

Organic N is converted to inorganic N through mineralisation, in which soil microbes break down organic N into amino acids and then NH_4^+, which then converts to into NO_3^- via NO_2^- by nitrification. These transformations are in equilibrium in the soil with immobilisation processes, through which inorganic N is taken up by both microorganisms and roots. These processes have a mutualistic relationship, in which excess inorganic N from the plant can be exuded and taken up by microorganisms in soil, preventing labile forms such as NO_3^- from leaching[24].

Inorganic forms of N were traditionally thought of as the main source of N nutrition for plants and microbes, yet more recent studies have shown that organic N, especially short chain amino acids, also plays a large role.

The DNRA (dissimilatory nitrate reduction to ammonium) pathway[25] helps to prevent nitrate loss through leaching by converting it to ammonium; this pathway uses anaerobic microbial processes, occurring more in marine environments and waterlogged soil, to convert NO_3^- to NO_2^- to NH_4^+, which is much less mobile in soil. The existence of this pathway in anaerobic conditions is essential in the soil environment, acting as a major sink of NO_3^- and preventing significant amounts of N from entering waterways, as well as reducing N_2O emissions and allowing nutrition to be provided to heterotrophic microorganisms.

With the increase of N found to be leaching from soil into rivers, a major shift in agricultural fertilisation strategy is needed. Through monitoring the level of N in soil, improved fertilisation schemes can be developed, both increasing efficiency and reducing the contribution of agriculture to pollution and climate change.

2.1.2 The N Cycle in Riverine Systems

An overview of N processes in riverine systems is given in (Xia et al, 2018)[26], outlining natural transformations and anthropogenic sources. Figure 2 gives an overview of the N transformations in riverine systems. This cycle highlights the difference in nitrogen processes between the water and the sediment underneath, with both parts mainly being governed through microorganisms.

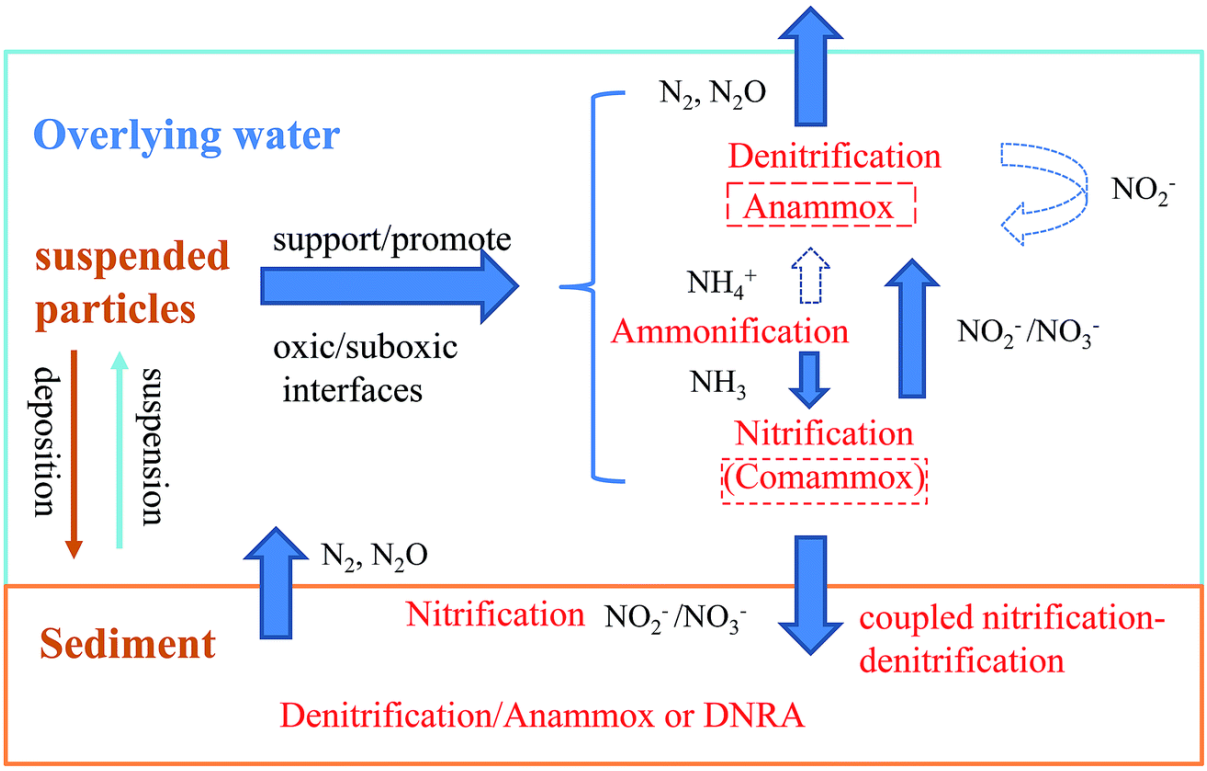

Figure 2 Schematic showing nitrogen transformation In river systems. Dashed boxes and arrows indicate potential pathways and coupling metabolism, respectively, which have not been determined so far. This figure was adapted from ref. [26] with permission from The Royal Society of Chemistry, copyright June 2018.

Denitrification processes (a group of processes which reduce $NO_3^- \rightarrow NO_2^- \rightarrow NO \rightarrow N_2O \rightarrow N_2$) tend to prefer anoxic conditions, with organic matter and nitrate present[27]. These conditions are best found in riparian environments and wetlands, and these areas have a significant impact in the removal of anthropogenic N. It has been estimated that approximately 30% to 70% of N that enters rivers/streams is converted to N_2 during its course to coastal water[28], yet there is a need for studies into the role of wetlands in denitrification.

2.1.2.1 Anammox

The anammox process, in which NH_4^+ is anaerobically oxidised (typically by NO_2^- or NO_3^-) to form N_2 and water, is a process that was only discovered in the early 1995 in a wastewater treatment plant[29]. However, this process has been found in several natural environments, such as riparian and marine sediment, in places where oxic and anoxic environments interface. Up to 50% of fixed nitrogen removal in the ocean has been attributed to anammox processes[30], yet In streams and rivers, its

contribution in removing N has ranged from 7%[31] to 86%. With further study into this area we will better realise its contribution to the nitrogen cycle.

DNRA, anammox and denitrification processes all play roles in the riverine ecosystem as ways of processing NO_3^- which enters waterways, allowing for the conversion of NO_3^- to either N_2 (anammox and denitrification) or NH_4^+ (DNRA). Through the use of in-situ analysers, the rate of removal under different conditions of NO_3^- can be monitored, allowing for a greater insight into N processing in rivers and the influence of anthropogenic sources can be tracked through the placement of sensors adjacent to known point sources such as wastewater treatment plant outlets or downstream from more diffuse sources, such as agricultural sites.

2.1.3 Phosphorus Species and the Phosphorus Cycle

Another key nutrient in soil is Phosphorus (P). P is an essential macronutrient for growth in both plant and animals, which is usually provided through decomposing matter, such as algae for water and plants for soil. These often come in the form of orthophosphate (PO_4^{3-}), as well as mono and dihydrogen phosphates (HPO_4^{2-} and $H_2PO_4^-$). However, there are common anthropogenic sources of phosphates that contribute heavily to the overall phosphate levels in both soil and water systems, such as phosphate-rich fertilisers, the effluent from wastewater treatment plants, and runoff from road surfaces. In these habitats the natural phosphorus cycle can stabilise itself through plants taking up phosphorus yet in rivers excessive levels of phosphate can lead to eutrophication, due to the rapid levels of phytoplankton growth, leading to the destruction of these ecosystems. In England, the leading cause of water bodies not achieving good ecological status was due to an exceedance of standards for Phosphorus[32].Unlike N, the phosphorus "cycle" is sedimentary[33], with most phosphorus originally occurring in most rocks as fluorapatite, which is slowly released during weathering as phosphate[34], which can then be taken up by plants, with it slowly transferring to waterways and then into oceans before settling in sediment, which then accumulates as mineral deposits, with this cycle taking thousands to millions of years. Small amounts of phosphorus deposited by riparian vegetation, migratory fish returning to spawning grounds[35] and animal waste contribute to natural riverine P, yet it has been estimated that anthropogenic sources of P has increased the worldwide freshwater level of P by 75% from preindustrial levels. The accumulation of P in upland soils through fertiliser use is providing a slow input into freshwater systems that is exacerbated by exceptional rainfall/erosion events through P entering rivers in soil particulates, with legacy sources of soil P creating knock-on effects that could devastate these riverine habitats decades after the addition of P to soil[36, 37].

In order to prevent P from devastating riverine habitats further, identification and management of point sources is required in our waterways. Modeling techniques alongside monitoring P using in-situ sensors at suspected point sources will allow us to identify and rectify anthropogenic pollution in waterways.

2.2 Overview of Soil Analysis Methods

2.2.1 Destructive Techniques

Many of the "gold standard" soil sampling techniques require the disturbance or destruction of soil, such as dissolution and filtering of the soil into a soil solution using KCl. This can then be analysed through many lab-based techniques, yet its destructive nature means that the soil is disturbed significantly, affecting the physical and chemical composition of the soil[38]. Off-line analysis a day after collection has found to have a profound external effect on nitrate, even if the sample has been refrigerated[38]. information concerning heterogeneity and availability of nutrients to the plant is lost. Important nutrients such as amino acids have a limited half-life in soil[39], meaning these destructive processes may also lead to further misinterpretation of soil conditions. However, the macronutrient content of soils is still determined using these techniques as the gold standard and shall be listed here.

2.2.1.1 Kjeldahl Digestion

The Kjeldahl method has successfully been used to measure N levels in organic substances since its inception in 1883[40] and is considered the reference method of total N determination. This method breaks down organic N, present in amino acids, proteins and amino sugars, using sulfuric acid at high temperature (370 °C) to convert the N in these substances to ammonium sulfate which, traditionally, was then quantified using titration by raising the pH with addition of a base (e.g. NaOH) or analysed via steam distillation. Newer methods of quantification using the Kjeldahl method directly measure the ammonium formed using ammonium ISEs[41] or spectrophotometric techniques, with Saez-Plaza et al (2013)[42] giving a comprehensive list of spectrophotometric techniques that have been paired with the Kjeldahl technique.

Whilst the Kjeldahl procedure is a reference standard for the determination of nitrogen in many different types of samples, the process has been found to omit certain forms of N. Nitrate and nitrite are typically not included in Kjeldahl-N, of which nitrate is present to a significant degree in soil systems. Also, the estimation of total N gives little information about the types of N available in the

soil; given how organic and inorganic forms supply N in different ways to plants, this method does not necessarily give reliable information on N pools in soil, especially with how much of other forms of N change into nitrate after taking a sample.

2.2.1.2 Dumas Combustion

An alternative to the Kjeldahl digestion method is the less commonly used Dumas combustion. In this method, soil is pretreated by heating a small sample to 800 – 1000 °C in the presence of pure oxygen, causing CO_2, H_2O, N_2 and NO_x gases to be liberated. These gases are then passed through a water removal method (such as perchlorate traps or thermoelectric coolers) and a reduction method, converting the NO_x to N_2. This method produces much less waste materials than the Kjeldahl method and allows for much faster sample throughput, yet the Kjeldahl method is able to be much more adaptable in the mass amount of the sample used and can be carried out using typical laboratory glassware instead of specialist equipment, hence why the Kjeldahl method is used more as a reference method.

2.2.1.3 KCl Extraction

For soil, the KCl extraction technique is commonly used for the analysis of available inorganic N, through extracting NO_3^-, NH_4^+ and NO_2^-. Whilst nitrate can be extracted from soil using water, ammonium binds to the soil surface. By adding KCl solution with a high enough concentration (typically 2 M is used) to a soil sample, the K^+ ions replace the NH_4^+ ions due to their similar ionic radii, liberating the NH_4^+ ions and allowing them to collect in solution. The soil slurry is shaken for 1 hour before being filtered and either analysed immediately or frozen for future analysis. Some ammonium will still be bound to the soil matrix, referred to as "fixed NH_4^+", which is typically included in the Dumas and Kjeldahl methods, yet its exclusion in soil analysis through this method gives us a clearer idea of soil nutrition pools.

2.2.1.4 Mehlich 3

The Mehlich 3 assay was developed as a generic extractant for a wide range of soils and has been used for recovering both macronutrients (including P, K, Ca, Mg) and micronutrients (Cu, Zn, Mn)[43] simultaneously, to allow for analysis via methods such as LC-MS, which can then measure all of these nutrients simultaneously, increasing uniformity in . The extracting solution is composed of glacial acetic acid (0.2 M), ammonium nitrate (0.25 M), ammonium fluoride (0.015 M), nitric acid (0.013 M), and EDTA (0.001 M). This extraction method has been well documented as a method for analysing

soil P, showing good correlation with crop response to fertiliser P in acidic soils. This method is unsuitable for inorganic N due to its composition, containing both NO_3^- and NH_4^+, but has good scope for complementing KCl extractions to give a full macronutrient profile; retrieving information about both K and NH_4^+ at the same time is close to unfeasible due to their similar ionic radii.

2.2.2 Non-Destructive Techniques

More recent techniques that have come to the forefront manage to sample non-destructively, allowing for the same area to be investigated at different time points. To achieve this a probe is placed in the soil from which samples can be taken, which are then typically frozen and stored for later analysis. Microdialysis probes, suction cup samplers and diffusive gradients in thin films are the most common of these, and their sampling methods shall be explained here.

2.2.2.1 Microdialysis

2.2.2.1.1 Principles of Microdialysis

Microdialysis uses diffusion gradients to extract nutrients from the soil by passing a fluid, known as a perfusate, through a section of tubing with a semi-permeable filter, allowing perfusate to diffuse out of the tubing and into the soil (Figure 3). The difference in concentration of nutrients inside and outside the filter creates a concentration gradient, causing nutrients of interest to diffuse through the filter. This fluid (now termed dialysate) then continues to pass through the tubing and can then

be processed. By continuously flowing perfusate through the concentration gradient is maintained, allowing for continuous sampling.

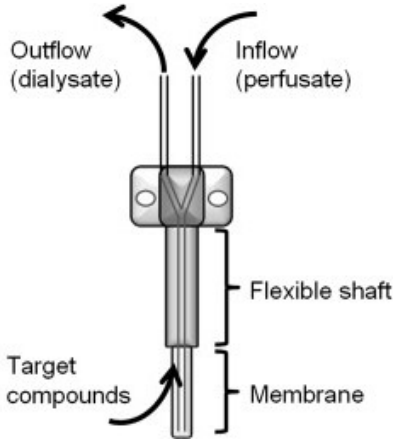

Figure 3 Typical layout of a concentric dialysis probe, based on the CMA 20 probe (CMA Microdialysis AB, Kista,Sweden). This figure was adapted from ref. [39] with permission from Elsevier, copyright June 2011.

In an ideal solution, diffusion can be described by Fick's First Law:

$$J_{Ax} = -D_A\left(\frac{\delta C_A}{\delta x}\right) \quad (1)$$

Where J_{Ax} is the molar flux of species A in the *x*-direction (mol m^{-2} s^{-1}), D_A is the diffusion coefficient (m^2 s^{-1}) and C_A is the concentration of A (mol m^{-3}). The assumptions made by an ideal solution are that the solution is homogeneous and that the concentration gradient is at a steady state. While this may be mostly true for water, this is certainly not the case for soil, a heterogeneous solution containing charged particles and varying saturation levels. This has led to equations modelling the complex interactions in soil to be developed, considering these inhibitors [44].

When considering microdialysis, the calculations for flux must take into account the three different regions diffusion takes place across: the external media (ext), the membrane (m) and the perfusate (d). Each of these regions can be said to have different "resistances" to diffusion (R_{ext}, R_m, R_d), which have the general form:

$$R = \frac{\Delta r}{D_{eff} S \varphi} \quad (2)$$

Where Δr is the length of the region, D_{eff} is the effective diffusion coefficient, S is the surface area of the probe and ϕ is the volume fraction of the region. By using these resistances, they can be summed together allowing for further resistances to be added easily, resulting in the following equation:

$$J = \frac{dC_{1-3}}{R_{ext} + R_m + R_d} \tag{3}$$

This was then further developed[45] to provide a measure of probe efficiency through relative recovery (E_d) by:

$$E_d = \frac{C_{out} - C_{in}}{C_{ext} - C_{in}} = 1 - \exp\left(-\frac{1}{Q_d(R_{ext} + R_m + R_d)}\right) \tag{4}$$

Where C_{out} is the concentration of nutrient in the dialysate, C_{in} is the perfusate concentration (typically 0), C_{ext} is the unperturbed soil concentration (Measured externally) and Q_d is the flow rate of the dialysate. The relative recovery can be a useful method of finding the concentration of a species in a sample, or to compare whether certain parameters influence solute recovery. Relative recovery is a key measure in biomedical studies using microdialysis due to the importance of concentration of a solute in a body, yet in soil it is common for flux to be the more important parameter.

Microdialysis was first developed to be used in medical research, to allow for samples to be taken with minimal intervention. Areas like the brain[46], inaccessible to many types of sensing, have been able to be probed using microdialysis due to its small probe size and diffusive sampling method.

2.2.2.1.2 Microdialysis in Soil

Buckley et al[47] gave a comprehensive analysis of the current work performed using microdialysis for soil sampling, outlining areas like how soil moisture content, “resistances” present in soil (Figure 4), perfusate composition and flow rate can affect the uptake of solutes into the probe. The review highlighted the potential for microdialysis to be used as a root simulator, through relating the flux of nutrients across the membrane of the probe to root uptake, giving an insight into bioavailability of the nutrient being studied. This look into bioavailability allows for the multiple factors affecting flux in the soil to be integrated together. This has allowed it to be used to investigate the bioavailability of soil N and P, showing good promise for further work in soil analysis.

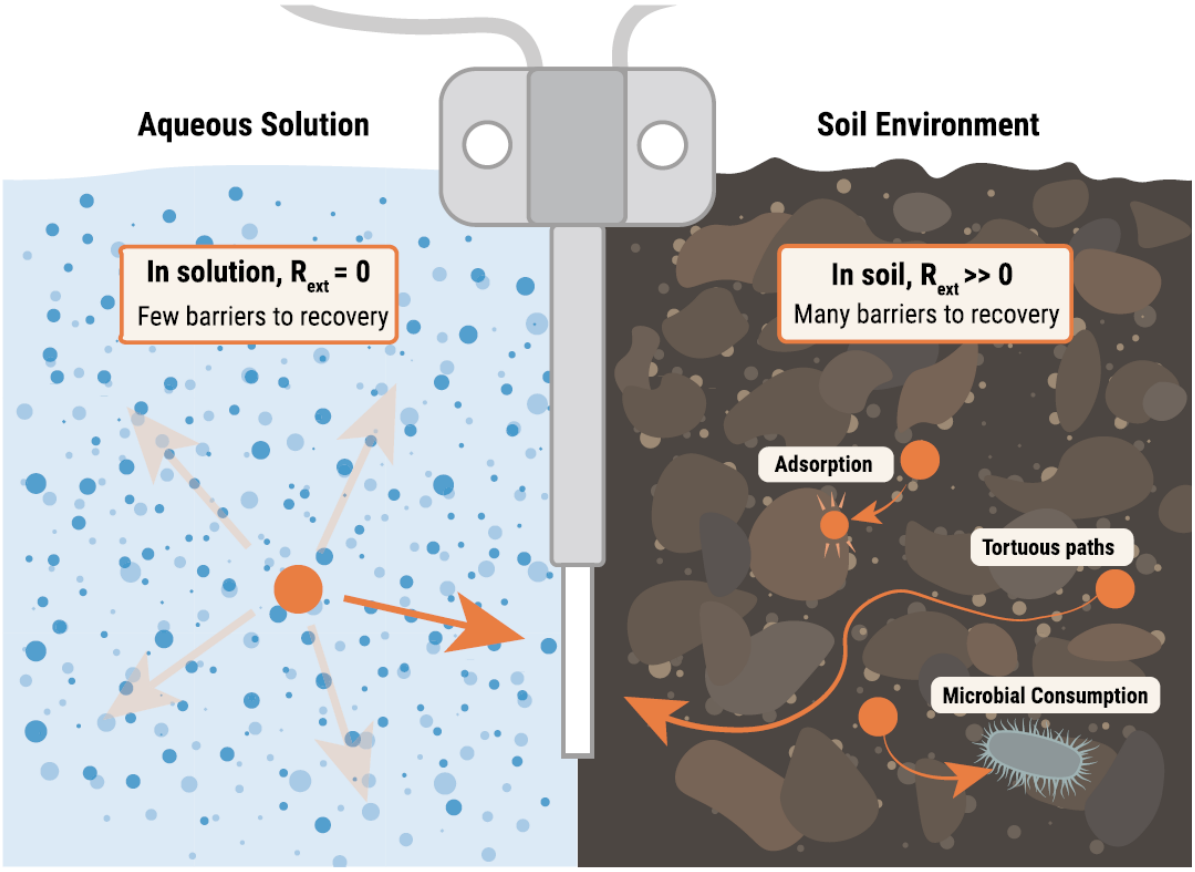

Figure 4 Buckley, 2020[47]. Diagram showing how the differences in external matrix can lead to greater "resistance" to diffusion. This figure has been adapted from ref. [47] with permission from Elsevier, copyright April 2020.

In measuring flux, we can measure how much of a given solute is exchanged between a media and the probe. This allows for a deeper look into what occurs in soils; the soil concentration could be artificially high using fertilisers, yet it would not necessarily change how much is adsorbed by a plant. Analyses performed on sugarcane roots found that by measuring the flux of nutrients such amino acids, it was possible to more closely mimic root uptake capacity and provide a better measure of nutrient availability [48].

With microdialysis we can more closely replicate what root systems would experience, allowing for a more precise measurement of nutrient availability. Phosphate, for example, is very abundant in most soils yet most of it is in the form of insoluble salts[49]. Roots exude organic acids, such as citrate and oxalic acid, to break down and mobilise these phosphate ions, allowing them to be absorbed through the roots. Through mimicking this process using retrodialysis, in which the perfusate is doped with a

species which then gets exuded into the soil, has allowed for researchers to study the root-soil interface and model P recovery in oilseed rape[50], showing good promise for this technique.

There are some key disadvantages to using microdialysis in soil. The small scale of the probe leads to issues in reproducibility of results, the heterogeneous nature of the soil could mean that it could take many measurements to analyse enough to cover a statistically relevant area. With the high resistance to diffusion in the soil, a "depletion zone", may form around the probe, with nutrients being extracted faster than diffusion can replace them. It may also be time consuming to allow the solute to reach a diffusive steady state. As solute is taken in by the probe, the change in concentration around the probe will require solute to diffuse through the soil to the probe. This could be beneficial, however, as it could allow us to either look at the local concentration around an area of interest, such as near a root surface, by doing a short-term measurement or allow the probe to run for a longer period to see more of a steady-state profile of the soil.

Continuous microdialysis has been used to assess how climate change parameters, such as elevated CO_2, temperature and an increase in drying-rewetting events, affect diffusive flux of different types of N in soil[51]. The method was able to track changes from both drying-rewetting events for both ammonium and nitrate, showing the short-lived increase in mobilisation upon rewetting dry soil shown in other studies.

The various methods in which microdialysis has been applied have allowed for many different parameters to be studied non-invasively, marking a large step forward for soil analysis; Continuous measurements of soil had been limited before microdialysis due to the limited supply of water to the soil, with other sampling methods (such as pore water sampling) having to actively take up water to analyse instead of using diffusive methods.

2.2.2.2 Pore water sampling

Whilst microdialysis has been becoming more prominent in soil analysis, other probes have also been developed. Pore water samplers (Rhizon, Rhizosphere Research Products B.V., Wageningen, The Netherlands) extract soil solution by applying a vacuum, allowing soil solution to pass through a porous polymer tip. After collection, the sample can either be processed immediately or frozen without any significant change to the chemical composition[52]. Smaller version of these samplers (MicroRhizon) have been used to good effect through collection and immediate analysis techniques in sediment sampling[53], working under both high and low moisture levels.

One major issue with these samplers, however, is due to how water is distributed through soil systems. The pore size in soil is often not uniform; when a force, such as suction, is applied to the soil, the largest pores empty first due to the lower capillary tension. As these larger pores empty, smaller pores are isolated and cannot empty. This causes Rhizon samplers to often bias the larger pores, not giving a complete picture of the concentrations present throughout the soil.

Most sampling techniques used with Rhizon samplers are still used with offline detection, with manual sampling techniques introducing potential error and contamination. Work has been done recently to couple a Rhizon sampler to a device for in-situ analysis, in which an electrochemical sensor for Cadmium detection was developed[54]. The pump connected to the Rhizon used quite high flow rates (3 mL/min), which would deplete soil moisture levels almost immediately and required a continuous supply of water on the surface of the soil to keep the soil hydrated.

The miniature samplers have promise for monitoring lab-based studies, in which soil moisture can be kept consistent, as well as with soils with high moisture content to prevent pore water from being depleted over time. A system connected to this can be run intermittently but the flow rate and sample frequency will have to be low enough that water can travel to the sampler without the area surrounding it being depleted.

2.2.2.3 Passive Sampling

For longer studies, passive sampling methods have been successfully used to monitor macronutrients in riverine, oceanic, and soil studies. These methods use a device that is placed in the medium, which slowly accumulate the target macronutrient. After the sampling period, the device is removed from the medium and the sorbent material within is typically treated with a solvent (typically acetonitrile or methanol) to provide a solution containing the macronutrients to be measured, which is then analysed through methods such as LC-MS, giving a time-weighted average of the concentration of the analysed macronutrients in the medium.

Passive samplers have been developed with commercial success, such as Chemcatcher®, consisting of a plastic or metal housing, a membrane for filtering (Typically polyether sulfone) and sorbent discs. The metal housing can accommodate up to 6 sorbent discs simultaneously allowing for two sets of triplicate studies to be done simultaneously with one device. A large range of sorbent discs to be used with Chemcatcher have been developed, allowing for different types of analytes to be

collected, including pesticides[55] and pharmaceuticals[56], yet many studies have used this housing with custom sorbent discs to good effect.

One passive sampling method that has been used for the analysis of macronutrients in soil is the diffusive gradients in thin films (DGT) technique. In this, a DGT device is inserted into the soil and absorbs nutrients through diffusion from the pore water, meaning the analyte amount sampled is dependent on both the pore water concentration of the analyte and its resupply rate from solids to pore water, giving insight into nutrient availability to plants.

A typical DGT device consists of an outer filter membrane, a diffusive layer and an inner binding layer, in which a binding agent allows for specific analytes to be collected. The diffusive layer, typically in the form of a polyacrylamide hydrogel, can be adjusted to its use cases through changing its diffusive properties through changing variables such as by adjusting the polyacrylamide composition and the polymerisation temperature[57], whilst the binding layer can be chosen for its specificity to an analyte (or analytes), to which it can chemisorb. Through formation of a diffusion gradient in the diffusive layer, a time weighted average concentration can be collected through analysis of the amount of analyte present in the binding layer.

(Kodithuwakku et al, 2023)[58] gives a comprehensive review on the use of DGT in soil for the analysis of NO_3^- and NH_4^+, comparing the DGT technique to KCl extractions. In this study, it was shown that whilst the two techniques give similar values for NO_3^-, the NH_4^+ concentrations differed. This was posited to be due to the KCl technique having greater access to soil-bound NH_4^+ whilst the DGT technique only samples pore water nutrients. However, one downside of using the DGT technique in soil is the potential volatilisation of NH_4^+ in basic soil environments through conversion to NH_3, preventing certain soil types from having access to this technique for long-term measurement of NH_4^+.

DGT techniques have also been applied to freshwater analysis[59, 60], analysing a vast range of analytes from trace metals (e.g. V, Mo)[61, 62] to pharmaceuticals[63, 64] to pollutants like organomercury[65]. In-situ analysers have also been developed for freshwater, combining a DGT device with a detector to monitor the accumulation of analytes in the binding layer. Using a suspension of gold nanoparticles attached to graphene oxide in water as a liquid binding layer, surface-enhanced Raman spectroscopy (SERS) was successfully combined with DGT[66]. The sensor was used to analyse sulfadiazine, an antibiotic, in pig breeding wastewater, and was able to do so under a wide range of environmental conditions (e.g. pH 5 to 9, 0.0001 – 0.05 mM NaCl). The gold nanoparticles attached to graphene

oxide enhances the SERS signal through the sulfadiazine adsorbing onto the surface of the gold nanoparticle, increasing the "wagging" vibration through the terminal amino group of sulfadiazine[67]. The system had an LOD of 10 ng mL^{-1}. The use of DGT for in-situ sensing is limited through its accumulative nature, with there being an upper limit to the amount of analyte bound to the binding layer. For long-term development, a careful balance must be made between enhancing the signal for it to be detected in-situ and not enhancing it to the point where the binding layer becomes saturated after a short period of time.

Passive samplers are now a key part of environmental analysis, providing time-weighted averages for long-term studies. However, these samplers are unable to capture short-term spikes in concentration well, highlighting that their use alone does not provide a total picture and can miss out on effects from rainfall events. These samplers can capture longer trends that are often overlooked well yet for studies with shorter timeframes other methods should be used instead.

2.2.2.4 Direct Electrochemical Methods

Along with these methods of sample collection, electrochemical sensors have also been developed that have direct contact with the soil solution. Many of these come in the form of Ion-selective field effect transistors (ISFETs)[68] and ion-selective electrodes (ISEs)[69]. However, these often require the formation of a soil solution due to the need for complete contact with the sensor to allow for these sensors' results to be comparable to one another, and these sensors often take a significant amount of time before a stable plateau can form.

Recently, a soil organic carbon (SOC) sensor system[70] has been produced through analysing charge transfer and charge-withholding capacities using a thin coating containing room-temperature ionic liquids (RTILs) which have a preference for binding to SOC species on top of metal electrodes. This sensor system was compared to a reference standard method, giving a 1-11% error. Whilst this method needs to be tested in the field, if similar ionic liquid membranes can be formulated towards soil nitrogen, this could be a boon for nitrogen sensing and soil science in general.

2.3 Sample Analysis

In the previous section we have seen how liquid samples can be extracted from soil. Here we will see how they can be analysed to determine key parameters.

By combining a sampler, such as microdialysis or pore water sampling, with a microfluidic system *in-situ* sampling could take place, in which a probe is placed into the soil or water and samples are taken and analysed at the location. This takes out human error from transferring the analyte from the sampler to the analysis equipment and allows for much quicker data acquisition.

In this section some of the laboratory methods used to quantify samples will be discussed, focusing on the ones that have been coupled with microfluidics, followed by a further look at the concepts governing droplet microfluidics.

2.3.1 Standard Laboratory Methods

Optical, wet chemistry and electrochemical methods are commonly used to analyse macronutrients, with each of them being used for analysing grab samples and in in-situ analysers. How each interacts with the sample and how they are implemented will be discussed here.

2.3.1.1 Optical

Optical methods use the interaction of the analyte with light as a means of detection. Examples of this include absorbance, fluorescence, and Raman spectroscopy.

In absorbance spectroscopy, electrons are excited into higher energy states by photons, reducing the signal that reaches the detector. The energy of the photons lost will be relative to the difference in energy between the ground state and excited state of the electrons in the sample, allowing for spectra to be developed if multiple wavelengths of light are used.

Fluorescence spectroscopy takes advantage of rigid, conjugated structures in the target molecule. Electrons are excited from the ground state to an excited state, which then undergo internal conversion, in which the molecule collides before transitioning back to the ground state, emitting a photon of a characteristic wavelength, higher than the wavelength of absorption.

Raman spectroscopy monitors inelastic scattering that occurs when light is scattered off a sample[71]. When a molecule is illuminated with light, there is a small chance (approx. one in every 10^8 photons) that the molecule will absorb a small amount of energy, with the photon being scattered at a different optical frequency. The change in frequency, known as the Raman shift, is dependent on the vibrational frequency of bonds present in the molecule, allowing for a spectrum to be analysed through analysis of the changes in frequency present. Surface-enhanced Raman Spectroscopy (SERS) has been

developed to significantly boost the weak signal generated in normal Raman scattering. Raman sensors have been paired with microfluidic architecture successfully[72], yet Raman sensors have not been miniaturised to the same degree as absorbance sensors, due to the requirement of a high-power laser.

Absorbance sensors take advantage of the linear relationship between absorbance and concentration of a species, at low concentrations, provided by the Beer-Lambert law:

$$A = -\log\frac{I}{I_o} = \varepsilon c l \tag{5}$$

Where A is absorbance, I and I_o are the intensity of the transmitted light and incident light respectively, ε is the molar extinction coefficient, c is the concentration of the analyte and *l* is the optical path length. Whilst it is possible for certain substances to be quantified in a mixture, difficulty can arise when interfering species have similar absorbance wavelengths. Techniques have been developed on a per-nutrient basis to "pick out" the chosen analyte, normally involving a chemical reaction involving a colour change.

One of the main benefits to using optical-based sensors is that they allow for analytes to be probed without the requirement of a surface reaction, allowing for less invasive sensing. In doing so, optical sensors do not have as much 'drift' in their performance, as the strength of the signal is based on the performance of the light source and the photodiode. This also allows optical sensors to run for a much longer time.

One issue with absorbance systems is that analytes of interest are often inhibited by low molar extinction coefficients, meaning the limit of detection (LOD) is often high as not much light is absorbed by the sample. Whilst a chemical reaction can be performed to give a compound with a higher extinction coefficient, this will increase the amount of waste produced. One way to combat this extra waste is by using a smaller sample size; with low flow rates and an intense chromophore, it is possible to create a very small amount of waste per sample.

One of the main aims of a microfluidic device is miniaturisation, which is antithetical to absorbance spectroscopy as a longer path length allows for potentially lower detection limits. To counteract this

tension, mechanisms have been developed to increase path length, such as by passing light through the sample and then reflecting it back through the sample en route to the detector. These “multipass” flow cells allow for a much greater path length than would be possible in these small sensors.

With continuous microfluidics, path lengths of similar distance or higher than those use in traditional spectrophotometry have been achieved in an in-situ optical sensor for Phosphate[73], using black PMMA as a flow cell material, chosen for its ability to absorb light not travelling along the inlaid optical cell path. This long path length system can struggle if air bubbles occlude the flow path, which is possible by getting stuck in the corners entering and leaving the flow cell, causing a lensing effect that impedes light from reaching the photodiode. Flushing techniques can be used to remove these and the inclusion of 2 flow cells instead of just one helps to mitigate this.

Cavity ringdown spectroscopy has also become popular in this regard[74-76], allowing for chemicals with low extinction coefficients to be analysed; this process uses two aligned mirrors with a very high reflectivity either side of the sample (Figure 5). A pulse of light, normally from a laser, is directed through the back of one of the mirrors. A small amount of light passes into the cavity and passes through the sample to the other mirror. Most of the light bounces off the mirror but as it isn’t fully reflective (often >99%) a small fraction of the light passes through to the detector. The remaining light bounces back and forth, with a small amount passing through each time. With each pass, more light is absorbed by the sample and an exponential decay of light intensity can be recorded.

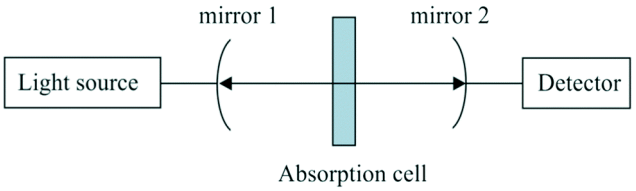

Figure 5 Schematic of a typical cavity ringdown spectroscope. This figure has been adapted from ref. [75] with permission from Royal Society of Chemistry, copyright December 2014.

One of the main benefits is that the technique is not sensitive to fluctuations in initial laser intensity[77] as the rate of decay is measured, which is independent of the initial intensity. This allows for a reduced signal to noise ratio, increasing the sensitivity. However, the system is also very dependent on the alignment of the two mirrors and typically requires a high-power laser, which may pose problems for in-situ sensing due to the large power requirements.

One issue with implementing these path length enhancement techniques into droplet microfluidic systems is that the curved nature of the droplet interfaces could lead to lensing effects, which could reduce the intensity with each pass as light refracts out of the cell. This effect may lead to a drop in sensitivity, so it may be necessary to pair these sensing techniques with techniques like droplet elongation or refractive index matching[78], which could reduce these lensing effects.

2.3.1.2 Wet Chemistry

For certain molecules, there are difficulties in accurately analysing levels due to interference, with species having overlapping absorbance spectra. Laboratory techniques can be incorporated in sensors, such as performing chemical reactions, to discern between these molecules. Absorbance spectroscopy can be tailored to specific molecules using chromophores, specific molecules that can selectively react with a reagent to form a highly conjugated molecule, absorbing light at characteristic wavelengths with a much larger extinction coefficient. Nitrite/Nitrate sensors can rely on the difference in electrophilicity between the two ions to analyse them separately using the Griess assay, which creates an azo dye, and has been used to detect nitrate/nitrite in many settings, ranging from biomedical[79] to environmental[80, 81]. Many such chromophores have been developed, using functional groups that target specific nutrients. These pre-treatment steps have been essential in driving down the limits of detection and improving the selectivity of microfluidic systems as more and more steps, such as filtering and mixing, are transferred to microfluidic devices.

2.3.1.3 Electrochemical

One of the main competing areas in environmental sensing is that of electrochemical sensors. Electrochemical sensors can detect the presence of species using chemical reactions at the surface of an electrical conductor, with electrons being transferred between the surface and the solution. The way in which the change is recorded differs between the three main types of electrochemical sensors: potentiometric, amperometric and voltammetric. Figure 6 shows an overview of the typical parts required for electrochemical sensors and how their signals are created.

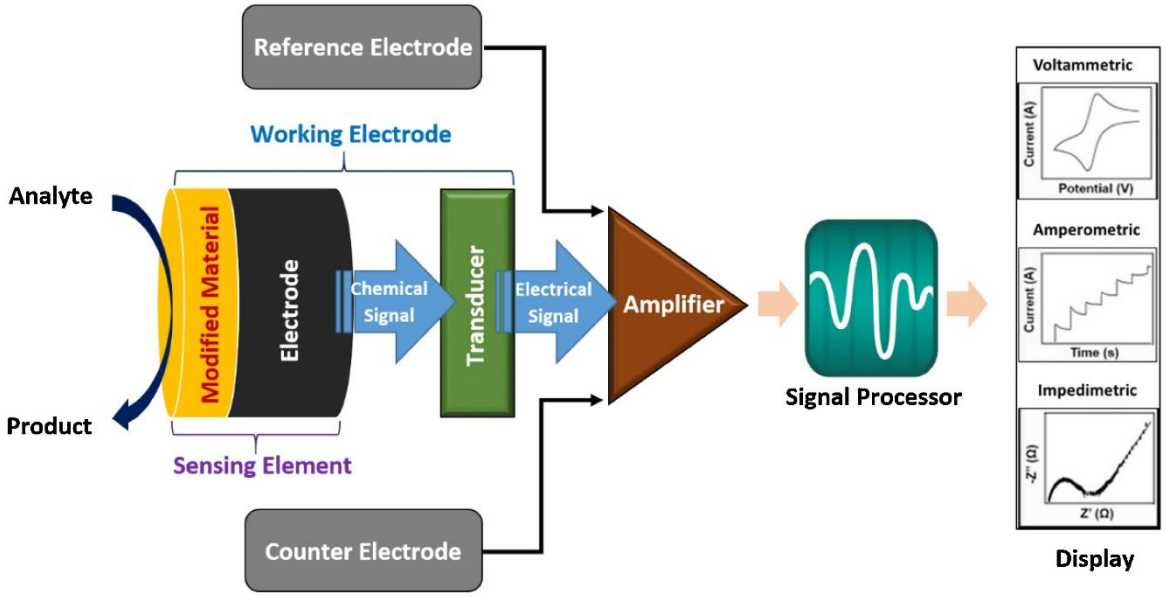

Figure 6 Schematic diagram detailing the processes of an electrochemical sensor. This figure has been adapted from ref. [82] with permission from Elsevier, copyright September 2021.

In potentiometric sensors, a change in analyte concentration is measured with a change in potential between the working electrode in contact with the solution and a reference electrode. In these sensors, very little to no current passes through. The potential has a logarithmic dependence on the concentration. Whilst these sensors can be very useful in detecting a wide range of levels of analyte, sensitivity issues arise due to the very small change in potential between similar concentration solutions. Ionophores have been extensively used in outer membranes for electrodes to selectively transport the analytes in question to the electrode to help mitigate this issue, leading to the formation of ISEs.

Many of these ISEs use liquid-contact, in which the outer ion-selective membrane is in contact with an internal solution to form an interface. These electrode configurations can give very good ion selectivity, yet the inclusion of an internal fluid leads to unsuitability for long term measurement, due to complex maintenance procedures. Solid contact ISEs (SC-ISEs) have since been developed to try and counteract this, using solid contact layers made from materials ranging from carbon nanotubes to metal nanomaterials. *Shao et al*[83] provides a comprehensive guide into the fabrication and development of these SC-ISE electrodes, developed for both environmental and wearable sensors. One key disadvantage of these ISEs is through ISEs often using a size-based pore for its ion selectivity. Other ions, with similar charge and size, can interfere by entering these pores. For nitrate, chloride and bicarbonate can be significant interferants[84], whilst ammonium is interfered with by potassium

and sodium ions[85]. Techniques such as introducing additional ISEs for these interferants can help in reducing their impact when analysing aqueous solutions or slurries yet are much less viable for in-situ soil measurements due to the heterogeneity of soil.

Voltammetric and amperometric sensors rely on probing specific redox reactions by applying a voltage and measuring the current; voltammetric sensors change the potential to “sweep” the system and measure the peak current whereas amperometric sensors have a fixed voltage.

Electrochemical systems tend to have a lower detection limit than optical sensors, yet the output often “drifts” from their starting signal over its lifetime, caused by degradation of the electrode surfaces during sampling[86]. These sensors therefore require frequent calibration, normally performed by either dipping the probe into a solution of a known concentration, adding a known quantity of the nutrient in question to the sample or by using a secondary probe and fitting the data to it. Also, as their signal is derived from a reaction on the surface of the electrode, biofouling can take place in which the sensor is contaminated. Electrochemical sensors can be very useful in giving quick results; without the need to perform a chemical reaction beforehand the detection process can be streamlined.

The direct implementation of electrochemical sensors in contact with soil has been an area of concern, with the contact between the sensor and the external medium being one of the major benefits of other electrochemical systems. Unlike in aqueous scenarios, the variability in soil moisture can cause the surface of the probe to dry out, leading to a rapid decrease in measurement. Also, the most common type of reference electrode (Ag/AgCl) has the potential to leach Cl^- out into the surrounding area, leading to a drift in the sensor's open circuit potential (OCP), causing a drift. Ali et al[87] have been able to use a layer of protonated Nafion to prevent this from occurring, which was able to keep the OCP from drifting over the course of their sampling window (32 days). Developments like this show great promise for the deployment of direct electrochemical sensors to be used in the field, yet their fluctuation with moisture content and biofouling are still major hurdles that still need to be overcome. Further work into such membranes may allow for an increased use in electrochemical sensors in soil sensing yet longer deployment times will need to be studied. With more stable sensor readings over time these would provide measurement without the production of waste, which would be advantageous to optical methods.

2.3.2 Macronutrient Analysis

Many of the sensing systems used for environmental study are lab-based, in that the samples are analysed away from the sampling area under controlled conditions. Whilst these are useful for some research purposes, and currently impossible with some techniques due to machine size, a move towards in-situ sensing will allow for many benefits. Having time-resolved data and remote monitoring allows for much more precise and informed decisions regarding fertiliser application or how certain meteorological events impact the soil

.

Table 1 Off-line Macronutrient Analysis for Water

NUTRIENT	METHOD OF DETECTION	SENSING ELEMENT	LOD (µM)	DETECTION RANGE (µM)	LIFETIME OF SYSTEM	FEATURES	REFERENCE
NO_3^-	Direct Optical	UV-Vis Absorbance	27	30-800		Uses optical fiber, requires pre-treatment methods Suggests higher precision through a smaller range of recoveries for nitrate Tested on lake, sewage and leachate water	[90]
NO_3^-	Potentiometric	Tetradodecylammonium bromide with 2-nitrophenyl octyl ether as plasticiser	7	$10\text{-}10^6$	1 month	Microfluidic system Tested on tap, river and well water Throughput of 12 samples per hour Cannot be used in saltwater due to Na^+ reference electrode	[91]
NO_3 + NO_2	HPLC-UV	Luminol (Chemiluminescence)	$2x10^{-3}$ (NO_2^-) $1x10^{-2}$ (NO_3^-)			Converted to Peroxynitrite after separation with UV irradiation using a low pressure mercury lamp Tested on river water, pond water, rain water, commercial mineral water and tap water	[80]

NUTRIENT	METHOD OF DETECTION	SENSING ELEMENT	LOD (µM)	DETECTION RANGE (µM)	LIFETIME OF SYSTEM	FEATURES	REFERENCE
NH_4^+	Ion Chromatography	Berthelot assay	0.3	1-2000	-	High-capacity ion exchange column, methanesulfonic acid eluent; tested on water and soil samples NH_4^+ extracted from soil samples using 26mM methanesulfonic acid with ultrasonication for 30 mins before filtering	[92]
PO_4^-	Ion Chromatography /UV	Molybdate assay	0.06 (SRP) 10 nM (IC PO_4^-)			Measured Orthophosphate/ SRP ratios and how it is affected by organic matter in shallow lake waters, SRP measured using molybdate method, orthophosphate measured through ion chromatography then molybdate method	[93]

Table 2 Environmental Sensors for Water

NUTRIENT	METHOD OF DETECTION	SENSING ELEMENT	LOD (µM)	DETECTION RANGE (µM)	LIFETIME OF SYSTEM	FEATURES	REFERENCE
NO_2^-	Impedimetric	Gold nanoparticle deposited on MoS_2 nanosheets on a glassy carbon electrode	0.09	10-2100	-	Enhanced accuracy over previous systems, with recovery rates between 99 and 103%	[94]
NO_2^- + NO_3^-	Colorimetric	Griess+ Assay	1.7	5-800	≥ 6 weeks	Droplet microfluidic system Low reagent consumption (2.8 mL/day) High rate of measurement (0.1 Hz), droplet microfluidic nature allows for longer deployments through avoidance of smearing and simpler, more robust system architecture than continuous microfluidic devices Low power consumption (1.5 W)	[95]
NH_4^+	Potentiometric	AlGaN/GaN High Electron Mobility Transistor with a PVC membrane with Nonactin	5.4	$10\text{-}10^4$	2 months	Significantly longer lifetime than previous work due to use of polymeric membrane	[96]

NUTRIENT	METHOD OF DETECTION	SENSING ELEMENT	LOD (µM)	DETECTION RANGE (µM)	LIFETIME OF SYSTEM	FEATURES	REFERENCE
NH_4^+	Potentiometric	Monoaminophthalocyaninato ionophore fixed to an acrylate membrane	0.004		6 months	Developed for use alongside an flow injection analysis system Lower LOD than previous works, lack of interfering ions	[97]
NO_3^-	UV Spectrophotometry	Deuterium Lamp (190 to 370 nm)	0.3	1 - 4000	900 hours (based on lamp lifetime)	SUNA V2 UV Nitrate Sensor (Sea-Bird Scientific) Can measure in both freshwater and seawater Rated down to 500 m depth Can correct for temperature and salinity with external temperature/salinity data	[98]

Table 3 Off-line Macronutrient Analysis for Soil

NUTRIENT	METHOD OF DETECTION	SENSING ELEMENT	LOD (µM)	DETECTION RANGE (µM)	LIFETIME OF SYSTEM	FEATURES	REFERENCE
$NO_2^=$	UV-Vis Lab-based	Griess Assay	3.2	5-65	-	Performed in a laboratory setting on dry soil samples	[99]

NUTRIENT	METHOD OF DETECTION	SENSING ELEMENT	LOD (μM)	DETECTION RANGE (μM)	LIFETIME OF SYSTEM	FEATURES	REFERENCE
PO_4^{3-}	UV-Vis	Molybdate assay	0.5	0.5-5	-	Required soil samples to be digested using HNO_3 and $HClO_3$, shows potential as a standard measurement method for phosphate in many environmental samples	[100]
PO_4^{3-}	Potentiometric	Hydrotris(3-phenyl-5-methylpyrazolyl)borate cadmium complex ionophore	1.5	1.5-10^4	1 month	Sampled on soil water Lifetime measurement based on the sensor being placed in 0.1 M NaH_2PO_4 when not in use $H_2PO_4^-$ selective, showed good agreement with colorimetric analysis (molybdenum blue)	[101]
P	UV-Vis	Malachite green with phosphomolybdate	0.2			Analyses total organic and inorganic P in soil water Uses centrifugation and filtering to extract P from soil Very pH dependent	[102]

2.3.2.1 Nitrate/Nitrite

The most common method of measuring nitrate/nitrite concentrations uses UV-vis spectrophotometry through the Griess assay, involving the reaction of nitrite with sulfanilamide and N-(1-Napthyl)ethylenediamine dihydrochloride (NEDD) in the presence of an acid, forming an azo dye.

The nitrate can first be reduced to nitrite to get a value for combined NO_3^- and NO_2^- (ΣNO_x^-). This method had been previously implemented whilst using continuous microfluidics by flowing the sample over copper-treated cadmium[81, 103]. Other methods have found success using VCl_3[104] as a reducing agent; whilst its reduction is significantly slower, the homogeneous nature of the reaction is useful in certain scenarios.

For soil, most nitrate measurements are derived from the use of the method from (Hood-Nowotny, 2010)[105], in which soil extracts are added to a microtiter plate, followed by VCl_3, NEDD and Sulfanilamide in a stepwise manner. After this, the solution is heated at 37.5 ^oC for an hour.. As these reagents are pipetted in a stepwise manner, there is an avenue for pipetting error to cause a small drift between samples, which could also affect any calibration curve that is developed in this method.

Electrochemical nitrite sensors have shown promise, offering lower detection rates than their wet chemistry counterparts. An impedimetric sensor using gold nanoparticles on MoS_2 nanosheets[94] offered a nitrite detection limit of 90 nM, having been tested on river water. A similar system has also been developed for soil nitrate sensing, using an MoS_2 and poly(3-octylthiophene) nanocomposite on a patterned Au electrode with a nitrate-selective membrane[87]. For long term measurements, electrochemical sensors tend to struggle due to both sensor drift and electrode deterioration. When using an Ag/AgCl reference electrode, Cl^- ions can leach during operation[106]. This sensor used a 15 nm-thick protonated Nafion layer to overcome this issue, preventing the movement of anions across the membrane during operation, resulting in a much longer lifetime (1 month). This system had a wide detection range (1 – 1500 ppm).

Several nitrate sensors have been commercialised successfully, such as the SUNA V2[98] (Sea-Bird Scientific). The SUNA V2 uses an ultra-violet spectrometer featuring a deuterium lamp for detection, measuring nitrate through analysing the UV signal of the seawater from 190 to 370 nm using a method developed by MBARI, decoupling the signal into its constituent parts through using a multivariant least squares method, taking into account the contribution of water and ions including bromine. This device has been used in both freshwater and seawater scenarios, yet has a fixed deployment limit due to its

deuterium lamp which has a lifetime of approximately 900 hours. This can still allow for long deployments through intermittent use, allowing for 3600 samples to be taken before needing to replace the device. This system struggles with high dissolved organic matter or high turbidity environments; with its open flow cell, there is no possibility for sample prefiltering. There is a "wiper" feature to prevent biofouling yet this would not aid with a turbid sample.

2.3.2.2 Ammonium

The most common ways of measuring ammonium using colorimetric assays involve the Berthelot method or the Nessler method.

The Berthelot method once used sodium hypochlorite and phenol to analyse ammonium, through the formation of a blue indophenol complex. This method has since been improved by incorporating salicylate instead of phenol[107], allowing for this process to be performed on-site without the risk of poisonous chemicals being exuded.

The Nessler method uses mercury potassium iodide (K_2HgI_4), which reacts with NH_4^+ to form a yellow compound. This method has fallen out of favour compared to the Berthelot method as the use of mercury salts cannot be avoided.

Previous versions of the Berthelot method sequentially mixed the 3 reagents, which was easily done in a laboratory setting. This often meant samples had to be collected and sent to a laboratory for analysis, allowing for contamination. If the method was directly implemented into a microfluidic system, this multi-step synthesis would have led to very complex microfluidic architecture, which would drive up the cost of both manufacturing and power consumption. A "simplified" method was developed[108] which allowed for microfluidic analysis through a one-step synthesis, in which the reagents were pre-mixed through pumping the two reagents into a small reagent mixing channel, then mixing this combined reagent with the sample in a 1:1 ratio. This simplification has allowed for a large reduction in complexity, driving down the cost per device, while still having a detection limit of 0.8 µM NH_4^+.

A popular way of measuring ammonium concentration in freshwater involves using nonactin as an ionophore to make an ISE[109]. These devices have the potential to give low detection limits for ammonium yet are hampered in their development by interfering K^+ and Na^+ ions. Ionophores work by reversibly binding to a species of a specific size and charge, allowing for similarly sized molecules to bind to the site. As NH_4^+ has a very similar ionic radius to K^+ (and Na^+ to a lesser extent), even though

nonactin binds preferably to NH_4^+ some binding to K^+ will still take place, artificially raising the detected level. Whilst these ISEs have been successfully used in freshwater scenarios, porting these technologies over to monitor soil ammonium levels has proven difficult, due to the abundance of K in soil.

The combination of electrochemical devices with microfluidic systems has also been used to good effect in monitoring ammonium, through development of multiparameter sensor measuring NH_4^+-N, dissolved oxygen, temperature and pH simultaneously[110], with high accuracy and good stability over a 10-day period. With a sample duration of only 3 seconds, the system was able to detect changes in ammonium from a range of 20 to 300 µM. However, long-term studies have not been performed with this chip and may suffer from the same drifting effects over time as other electrochemical sensors.

2.3.2.3 Phosphate

In agriculture, it is common for phosphorus stocks to be depleted after harvesting. Whilst this is normally managed through crop rotation, having easier access to how much phosphorus is available will allow farmers to better tailor their methods, increasing efficiency. Developing a user-friendly method for this will be essential in the future of smart farming.

The molybdenum blue method is the most commonly used colorimetric method for analysing phosphate in water in which PO_4^{3-}, ammonium molybdate and ascorbic acid react to form a blue complex. This method has had good success in being adapted to microfluidics for water samples and has also been used on digested soil samples [100]. The current method has yet to be adapted to measuring intact soil samples.

Electrochemical phosphate sensors for soil have also proven to be effective. Development of a potentiometric system using a cadmium complex ionophore[101] has shown good agreement with colorimetric analysis, and has shown good selectivity towards H_2PO_4. Having electrochemical phosphate soil sensors would be very useful due to the minimal reagent consumption, so this is promising work. Claims are made that the system has a lifetime of a month yet this is based off of it being stored in NaH_2PO_4 when not in use instead of it being used continuously, so this may need further field testing to ratify.

Absorbance-based microfluidic sensors for phosphate in water have required innovations in increasing path length to be effective; the high detection limit of many absorbance systems combined with the low levels of phosphate concentration in water has proven challenging. (Morgan et al.)[73] have had success through the use of elongated path lengths, in which the molybdenum blue method was used in conjunction with long length flow cells (10.4 mm and 25.4 mm), using two sizes of flow cells to extend the range of the sensor, being able to measure concentrations as low as 100 nM.

Commercial probes have also been developed for absorbance detection of phosphate in water, including the WIZ probe (Systea S.p.A, Anagni, Italy), which consumes only 30-60 microliters of reagent per analysis, and the ClearWater Lab-on-Chip Phosphate Sensor (Clearwater Sensors, Southampton, UK), which is capable of measuring down to depths of 6 km and can measure up to 20 µM with an LOD of 50 nM. However, such systems have not yet been innovated for soil studies.

2.3.3 Microsample Analysis & the Advantages of Microfluidics

The increased implementation of microfluidic systems in our society has led to the miniaturisation of many essential tasks, allowing for wearable sensors and environmental sensors to be much more efficient in both response time and reagent usage. Whilst these have been implemented successfully, there are still areas that have yet to develop such infrastructure, including soil sampling.

Chemical soil sampling methods often use microdialysis to non-destructively extract nutrients[51, 111-114], allowing for flux measurements to take place. These can give a more detailed look into nutrient availability than destructive methods, as many nutrients are trapped in deposits that cannot be accessed without microbial activity which are unavailable for direct take-up by plants. Microdialysis also allows for a much greater spatial and temporal resolution, with systems incorporating multiple probes to “map” areas, performing analysis within minutes of sampling.

Through implementing microfluidics, this analysis time can drop even further with the detector being attached to the probe itself, allowing for portable soil sensors to be developed without needing to preserve and transport samples. This will be a great help to the current analytical methods, involving collection and freezing of samples, as the act of freezing has been shown to alter the chemical makeup significantly. Whilst there have been many microfluidic macronutrient samplers for water analysis[81, 95, 115], it has taken a long time for these types of sensors to be developed for soil analysis.

The ability to perform analytical techniques on-site allows for a marked increase in efficiency, cutting down on the amount of time and resources taken to transport samples from an area of interest to a

laboratory, allowing for rapid analysis of samples. This drive for efficiency has also led to the miniaturisation and automation of laboratory procedures, allowing devices to be developed that can be used by people with minimal training without fear of cross-contamination.

Table 4 Example of Microsample sensors (<100 µL sample volume)

NUTRIENT	METHOD OF DETECTION	SENSING ELEMENT	LOD (µM)	DETECTION RANGE (µM)	LIFETIME OF SYSTEM	FEATURES	REFERENCE
NO_3^- + NO_2^-	Colorimetric	Griess assay	1.7	2-800	9 months	Droplet microfluidic system, uses V(III) to reduce nitrate to nitrite to give separate measurements of nitrate and nitrite Consumes 2.8 mL/day of sample/reagent (0.32 µL/droplet)	[95]
NO_3^-	Potentiometric	Poly(3-octyl-thiophene) and Molybdenum Disulfide nanocomposite layered on a PCB	22	16-2400	1 month	Solid state miniature sensor Tested on extracted soil solution using a suction lysimeter, showed good agreement with commercial sensor ((LaQua Horiba nitrate sensor),	[87]

NUTRIENT	METHOD OF DETECTION	SENSING ELEMENT	LOD (µM)	DETECTION RANGE (µM)	LIFETIME OF SYSTEM	FEATURES	REFERENCE
						Use of polymeric layer on top of the Au electrode allowed for a longer lifetime than previous studies	
NH_4^+	Colorimetric	Berthelot assay	0.8	1-170	6 months	Low cost microfluidic system with automated calibration Tested for fresh and salt water	[108]
PO_4^{3-}	Colorimetric	Phosphomolybdate assay	0.10	0.3-100		Miniaturised system, able to work at temperatures between 17 and 35 ^oC, with wireless capability Interference with arsenate and silicate	[116]

NUTRIENT	METHOD OF DETECTION	SENSING ELEMENT	LOD (µM)	DETECTION RANGE (µM)	LIFETIME OF SYSTEM	FEATURES	REFERENCE
PO_4^{3-}, H_4SiO_4, NO_3^-, NO_2^-	Colorimetric	Phosphomolybdate assay (PO_4^{3-}), Silicomolybdate assay (H_4SiO_4), Griess assay (NO_2^- and NO_3^-)	PO_4^{3-}: 0.18 H_4SiO_4: 0.15 NO_2^-: 0.45 NO_3^-: 0.45	PO_4^{3-}: 0.2–100 H_4SiO_4: 0.2–100 NO_2^-: 0.4 - 100 NO_3^-: 0.5 - 100	46-day deployment	Continuous microfluidic system, washing solution of 0.1 M	[117]
NO_3^-, NO_2^-, PO_4^{3-}, NH_3	Fluorimetric (NH_3) Colorimetric (NO_3^-, NO_2^-, PO_4^{3-}) UV (NO_3^-)	o-Phthalaldehyde (NH_3), Griess (NO_2^-), Griess+ using VCl_3 (NO_3^- Colorimetry), Molybdate Blue (PO_4^{3-})	<0.07 (NH_3) <0.14 (NO_3^- Colorimetry) <20 (NO_3^- UV) <0.07 (NO_2^-) <0.07 (PO_4^{3-})	0.2 – 35 (NH_3) 0.4 – 70 (NO_3^- Colorimetry) 60 – 700 (NO_3^- UV)	Up to 2.5 months (depending on water temperature)	40 minute cycle time per measurement 10 m max depth 8 W power consumption On-board calibration after reagent replacement	[118,119]

NUTRIENT	METHOD OF DETECTION	SENSING ELEMENT	LOD (µM)	DETECTION RANGE (µM)	LIFETIME OF SYSTEM	FEATURES	REFERENCE
				0.2 – 20 (NO_2^-) 0.2 – 30 (PO_4^{3-})		Option to have a 0.25 µm self-purging microfilter RS232 data output allows for integration with control systems	

Altahan, 2022[117] has shown the development of a multiple analyte on-site sensor, showing capabilities of measuring NO_2^-, NO_3^-, PO_4^{3-} and H_4SiO_4 simultaneously for a month. These nutrients were analysed through wet chemistry methods in a microfluidic system, using syringes and valves to control mixing and heating time. This analyser adapted the VCl_3 method of monitoring NO_3^- over the copper-coated cadmium column typically used, allowing for a significantly longer deployment time without maintenance (1 day with Cd-Cu column, 1 month with VCl_3). The use of wet chemistry methods is significant, as it was one of the first long-term deployment sensors that was able to analyse multiple macronutrients at once.

Microfluidic devices use microchannels to manipulate the flow of fluid; by incorporating pumps and valves, precise control of flow can be achieved. The phenomena that occur in these microchannels are significantly different due to the dimensional constraints of the channel, with limited width and height.

In continuous microfluidics, the small channel dimensions lead to the formation of laminar flow, in which the fluid moves through the system as if it was in the form of layers. At the walls of the channel, the fluid is stationary. Each layer acts on the layer above it in the form of frictional drag, leading to a parabolic flow pattern, with the fastest fluid being in the centre of the channel (Figure 7). This disparity in flow rate, known as Taylor Dispersion, leads to sample smearing and potential cross-contamination between samples.

2.3.3.1 Droplet Microfluidics

With conventional in-situ microfluidic analysers, it is necessary for a sensor to carry all its necessary liquids onboard in order to leave the sampler for extended periods of time. By using droplets instead of a continuous flow, the amount of reagent per experiment can be precisely controlled, allowing for much lower per-sample quantities. With regular microfluidics, as the analyte can be in contact with the wall of the flow cell, smearing can also occur (Figure 7). This smearing can be detrimental to the accuracy of the system, meaning the system will need to be flushed every so often which can require complex microfluidic systems. With droplets the sample being processed will not touch the walls of the tubing, allowing for less contamination to build up over time.

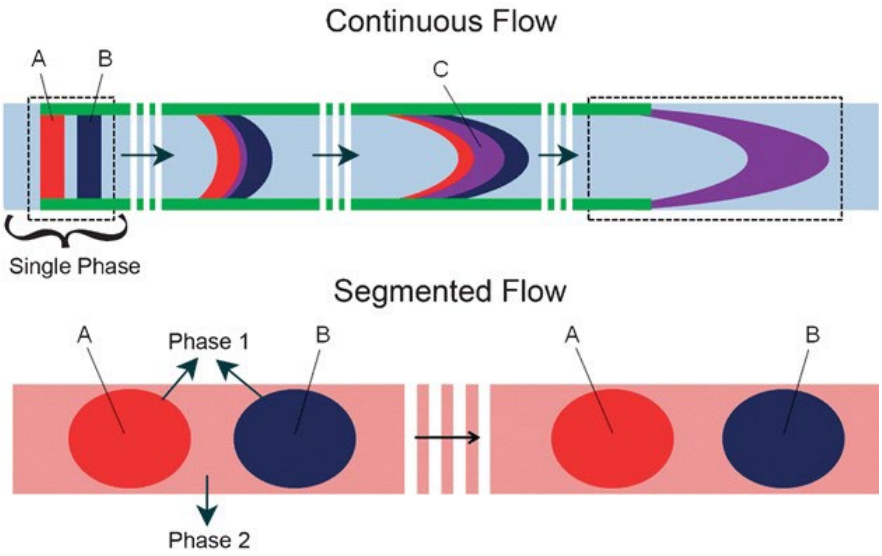

Figure 7 Comparison of Continuous and Droplet microfluidics, with droplet systems containing two immiscible phases. Segmented flow regimen highlights the lack of Taylor dispersion in droplets, with less sample cross-contamination. This figure has been adapted from (Solvas and deMello, 2010)[120]. Copyright 2010 Royal Society of Chemistry.

Another major benefit of droplet microfluidics is the facility of mixing. In continuous microfluidic systems, it is often required to extend the length of the fluid channel to increase diffusion, using serpentine channels to induce mixing. Whilst some systems have incorporated methods such as channel grooves[121] to disrupt laminar flow, these systems also have issues with production as the tolerances needed require specialist equipment. Inside droplets, turbulent flow dominates and mixing is achieved in small timescales. This fast mixing is beneficial in allowing for more controlled reactions by giving a much more precise start time[122], which can be essential when monitoring kinetics. This feature, combined with the lack of cross contamination, allows for a discrete droplet to be monitored throughout the course of its reaction.

To form these droplets, two main techniques have come to the forefront (Figure 8). T-junctions are typically used for larger droplet generation whilst flow-focusing techniques are better for making smaller droplets and are a good solution when using more viscous fluids. Droplet systems can be split into a disperse phase (droplet) and a continuous phase (carrier fluid), with the continuous phase preferentially wetting the channel wall. Fluorinated oils are often used as a carrier fluid with PTFE channel walls. The use of fluorinated carrier fluid such as FC-40 has been advantageous in preventing droplet cross-contamination as they are immiscible with most organic substances.

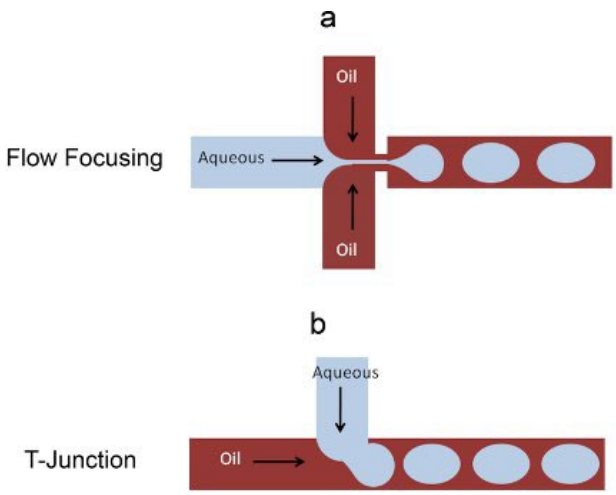

Figure 8 Comparison of typical methods of droplet formation, with a) a planar flow-focusing regime and b) a planar T-junction regime. This figure has been adapted from (Solvas and deMello, 2010)[120]. Copyright 2010 Royal Society of Chemistry

In a T-junction, the two phases are injected into the two branches of the "T"; at the interface of the two sections, the disperse phase enters the channel of the continuous phase and is then cut off by the forces of interfacial tension and shear force. The degree of this cut-off can be controlled through manipulation of the flow ratio, with faster continuous phase flow rates resulting in smaller droplets. If the flow rate is too fast, laminar flow can be observed in the channel. With more viscous solutions, this threshold appears at lower flow rates (Figure 9c).

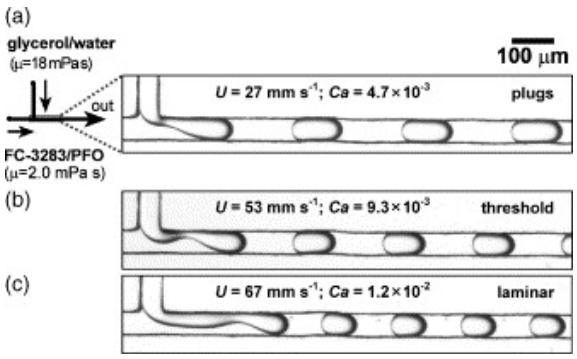

Figure 9 Depiction of the 3 flow regimes exhibited in T-Junction droplet formation, where U is the flow velocity and Ca is the capillary number. At low flow rates (a), the droplets are formed at the junction; as the flow rate increases, a laminar segment forms before the droplets are

cut off. (B) represents the threshold, which is determined by the flow velocity and the viscosity of the sample fluid, after which laminar behaviour is observed (c). This figure has been adapted from (Tice et al, 2004)[123], with permission from Elsevier, Copyright April 2004

The flow-focussing technique can be utilised here allowing the production of small, monodisperse droplets by passing the fluid through a narrow gap into a wider channel. These methods do typically require more complex fluidic architecture yet can be very useful when handling more viscous substances. The smaller droplets formed are good for high-throughput assays and could be used for applications like PCR, yet are less suitable for soil-based macronutrient analysis due to the generally low concentration of analyte in the soil, which would be harder to detect in smaller droplets. The complexity of the system also inhibits its uses in field sensors, which typically need to be more robust.

Many droplet microfluidic devices currently use polymers such as poly(dimethylsiloxane) (PDMS) or poly(methylmethacrylate) (PMMA) for chip fabrication with a fluorinated oil as the carrier fluid. The surfaces undergo fluorination to make the surface more hydrophobic, allowing the carrier fluid to preferentially wet the surface. This surface treatment tends to be thin and wears off over time, leaving the exposed polymer underneath, which leaves the surfactant to be present in the carrier fluid and prevents the carrier fluid from being reused without a costly separation method. Through using fluorous chip materials, such as Dyneon THV 500GZ[124], this can be overcome and longer chip lifetimes can be achieved. Whilst this sort of material may be applicable to nutrient sensors, biomolecular sensors may not transition over from using PDMS as PDMS is merited for its gas permeability, allowing for cell cultures to last longer as they can get access to oxygen, which may not be the case with fluoropolymer-based chips.

A droplet microfluidic method of measuring nitrate and nitrite separately in one device[95] used VCl_3, due to the inability to use a surface-based catalyst. As the reduction step was much slower than the Griess reaction, it was possible to first measure nitrite absorbance after the initial nitrite-Griess reaction was finished and then heat the mixture using an inline heater to speed up the reduction of NO_3^- to NO_2^-, followed by a second measurement to quantify the ΣNO_x^-(Figure 10). As this system was able to monitor nitrate and nitrite separately without adding extra reagents post-droplet formation, this method allowed for much simpler microfluidic architecture.

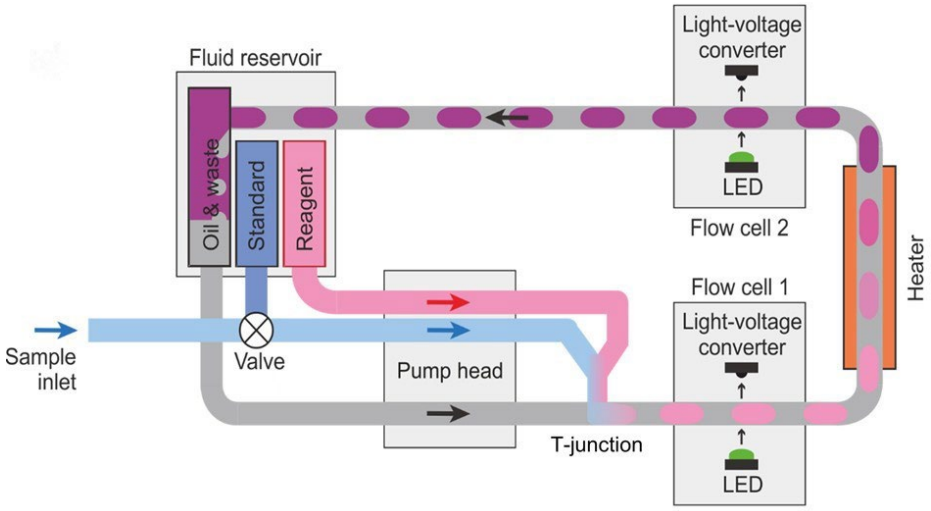

Figure 10 Schematic of the combined Nitrite+Nitrate measuring system, using an in-line heater to drive the reduction reaction, with an in-built oil recycling system to reduce waste. Reprinted (adapted) with permission from (Nightingale et al, 2019)[95]. Copyright 2019 American Chemical Society.

There has been work in incorporating electrochemical and optical sensors into a singular device, using the electrochemical sensor to give a continuous data output and then using the optical device to calibrate it. This would take into account the sensor drift, yet it would not be able to be incorporated with a droplet microfluidic system unless two fluid lines were maintained at once, given that droplet microfluidics cannot be used with surface-based sensors, as the carrier fluid separates the sample from the surface of the tube it passes through resulting in continuous microfluidics being used instead.

There have been developments in droplet microfluidic electrochemical sensors in an attempt to overcome the surface-based issues normally faced. Due to the immiscibility of the aqueous and fluorocarbon phases, placing electrodes on the channel walls would traditionally not allow for the aqueous phase to be studied. One interesting method involved reducing the width of the channel to elongate the droplets, reducing the distance between the droplet and the surface (Figure 11)[88]. In doing so, the system mimicked pressure-driven continuous flow, allowing for the chronoamperometric method to be carried out. This system was able to analyse nanolitre-scale droplets, yet it may be difficult to replicate in robust, in-situ sensors as the very small channel dimensions may be significantly hampered by biofouling.

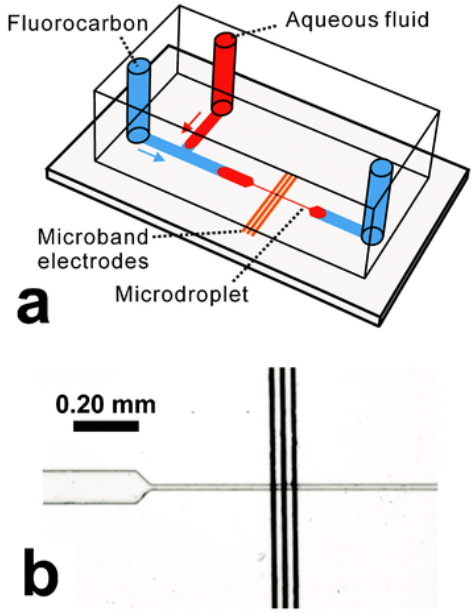

Figure 11 a) Schematic of droplet elongation technique to perform electrochemical sensing, b) Microscopic image of the narrow section. This figure has been adapted from ref. [88] with permission from Elsevier, copyright February 2013

Attempts have also been made to install electrodes into the microfluidic network that point into the channel to probe inside droplets[89]. This system managed to sense glucose levels in fluid droplets with reasonable accuracy, yet long term stability of the electrodes and cross-contamination between droplets needs to be examined. Nevertheless, this poses a potential for electrochemical devices to be incorporated into droplet microfluidic systems, allowing for more combined optical and electrochemical sensors in the future.

2.3.3.2 Microfluidics with Microdialysis

Certain disciplines have already created microdialysis probes coupled to microfluidic devices; biosensors have been made incorporating the two techniques, allowing for wearable technology to be used due to their small size. Both continuous and droplet microfluidic systems have been incorporated; Glucose has successfully been monitored using a continuous flow electrochemical sensor, with a high temporal resolution, to analyse the events following a traumatic brain injury in mice [46, 125].

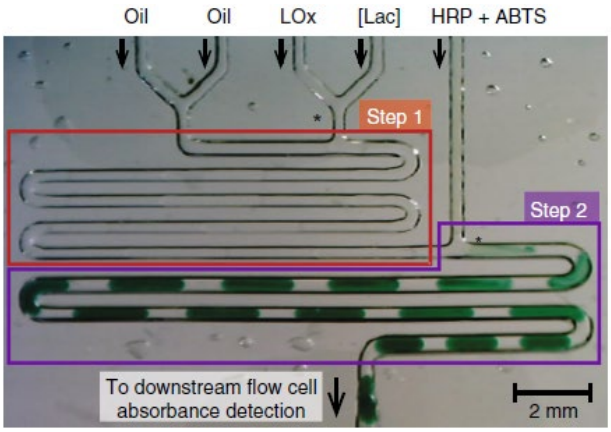

Figure 12 A droplet microfluidic system used to measure absorbance for a lactate assay; in step 1, the sample is mixed with lactate oxidase to form H_2O_2 and pyruvate before a second T-junction adds horseradish peroxidase (HRP) and 2,2'-azino-bis(3- ethylbenzothiazoline-6-sulfonic acid (ABTS), which gets oxidised by the H_2O_2 to form a blue-green compound, which can then be detected downstream. This figure was adapted from (Nightingale et al, 2019)[125] with permission from Springer Nature, Copyright June 2019.

Nightingale et al[125] were able to produce a wearable droplet microfluidic-based sensor, with an ability to be targeted towards different biomarkers (Figure 12). The system incorporated a microdialysis probe and a microfluidic system, driven by a screw-threaded pump, with an in-built absorbance flow cell. The pump allowed the push-pull mechanism needed for in-vivo microdialysis whilst also providing the segmented, out of phase flow needed for droplet microfluidics. The system was shown to be versatile, allowing for both glucose and lactate assays to be developed. By using droplet microfluidics, it was possible to avoid drift in the LED sensor by factoring in the absorbance of the oil phase, which remained constant, using the following correction to the Beer-Lambert law:

$$A = -\log_{10}\left(\frac{I_{d,sample} \times I_{o,blank}}{I_{d,blank} \times I_{o,sample}}\right) \quad (6)$$

Where I_d refers to the intensity in the droplet phase and I_o refers to the intensity of the oil phase, with the sample and blank notation referring to what was being measured at the time. This corrective step decouples the LED intensity from the absorbance, as the oil absorbance does not change.

This method coupling microdialysis to droplet microfluidics has also been used to monitor several neurotransmitters with high temporal resolution[126-128], through collection of a droplet train into tubing

which can then be analysed using liquid chromatography mass spectrometry (LC-MS) or more recently electrospray ionisation-tandem mass spectrometry (ESI-MS/MS), which is an excellent technology to use with neurotransmitters as the ionisation method does not break down these complex molecules, allowing for easy analysis of a solution containing multiple neurotransmitters at once.

Droplet microfluidics coupled with microdialysis has had potential to transform point-of-care analysis in the biosensor industry; through using a similar system in soil we have the potential to do the same for in-situ agricultural analysis. Many current microfluidic analysers have been developed for water analysis, yet the use of microfluidics for soil macronutrient analysis has not been explored. Through the pairing of soil sampling techniques, of which ultrafiltration and microdialysis have both been used, with a microfluidic system it would allow for a much more detailed look at short-term fluxes, whilst also having access to a robust sensor system for longer deployments.

2.4 Multinutrient Analysis

In many environmental systems, the need to analyse multiple nutrients at once has come to the forefront as the next step in macronutrient analysis. Being able to see the interplay of different nutrients in real time is a very powerful tool in gaining insight into both biogeochemical processes and agricultural processes. The increase in popularity of aquaponics, in which fish-farming is coupled to hydroponics, has led to an increased importance of tracking different forms of nitrogen simultaneously. Recording these in tandem will allow for better maintenance of both the fish and the crop, due to the fast-changing nature of inorganic nitrogen in the system.

Both ammonium and nitrite have to be kept at a consistent low level for aquaponic management, with several sources and sinks being kept in a delicate equilibrium (cumulative NH_3 and NH_4^+ levels between 1.6 and 2.9 mg N/L, NO_2^- levels between 0.4 to 1.1 mg N/L)[129] with fish producing ammonium through urine excretion, which is then processed by ammonia oxidising bacteria in the water into nitrite. This is then converted with nitrite oxidising bacteria to nitrate. This nitrate, as well as some nitrite and ammonium, can be taken up by the plants present through N fixing. If the amount of feed is too high, both ammonium and nitrite will not be processed quickly enough and potentially toxic levels of these chemicals will build up and endanger the fish. Introducing in-situ analysers will allow for such conditions to be avoided through control measures, such as changing feeding regime or by circulating a portion of the water in the system for fresh water to artificially lower concentrations in severe cases.

Wastewater treatment plants and bioreactors also are in need of multinutrient analysers. Having the ability to precisely monitor conditions for bacterial growth allow for much more efficient growth strategies to be developed, with the ability to non-invasively monitor nutrients reducing the amount of human error induced through grab sampling and wet chemistry analysis. Feedback loops can also be set up alongside these analysers to create self-sustaining bacterial culturing systems, which would be a boon for bacterial research in improving the reproducibility of culturing.

Document scanners and cameras have been used to good effect in quantifying nutrients through the same chromogenic methods as those found in the lab, being able to monitor the kinetics of multiple reaction cells in a similar fashion to a plate reader, typically coupled with paper-based microfluidic techniques. Up until recently these processes have been confined to the laboratory yet (Lin, 2019)[130] showed promise by integrating this type of scanner-based analyser into a portable system, allowing it to be deployed to take water samples in-situ. The unit would have multiple cells open to the environment that could collect small volumes of water (approx. 2 mL) which would then close and seal, allowing the collected volume to diffuse and mix with pre-loaded dried reagents on glass wool that would allow a colour to form in the cell. This colour could then be scanned and recorded over a period, allowing the analysis of kinetics, before the reaction plateaued and an endpoint could be analysed. Whilst there are limitations based on the amount of cells that are present, their single use nature, and the length and imaging quality of the scanner, the potential to measure multiple analytes in tandem with a customisability to use any colorimetric reaction thanks to the greyscale recording of the scanner shows promise for timed “grab sampling” events in-situ.

Many electrochemical sensors have been developed to track multiple analyte concentrations as once. Their small form factor is ideal with complexing multiple analysers into a single device, which have been implemented into both environmental and healthcare settings. The development of technologies as laser induced graphene (LIG)[131] and nanocomposite antifouling coatings[132] have allowed for electrochemical sensors to measure multiple analytical biomarkers simultaneously and will lead to much improved sensor lifetimes; in-situ optical analysers must start to incorporate multiple analytes. Bead-based microfluidic assays have great potential to analyse multiple biomarkers simultaneously; such beads have been functionalised through droplet microfluidic techniques to allow targeting for specific analytes, yet the way such beads target these biomarkers, through attaching antibodies is incompatible for macronutrient analysis.

Electrochemical inorganic nitrogen analysers have had good commercial success; the TL–2900 Dual Channel Analyser (Timberline Instruments, USA) has the capability to measure both ammonium and combined nitrate-nitrite through electrochemical analysis of ammonia gas. Nitrate and nitrite are converted into ammonium through reduction by a zinc column before being converted to ammonia using a pH 11 solution. This system can give analyses at a rate of 90-120 seconds per sample with low maintenance requirements yet is unable to differentiate between nitrate and nitrite through its reduction method.

Most environmental microfluidic analysers focus on a single analyte, needing to be positioned in-situ next to other competing analysers to track multiple analytes at once, increasing both power consumption and not being applicable to areas with high spatial variation such as soil or with a limited supply of moisture. Some multinutrient probes are commercially available, such as the WIZ and NPA probes (Systea S.p.A, Anagni, Italy)[119], capable of measuring Nitrate, Nitrite, Ammonium and Phosphate simultaneously with an in-situ filtration device capable of measuring in both freshwater and seawater scenarios, through using wet chemistry techniques. The WIZ probe has a reagent consumption of 30 to 60 µL per sample and a cycle time of 40 - 60 minutes, with a power consumption of 8 W. Through using a droplet microfluidic system instead, this cycle time and power consumption can be reduced through not requiring cleaning steps, with biofouling being significantly less of an issue due to the use of a carrier fluid, preventing buildup in channels and flow cells. This would also reduce the amount of waste the system would create, allowing a longer period between cartridge replacement.

2.5 Conclusion

Microdialysis has shown to be a useful tool in both environmental and medical sensing, with its passive sampling approach allowing for minimal disturbance to the sample, whether in a soil matrix or a blood vessel. Whilst microdialysis has been put to good use in taking samples to be measured off-line in soil studies, an in-situ analyser for soil has not yet been developed using it. Through combining droplet microfluidics and microdialysis, an in-situ sensing system will be developed in this project. Many microdialysis-based systems paired with optical approaches are currently impeded by having to collect a large amount of sample to get relevant data, requiring long sampling times due to the low flow rates used. This is not the case with droplet microfluidics, which is able to break up the continuous stream of perfusate into separate reaction vessels, giving a much better time resolution than previous wet

chemistry methods. Through probing the soil in-situ, human error can be avoided and analysis systems can be run autonomously without having to worry about sample degradation.

Optical and electrochemical techniques of macronutrient sensing in environmental settings have been compared, with electrochemical sensors giving lower limits of detection at the cost of lower reproducibility and potential sensor drift. Droplet microfluidics is a key area of development that allows for assays to be performed with a much lower risk of cross-contamination than continuous microfluidics. The formation of a “reaction vessel” also allows for easier manipulation of samples, allowing for stepwise processes to be performed. This has been crucial in the development of in-situ sensors by allowing wet chemistry techniques to be used remotely, which will be the fundamental basis for the work done in this project.

Chapter 3 Development of Soil Nitrate Analyser

This chapter describes the development of a droplet microfluidic system using microdialysis (MD) probes and ultrafiltration (UF) probes to examine nitrate levels in both soil and water using the Griess+ colorimetric assay.

Much of this chapter was adapted from a published paper (Lu et al, 2024)[133], of which I was a co-author. My contribution was in experimental planning and preparation, including preparing reagents, soil samples for analysis, and calibration of the analyser. I also helped with the maintenance of the sensor in the Writtle forest deployment, as well as with data analysis for soil WHC calibrations, the Glucose addition test and the Writtle deployment.

3.1 Introduction

The current area of soil sensing relies heavily on off-line measurement, with some areas starting to use in-situ systems, mainly in the form of electrochemical sensors, which have been used to analyse both NH_4^+ and NO_3^-, with NH_4^+ sensors showing potential for long term measurements when using nonactin ionophores. However, NO_3^-electrochemical sensors still have significant issues with drift over time. An on-line mass spectrometry system has been developed[134] for analysing soil samples using microdialysis yet it will take considerable time before such equipment can be deployed in-situ. Miniaturised absorbance sensors have already been coupled with droplet microfluidics for the development of both environmental and medical sensors, whilst microdialysis is being used for environmental sampling to extract macronutrients from soil with minimal disruption to the soil matrix for off-line analysis[47, 135]. If these collection methods (coupled to droplet microfluidics) can be developed for soil it would likely allow many other types of sensors to benefit from the passive nature of microdialysis sampling and the "reaction vessel"-like nature of droplets which would allow for the manipulation of time-relevant samples with little cross-contamination.

This NO_3^- analyser was adapted from our group's previous work, which was used to quantify riverine NO_2^- and NO_3^- concentrations[95], making use of a peristaltic pump instead of a screw-driven pump. Due to the low level of nitrite in soil, the detector for NO_2^- was not used.

Objectives:

- Modify the Niu group microfluidic platform to incorporate microdialysis and improve robustness to allow for monitoring in soil environments
- Further optimise the Griess reagent assay used in (Nightingale, 2019) to analyse a broader range of nitrate, due to the higher level of nitrate present in soil
- Compare the performance against the standard laboratory Griess+ assay using standards in both water and soil samples
- Deploy this system on-site to analyse soil nitrate over an extended period (2 months to 1 year)

3.2 Materials and Methods

Unless stated otherwise, all chemicals were purchased from Sigma-Aldrich (now Merck), UK. Ultrapure water was obtained from a Milli-Q Direct Water Purification System, with a resistance of 18.2 MΩ (Millipore, Merck).

Griess+ Reagent was made by first adding VCl_3 (1.25 g) to 30 mL Ultrapure water. HCl (15 mL, 37%) was then added, followed by Sulfanilamide (1.25 g) and N-1-naphthyl ethylenediamine dihydrochloride (NEDD, 0.125 g), before being shaken until all solids were dissolved. The solution was then made up to 250 mL with Ultrapure water and was then stored in capped aluminium-lined bags to prevent oxidation and stored at 4 ^{o}C before use.

A 50 mM nitrate stock solution was prepared by dissolving Sodium nitrate (1.06 g) in Ultrapure water and filling up to 250 mL. Nitrate standards were made up from the nitrate stock solution through serial dilution.

Soil used in the glucose test was collected from Stoneymore Wood in Writtle Forest, Chelmsford, UK (51°41'37.9"N 0°22'20.4"E). This soil was sieved below 1.4 mm particle size and had a pH around 4 (5g soil in 12.5 mL ultrapure water), as well as an organic matter content of 13.54% (ignition at 500 °C). Its maximum water holding capacity was 0.5 g H_2O/g dry soil.

3.2.1 System Design and Fabrication

The microfluidic system can be broken down into 5 crucial parts (Figure 13); the pump, the probe, the chip, the heater and the detector. Nitrate is sampled from either probe, which then flows into a T-junction microfluidic chip, in which Griess+ reagent is added and droplets are formed. These droplets then flow through a heater, required to reduce the time required for the VCl_3 to reduce the NO_3^- to

NO_2^-, which then reacts with the sulfanilamide to produce a pink solution. The intensity of this solution is then measured using the in-line flow cell at 535 nm, which is then converted into an absorbance using the Beer-Lambert law.

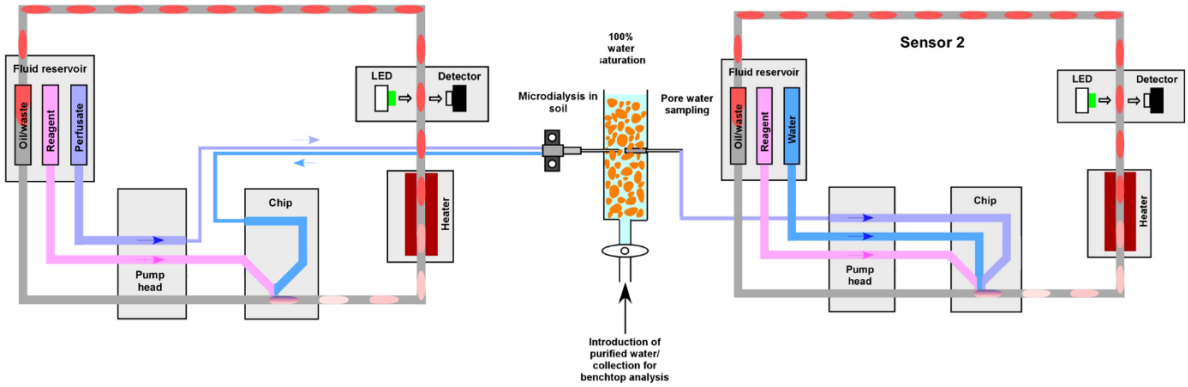

Figure 13 Layout of the nitrate sensor, using microdialysis (Sensor 1) and pore water sampling techniques (Sensor 2). In the pore water analyser, water was introduced to raise the potential range of the sensor.

The peristaltic pump system and microfluidic chips were made in-house using parts printed on an Ultimaker 3 in tough PLA (Parts for the peristaltic pump were designed by Liam Carter and Bingyuan Lu, flow cell designed by Liam Carter). Electronics were developed by Liam Carter and Ken Yeung. Heating elements were developed by SouthWestSensor. Motors were acquired from StepperOnline, which were connected to rollers which would compress on the pump bed, producing a flow. This peristaltic pump system was made as the screw-based system used previously gave significant backpressure, which gave a noisy signal. Using a peristaltic pumping system also allowed us to easily tune the ratio of water:sample:reagent:oil, allowing us to change dilution factors as needed during the system's development.

Santoprene microbore tubing (Altec, UK) was used as pump tubing, PEEK tubing was used as connector tubing to the microfluidic chip, AWG30 PTFE tubing (Adtech, UK) was used for the tubing between the pump and chip and UT7 was used from the chip through the heater to the detector. Short sections of small bore silicone tubing were used to connect AWG30 to PEEK. Fluorinert FC-40 (3M, UK) was used as the carrier fluid.

3.2.1.1 Pump

Inside each pumping system (Figure 14) a spring (LC072H0S, Lee Spring) pushes a pump bed, in which Santoprene (0.76 mm ID) is glued (using Loctite 406) into grooves that then rest onto a 4-line roller. These rollers have grooves of particular sizes which, when rotated using a stepper motor, allow fluid to be pumped through each of the santoprene lines when the pump bed is compressed. All pump parts (Pump bed, chassis, pump head and roller) were printed at 100% infill with Ultimaker Tough PLA (part no. 202303, Ultimaker). As roller designs were finalised, the roller was changed from tough PLA to a stainless steel roller with a 0.02 mm PTFE Coating (3a Prototype, Hong Kong), allowing for a longer deployment without roller breakage.

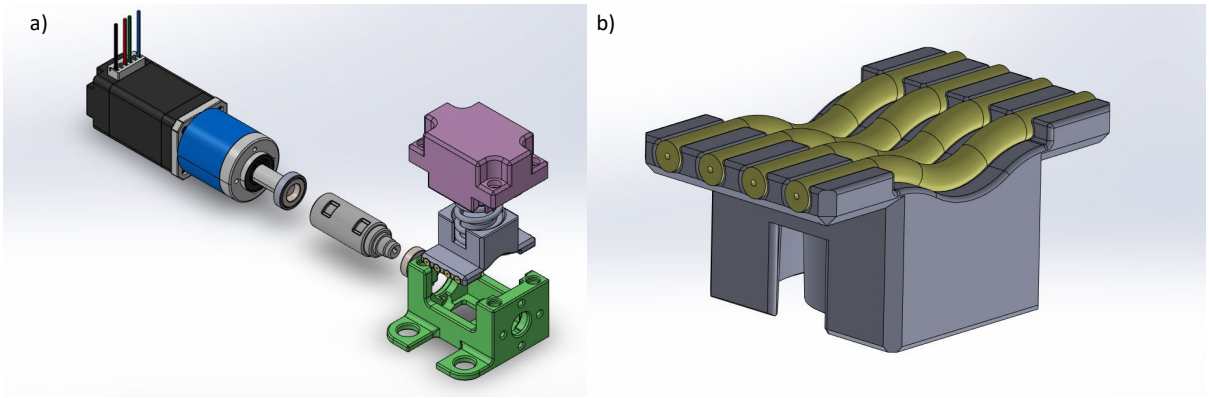

Figure 14 a) Exploded View of pump system, showing the roller that sits on the D-shaft of the stepper motor and the pump bed which the tubing is glued to. b) Close-up of the pump bed, showing the area that gets compressed by the roller.

The pump beds were assembled by putting a thin layer of super glue (Loctite 406) into the grooves of a custom 3D-printed pump bed, then placing 0.76 mm ID santoprene into the grooves. This is then compressed in a jig using a vice for 30 minutes to ensure good adhesion. After assembly, the pumps were run dry for 1 day to help make the tubing more flexible, allowing for consistent pumping.

3.2.1.2 Chip

The microfluidic chips made for the first part of this project were typically made in tough PLA (Ultimaker, The Netherlands) using an Ultimaker 3. This FDM printer was not ideal for making long-lasting or fully waterproof chips due to the potential for leakage to happen through the chip, due to the voids created in between layers of FDM printing. This manufacturing method was used due to its ease and speed of prototyping, allowing us to try several form factors with different sizes of pumps.

This was good for making chips used for testing processes but as the designs of the system as a whole were finalised we moved over to resin-based chips (Figure 15), using the same microfluidic designs, printed using an Elegoo Mars 3 (Elegoo, China). These chips had much better long term performance and were used in the field deployable analysers.

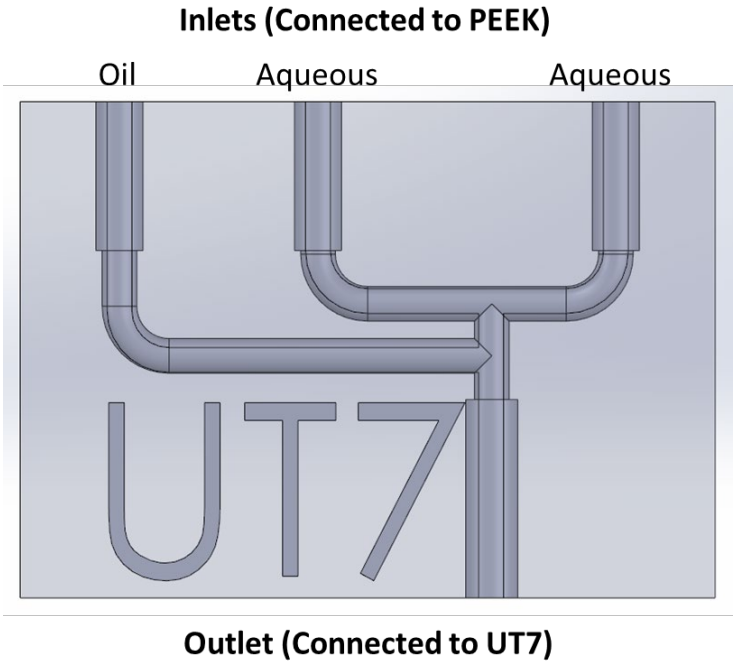

Figure 15 Microfluidic Chip Design, in which the PEEK and UT7 are inserted and glued in place with Epoxy (Araldite 2012, Huntsman Corporation)

The chip body was then glued to small sections of PEEK for the inlets and a section of UT7 PTFE Tubing (Adtech, UK) for the outlet. The fluoropolymer nature of the UT7 tubing is crucial for droplet stability as the FC-40 oil wets this preferentially, allowing the droplets to keep form throughout the length of UT7. Both 3-line and 4-line chips were made to allow for dilution to be added to the sample.

3.2.1.3 Heater and Flow Cell

The custom heater board, developed by SouthWestSensor Ltd. for previous analysers developed by our group, was incorporated with a 3D-Printed guide to keep the UT7 in contact with it for the correct duration (Figure 16a). This guide had multiple routes that could be taken to exit the heater, allowing for different heater times to be configured. The heater, when set up, would take around 5 minutes to

get to temperature, after which the droplets can be introduced into the heater for uniform heating (Figure 16b).

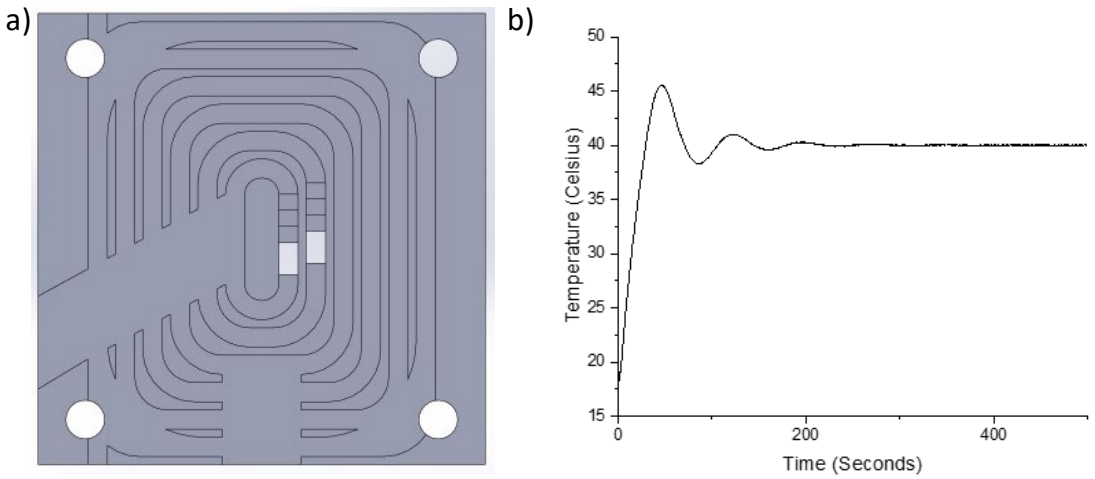

Figure 16 a) 3D Design for the guide (Designed by Bingyuan Lu) used to control the length of UT7 in contact with the heater. b) Typical heater response from heating up, taking approximately 5 minutes to stabilise.

After the UT7 is put through this guide, the UT7 travels into a flow cell screwed into the back of the guide. This flow cell (Figure 17,designed by Liam Carter) contains a photodiode and an LED (540 nm wavelength for the Griess Assay). Light is emitted from the LED and passed through the sample in the UT7 tubing before being captured by the photodiode.

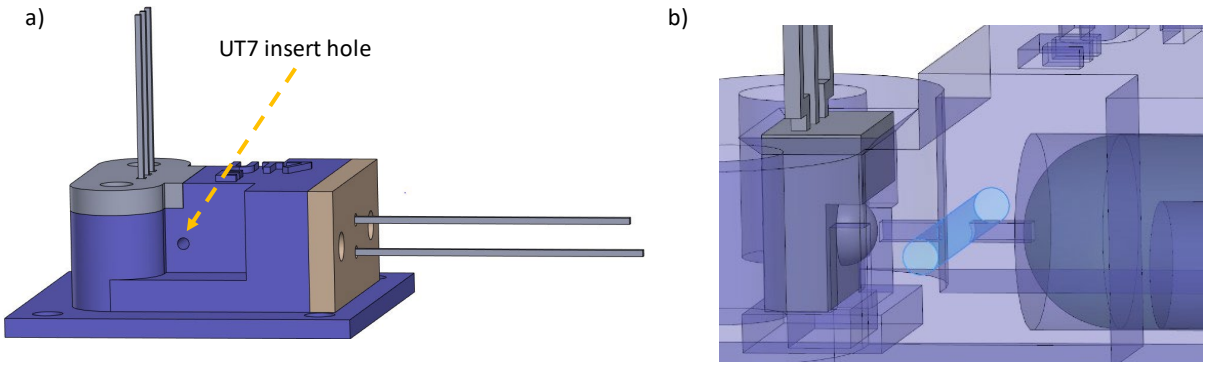

Figure 17 a) Flow Cell subassembly, with guiding covers for the LED and photodiode. b) View highlighting the UT7 tubing route (blue), passing between the LED and photodiode. Droplets pass through this UT7 and the change in absorbance is recorded.

This heater-flow cell subassembly was then insulated with foam insulation, with a 3d-printed shell surrounding this. This heater-flow cell combination allows for the flow cell to be kept at a constant temperature, which is necessary for deployment. Earlier prototypes of the system (i.e. Figure 18) had the flow cells separate from the heaters, which was quickly changed to all-in-one systems.

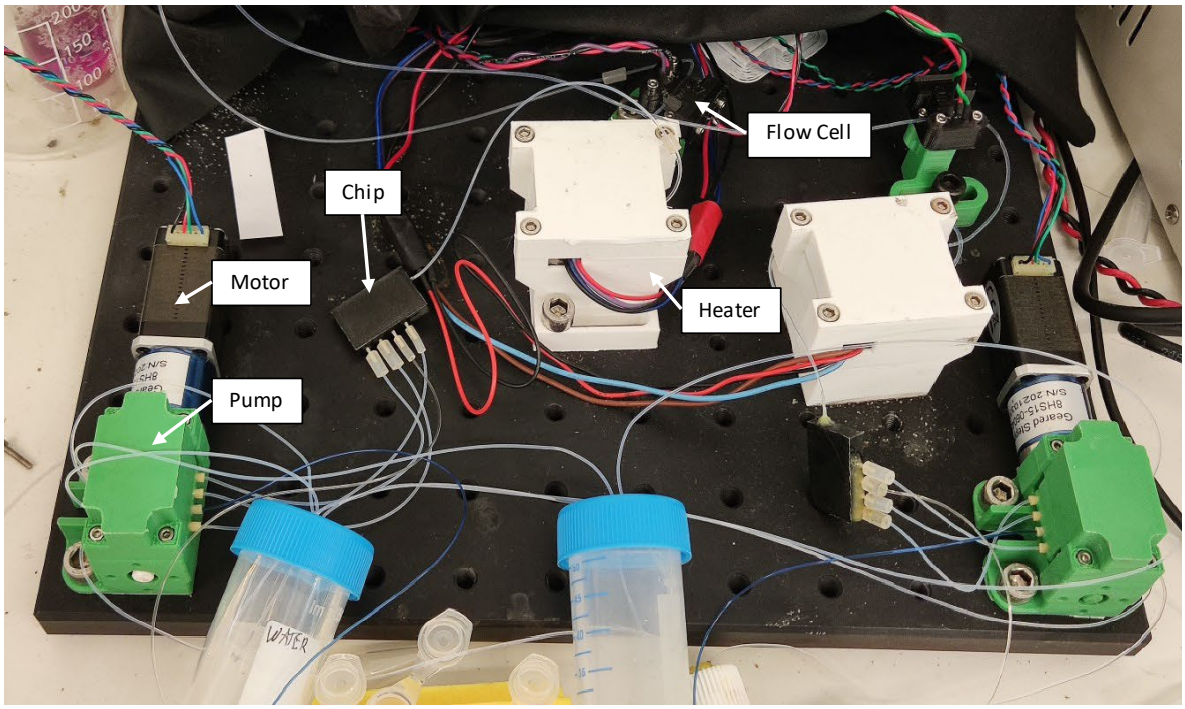

Figure 18 Two early prototypes of lab-based systems side by side, with the pumps flowing fluids to the microfluidic chips, which then pass through the heaters before passing through to the detectors.

3.2.1.4 Probes and Soil Columns

CMA 20 Elite Microdialysis probes (CMA8010436, Harvard Bioscience) with a 10 mm membrane length and a 20 kDa molecular weight cut-off (MWCO) were purchased, along with MicroRhizon pore water samplers (no. 19.21.82, Rhizosphere Research Products).

Soil columns (Figure 19) were created by drilling holes into the side of 25 mL centrifuge tubes or syringes with a pillar drill (0.9 mm diameter holes for the MD probe, 1.4 mm for the ultrafiltration probe) at the 10 mL mark. Parafilm (Bemis) was used for sealing the holes by piercing the film with a small needle and inserting the probe, ensuring a tight fit around the PEEK on the probe to prevent water leakage. Soil and water were added stepwise until the 10 mL mark, after which the ultrafiltration and MD probes were inserted and the parafilm was sealed to the outer surface of the column, after

which the remaining soil and water were added. This was to improve probe-soil interaction to improve recovery. Parafilm was added to the top of the column to prevent moisture loss through evaporation.

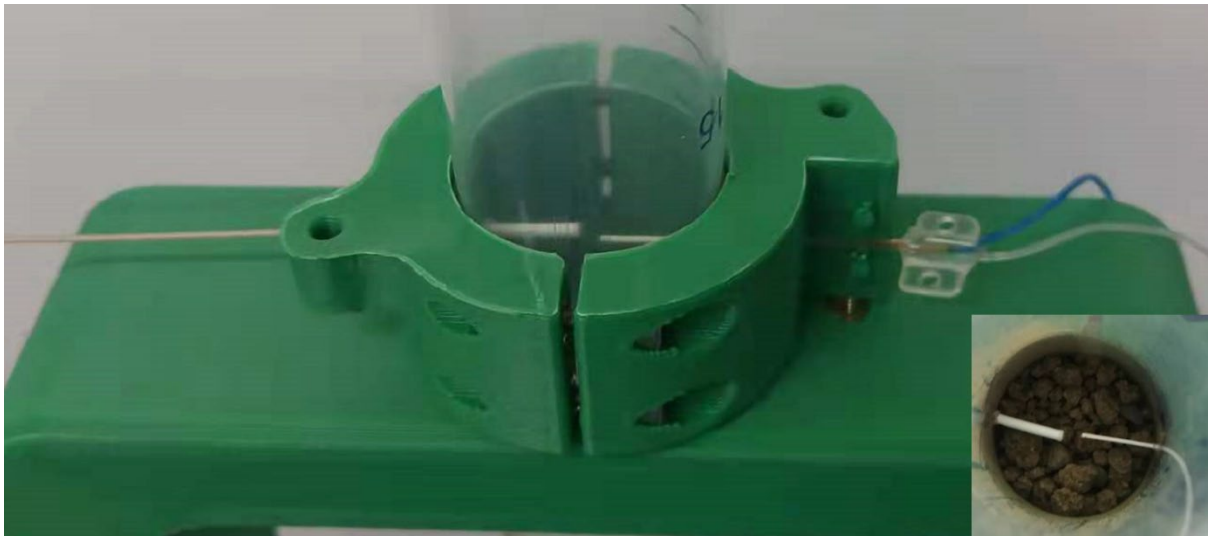

Figure 19 Setup of a soil column, with an ultrafiltration probe (left hand side) and microdialysis probe (right had side) inserted through holes drilled through the side of a syringe and supported by a 3D-printed structure; from this point, soil and water are added on top layer by layer to cover the probes.

3.2.2 Data Processing

The intensities throughout each experiment using the system were recorded to a .csv file, which was then processed using a MATLAB script (made by Adrian Nightingale and Liam Carter)[136] to discern between oil droplets and sample droplets, with the intensities of each droplet being averaged (Figure 20), taking into account the shift of oil droplets with temperature by shifting all oil levels to a single value and adjusting the aqueous droplets in turn. The droplets were sorted between aqueous and oil through finding stable plateaus in the data, signifying a droplet was in front of the detector, then determining if the intensity value is above a user-inputted threshold. As the carrier oil gives a higher intensity than an aqueous droplet, as it absorbs less light, through placing the threshold between the intensity values of oil and the blank values for droplets the oil and aqueous phases can be easily separated. The aqueous droplet intensities are then collated into a .csv file, with the average time of each droplet. For intermittent sampling, the intensity data from each photodiode was collected onto

an onboard SD card at the end of every measurement period but for continuous sampling and calibration the data was logged using a connected laptop.

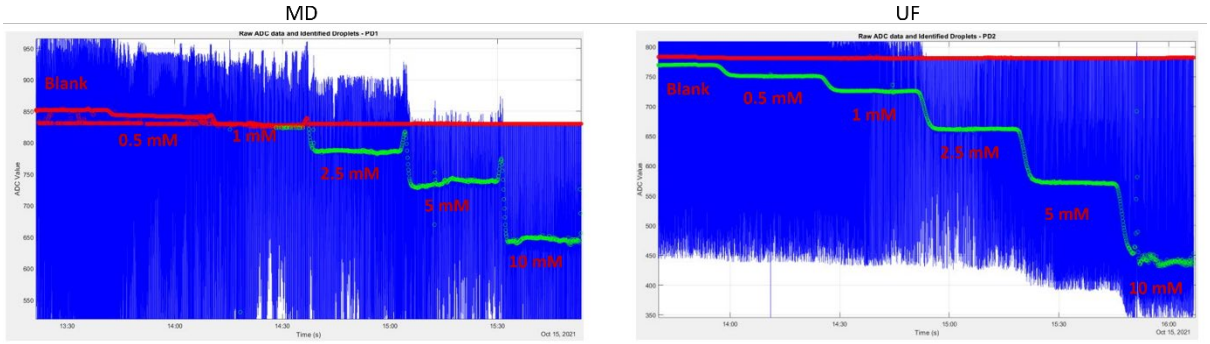

Figure 20 Processed data from the microfluidic system from a calibration in solution.

The red appearance of some of the microdialysis samples in Figure 20 was due to part of the processing during the early stages of the system development. Ideally, there should be a gap in intensity between the oil and sample droplets (with the oil being at a higher intensity) to allow for easier data processing, to prevent confusion between oil and sample. The intensity of the oil droplets can sometimes shift due to a misalignment in the flow cell, which can occur if the tubing is not a tight fit for the flow cell, making the oil and sample droplets overlap in intensity. An early version of the code would consider the oil to be a higher intensity than the sample, so all data points at or above the oil level were classed as oil droplets. This was later fixed so the bounds of the oil level (above and below the oil level) could be clearly defined, yet one future step in fabrication included flow cell testing with FC-40 and water to make sure the oil droplet intensity was significantly higher than any aqueous droplet intensity. Intensities were converted into absorbances using Beer's law, with the blank intensity being recorded before each calibration run and deployment. This absorbance could then be converted into concentration through using a calibration curve. The intensity given by each concentration in the calibration was calculated by averaging the intensity of the droplets made by that standard.

For the purposes of calibration, samples that gave a signal that was not consistent (e.g. when the probes were inserted into soil) were analysed by taking an average of the first 12 droplets after the droplet with the lowest value.

2 different soil samples were obtained from the Writtle Forest (Essex, UK); one of which had a very low nitrate level (Stoneymore) and one with a much higher nitrate level (Little Edney, approx. 2 mM NO_3^-). With the inherently low nitrate level, the Stoneymore soil was used for calibration purposes as

if a calibration solution was added there wouldn't be too much of a difference in absorbance. The soil was dried in an oven at 30 ^{o}C for 3 days, then sieved to 2 mm diameter before being used in tests.

3.2.3 Testing of Different Pumping Mechanisms for Microdialysis

After the pumps were constructed, a mock system was set up in which the pump was connected to a liquid flow sensor (SLF3S-0600F, Sensirion AG, Switzerland), which was then connected to a MD probe in a nitrite standard solution. 2 modes were tested; a push system, where the outlet of the MD probe fed directly into the microfluidic chip, and a push-pull setup in which the outlet of the MD probe was fed back into a second line of the peristaltic pump.

The two pumping methods were then compared to that of a conventional syringe pump (Harvard Apparatus PHD 2000 Programmable). Probes were placed in $NaNO_2$ solution (100 µM) and 500 uL was collected for a range of flow rates for each pump system (0.5 to 5 $\mu L min^{-1}$). This was then added to 500µL of Griess reagent, which was then analysed via a spectrophotometer. The absorbance was then compared to the absorbance given by the standard solution, giving a relative recovery (Figure 21). A higher relative recovery gives better consistency between results and improves measurement accuracy.

Theoretically, a push-pull system would be preferable as it would give greater control over the flow rate through the rest of the system, leading to more stable flow rates within the heater, and could also prevent backflow from the system into the MD probe if the system was stopped. However, it was found that it was difficult to properly synchronise the push and pull features as each pump line would be different, with slightly different amounts of glue attaching to the santoprene tubing, with each tubing wearing at slightly different rates. This would lead to slight changes in flow rates between different pump lines using our current pumping setup, which wouldn't make much difference when coming to measurement (due to the calibration performed before the test) but would have an effect on the pressure in the MD probe. This pressure could lead to a significant drop in recovery, due to the exudation of water through the probe.

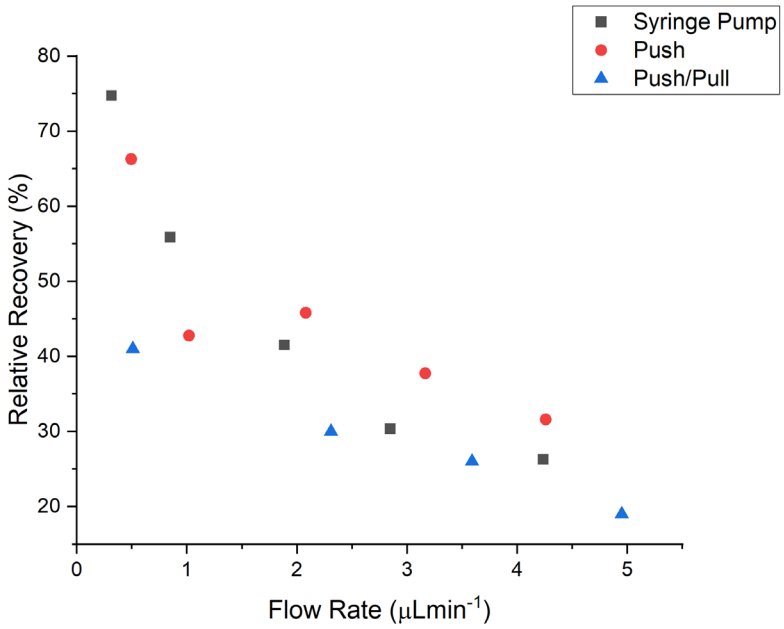

Figure 21 Comparison of relative recovery from a MD probe at different flow rates using different pumping setups.

At low flow rates (sub 1 $\mu Lmin^{-1}$) we would expect the recovery for all pumping systems to be very high as the perfusate in contact with the membrane would have more time to equilibrate with the external concentration, meaning that more nitrate would have diffused into the perfusate. With an increase in flow rate, we would expect a significant drop in recovery, in line with what was observed, as there would have been less time for the analyte to diffuse through into the perfusate in contact with the membrane.

In the experiment, the push method using a peristaltic pump gave higher recovery than the syringe pump method for the higher flow rates. This is probably due to the pulsatile nature of the flow in the peristaltic pump method, giving a greater time for the solution to diffuse through the membrane and collect. However, we would also expect the push-pull system to give a greater recovery than the push system as there should be less loss of perfusate through the membrane. The push system should create a slight flow of perfusate to the external solution due to the slight pressure at the membrane, whereas the push-pull system should have mitigated that by having no net pressure there (with dialysate being sucked out of the probe whilst perfusate is flowed in).

The recovery from the push-pull method seemed to be far lower than the push method across all flow rates tested. This may have been due to a slight imbalance of the two flow rates for push and pull,

which may have caused a slight pressure build-up in the probe. This could have been caused by different levels of wear on the tubing of the pump bed, leading to a slight difference of volume being pumped per revolution. Work will need to be done to optimise the push-pull setup, as it should give more consistent recoveries than the push setup, yet the push method gave recoveries in line with the syringe pump, so this push method was used for the microdialysis analyser. A flow rate of 4 $\mu Lmin^{-1}$ was used moving forward as a compromise of relative recovery to sample to signal time, with a lower flow rate requiring more time for the sample from the microdialysis probe to reach the detector and, if using an on-board power source, would increase the sampling interval and negatively affect battery life requiring more frequent maintenance. This flow rate was also used for the ultrafiltration probe to keep consistency in heater time between the two sampling techniques.

For microdialysis probes with a higher MWCO the push method would be unfeasible as more perfusate would be lost each pump revolution as there would be less resistance against the backpressure of the rest of the microfluidic system. As we were dealing with small molecules instead of proteins, this was not an issue.

3.2.4 Integration of the Field Deployable Analyser

The lab-based system was then modified to be used in the field. Several changes were made to the design of the sensor, with the sensor then being placed into a waterproof box.

For the field deployments, the flow cell was housed inside the heater unit to prevent fluctuations with temperature as well as stray light. SD card storage (Kingston Technology) was implemented, which would save a file after each sampling event, and a timer (DC 12V-16A, Camway) was added to allow for the system to turn on and off periodically to allow for easier control of intermittent sampling. A liquid cartridge was 3D-printed to hold the aluminium-lined bags containing Griess+ Reagent, Milli-Q purified water, FC-40 and the waste from the analyser. A battery (EL12.8-24, Groves Batteries) was used to power the system (). The system was stored in a waterproof casing (IP 66, Uriarte Safybox, Spain). The sampling probes and moisture sensor in the soil were connected to the system through a waterproof cable gland (RS, UK).

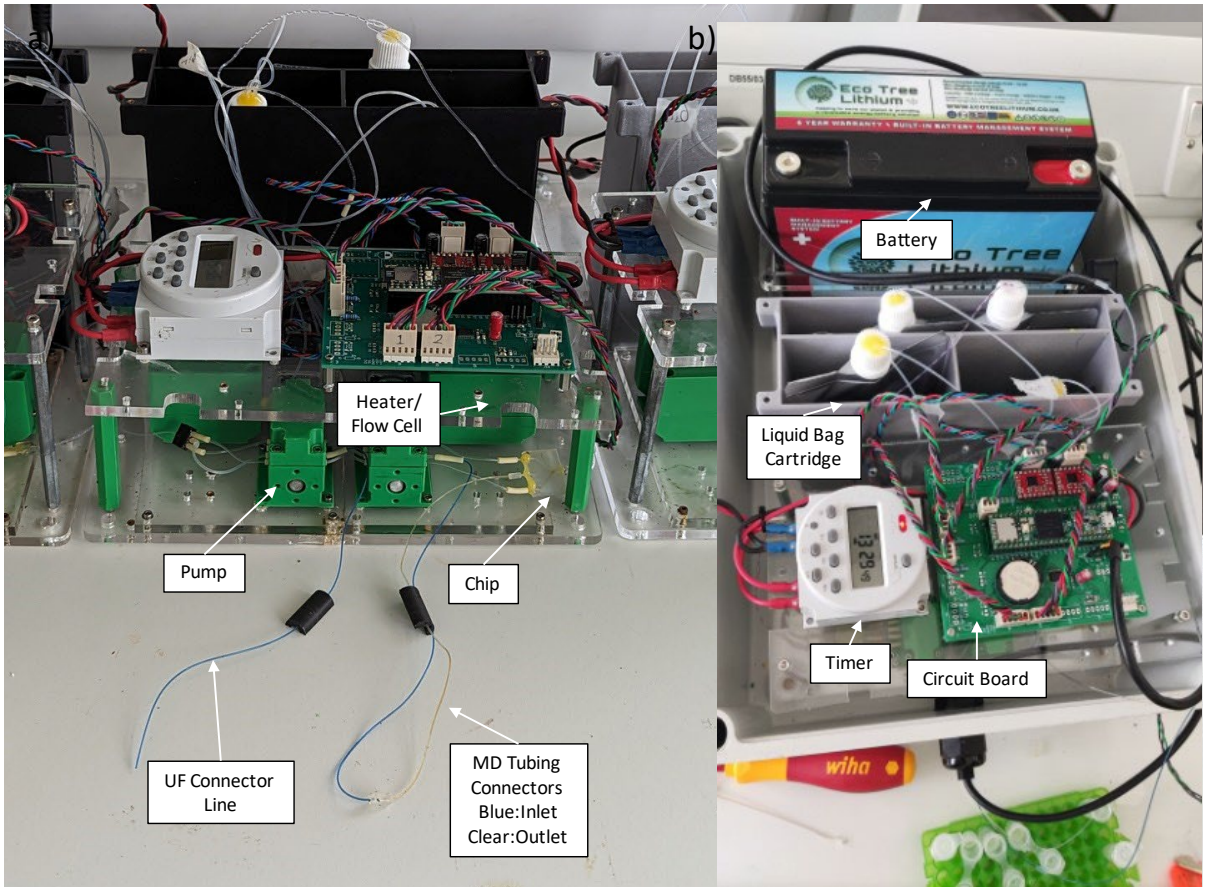

Figure 22 Later prototypes of the Soil Nitrate Analyser for field deployment. a) Outside of the box, one analyser with tubing for one ultrafiltration system (left-hand side) and one microdialysis system (Right hand side) b) Overview of a complete system, with liquid bags and battery.

In the Writtle deployment, soil moisture was evaluated with every measurement to allow for recovery to be calculated. This was calculated onboard the analyser with a capacitive soil moisture sensor (SKU:SEN0308, DFRobot). To calibrate this sensor, it was placed in soil collected from Writtle with different moisture contents (50 to 100%) and left to settle for 5 minutes before a reading was taken. The signal was normalised by using the following equation:

$$Moisture\ reading = \frac{ADC_{Air} - ADC_{Soil}}{ADC_{Air}} \quad (7)$$

Where ADC_{air} is the ADC value given by the sensor when in air and ADC_{Soil} is the ADC value when placed in soil.

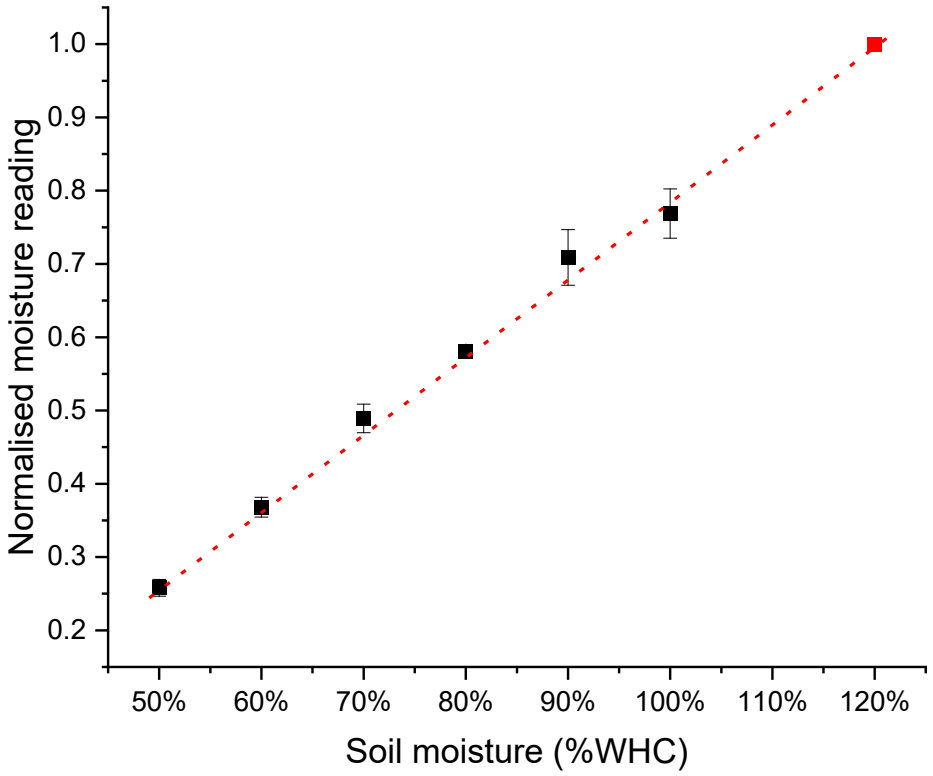

Figure 23 Soil moisture sensor calibration curve, in which the moisture sensor was placed into a centrifuge tube containing soils of different moisture levels. This figure has been directly adapted from (Lu et al, 2024)[133] with permission from ACS, Copyright January 2024.

This soil moisture calibration showed good linearity with soil moisture level (as a percentage of the maximum water holding capacity) so this moisture sensor was used moving forward. Collecting soil moisture data allows us to convert the data from mM to µg NO_3^- /g dry soil

3.3 Results and Discussion

3.3.1 Calibration of Nitrate Analyser

3.3.1.1 Calibration in Solution

The system was tested by inserting the probes into nitrate stock solutions of known concentrations, showing very good calibration curves both with and without dilution (Figure 24).The system without

dilution was used for the field deployments whilst the dilution system was used for the glucose test (Chapter 3.3.3) due to the high nitrate levels present in the soil. The method without dilution gave an LOD of 2 µM, which was calculated using the 3-sigma method: This increased to 99 µM in the dilution system., given by the formula:

$$Limit\ of\ Detection\ (LOD) = \frac{3.3 \times \sigma}{S} \tag{8}$$

Where σ is the standard deviation in the blank absorbance and S is the gradient of the calibration slope.

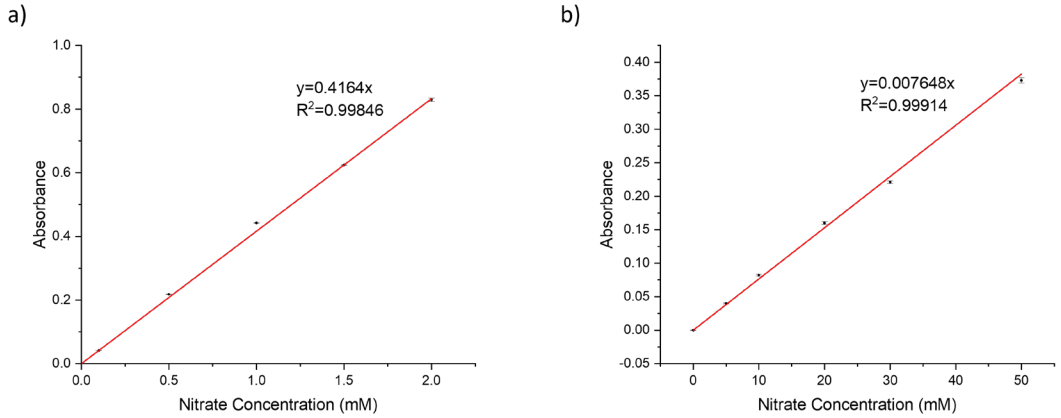

Figure 24 Calibration of the Nitrate analyser both with a) without dilution (1:1 Sample:Griess Reagent) and b) with dilution (1:2:2 Sample:Reagent:Milli-Q). This figure has been adapted from (Lu et al, 2024)[133] with permission from ACS, Copyright January 2024.

A perfusate flow rate of 4 µLmin^{-1} was used for the MD probe, which was kept consistent with the suction rate of the ultrafiltration probe. The droplets were heated for 3 minutes at 40 ^{o}C before being passed to the detector. This drop in temperature was used to increase the concentration range compared to previous studies[95], giving good linearity to 10 mM. Whilst the reaction would not go to completion the consistent pumping strategy would provide a consistent heating time, meaning with calibration it can be used. The ultrafiltration probe was used as a baseline from which the relative recovery of the MD probe was derived, which was found to be from 45 to 50% in solution at 4 µLmin^{-1}.

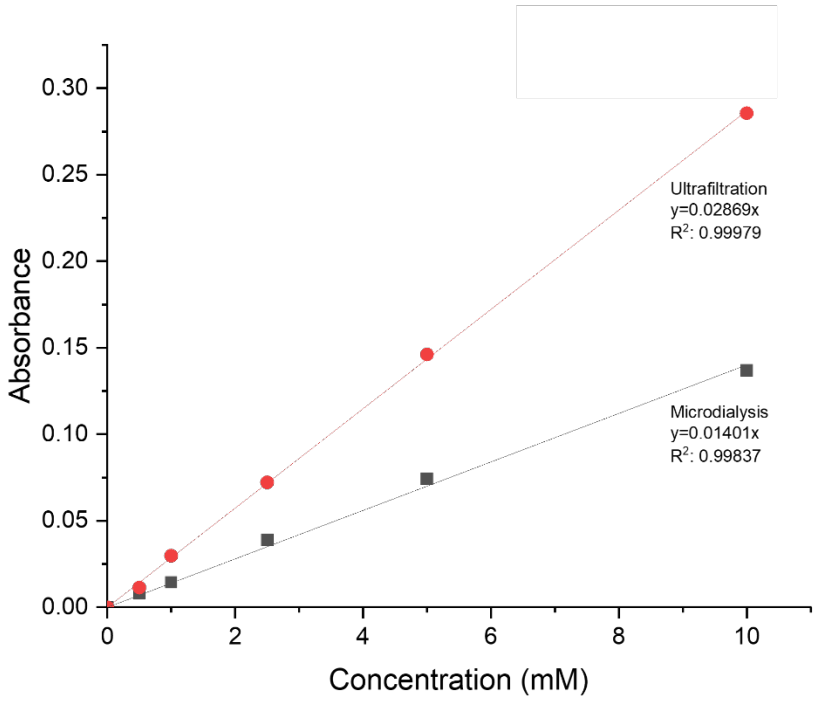

Figure 25 Solution-based Calibration with microdialysis and ultrafiltration, showing the difference in absorbance between the two sampling methods.

3.3.1.2 Calibration in Soil

In order to prevent drift over time, a minimum sampling time needed to be established for using the microdialysis probe intermittently. To do this, a microdialysis probe was inserted into the soil column and was connected to the analyser. The soil column was doped with sodium nitrate and the soil was intermittently sampled at different stop times. From the 1 and 2 hour stop time, a slight downward trend can be observed; through sampling too often, a depletion zone would form around the probe due to nutrients not being able to travel back to the depleted area around the probe quickly enough.

The two types of probe were inserted sideways into several soil columns spiked with different concentrations of sodium nitrate and the system was run, keeping the moisture level consistent between samples to allow for the formation of calibration curves for each moisture level (Figure 27a,b). Both probes showed good linearity across the range of concentrations (0.8 to 20 mM), with R^2 values above 0.99.

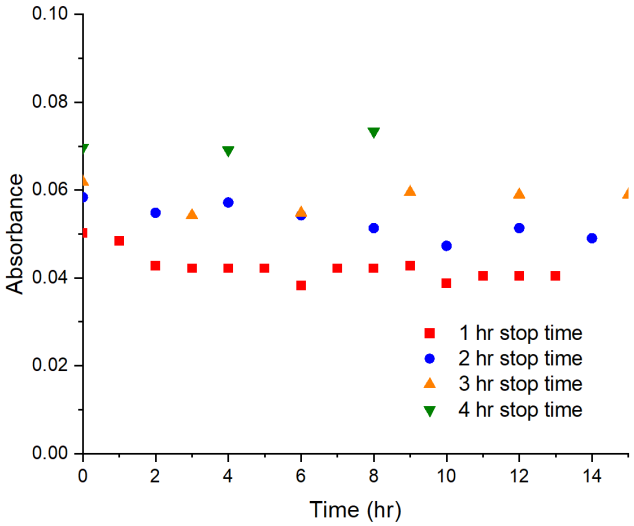

Figure 26 Variation of absorbance with stopping time from a spiked soil, showing how an increased stopping time leads to better recovery

Further tests were then done looking at 6 and 12 hour stopping times, as these would be needed to allow the system to keep running for longer in the field. The moisture level was changed while keeping the concentration of nitrate consistent, allowing for relative recovery curves to be formed for the longer stop times as these were the ones to be used in field deployment. (Figure 27c)

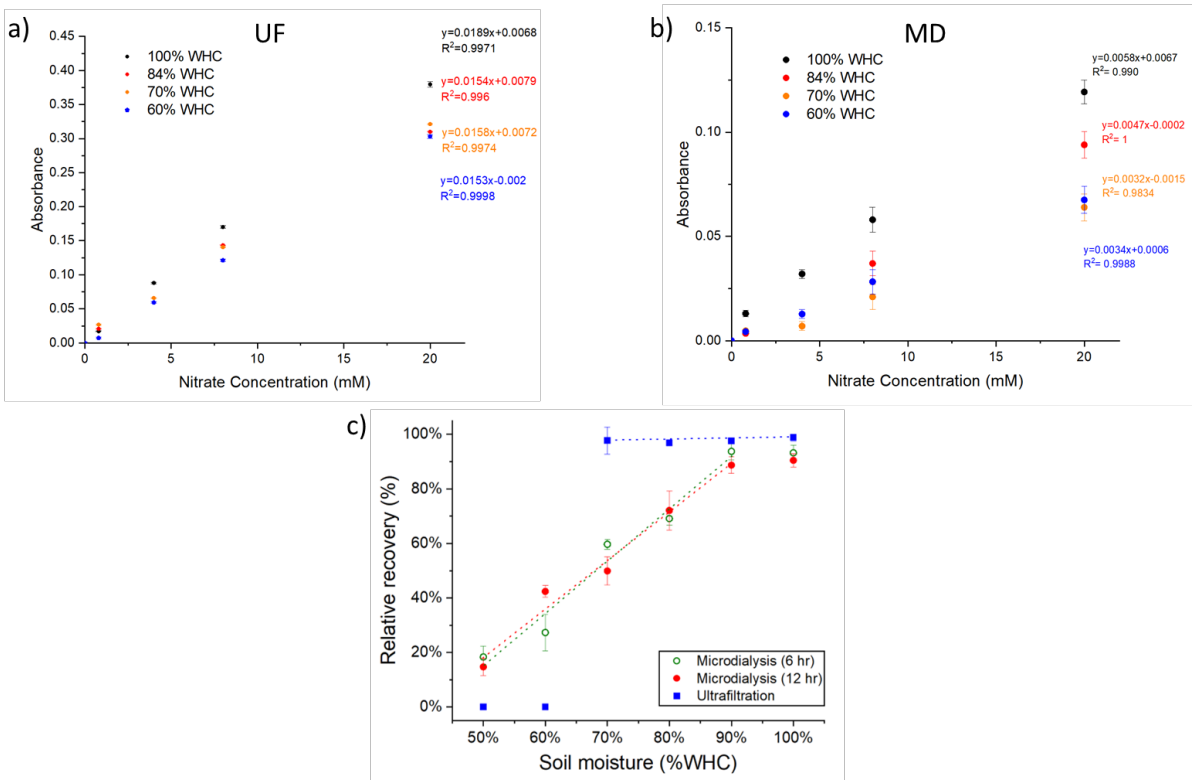

Figure 27 Calibration of NO_3^- standards in soil using both a) ultrafiltration and b) MD at varying moisture contents, with c) a further comparison at lower water holding capacities, including both 6 and 12 hour wait times for microdialysis.

It was hypothesised that there would be a dependence on moisture level for relative recovery with the MD probe, so this was tested during calibration. The signal given by both probes was divided by its equivalent when performing solution-based sampling, giving a relative recovery. In the ultrafiltration sample, there was a steep drop below 60% WHC. This may be caused by the reduction in sample picked up in each droplet, due to the lower moisture content. This may be caused by an increased backpressure, with less of the UF probe surface being wetted, requiring more force to draw up the liquid. These lower moisture levels also caused air bubbles to form in the system (Figure 28)

The gradual decrease in the absorbance for MD is due to the dependency on diffusion as the semipermeable membrane requires solution to be both inside and outside; at lower moisture levels the contact between the probe and the soil is lessened, leading to a drop in signal due to a lower flux. These measurements at lower moisture contents can be useful considering that moisture also affects the bioavailability of nutrients, given that more nutrients will be bound to soil at lower moisture contents.

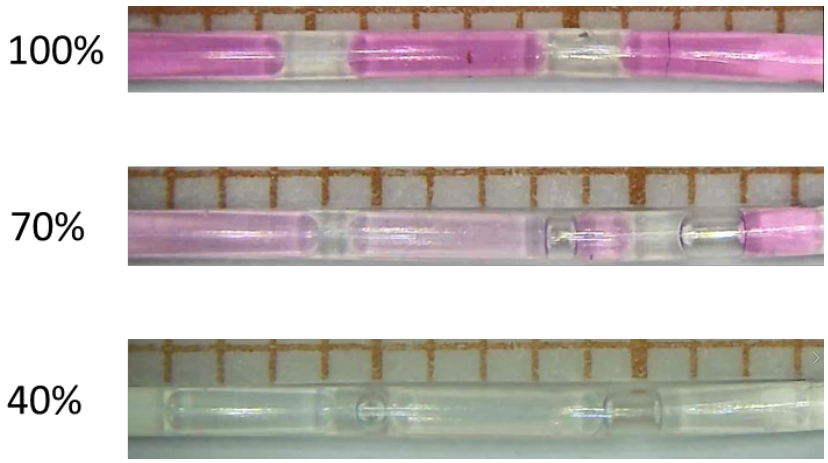

Figure 28 Bubbles observed at lower moisture contents whilst using the ultrafiltration probe, along with a strong decrease in absorbance due to the disruption of droplet formation

Ultrafiltration merely takes up pore water, so whilst there will be a greater inconsistency in results at lower moisture levels (with the inclusion of more air) the value between 60 and 80% is much more consistent. This comes at a cost of taking up water with every measurement, meaning there will be a smaller window before which the area around the probe will dry out.

Using eq. (8), LODs were calculated to be 0.07 µg NO_3^- per g dried soil for the microdialysis method (calculated from the recovery at 100% WHC) and 0.06 µg NO_3^- per g dried soil for ultrafiltration.

3.3.2 Continuous Monitoring

After calibration, continuous monitoring was run on a soil from Bangor with a small particle size (Sieved below 1 mm, moisture at 100% WHC) as well as a high nitrate content (~25 mM). The aim of this experiment was to see if the system could detect short-term changes in nitrate levels. Both probes gave a similar first spike after water was added, after which the concentration appeared to drop. This is consistent with other soils for microdialysis but the trend from the ultrafiltration probe had changed. This may be caused by the nitrate not releasing from the soil, which then recovers after a short period of time as an equilibrium is formed.

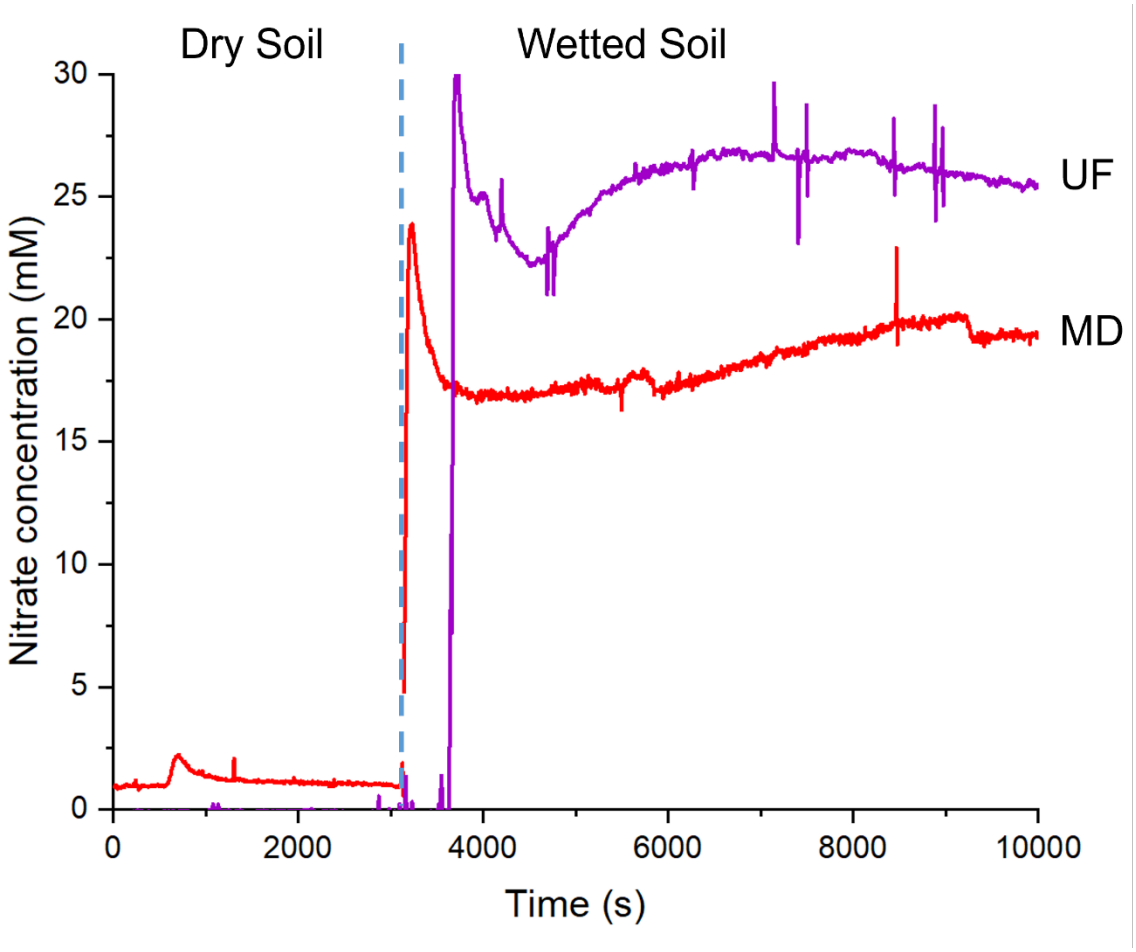

Figure 29 Continuous monitoring performed of a small particle size soil from Bangor with a high nitrate content (Provided by Tiina Roose); The first 5 minutes are with both probes in dry soil, after which it was then wetted to 100% WHC. The drop after the initial rise is due to the formation of depletion zones around the probes (MD: decrease in nitrate ions, UF: decrease in moisture content)

As both probes were inserted into the same soil column, you would expect the wetting to become apparent at the same time. The gap between the two measurement points is due to the difference in tubing between the two probe setups; the tubing connected to the UF probe had a wider inner diameter than the tubing used in MD and the UF sample also had to pass through the pump to get to the chip, which also would make the system longer. The difference in recovery method was also highlighted through the lower concentration for MD.

Continuous monitoring was not possible using both probes in one soil column for a longer period as the soil would dry out due to the rate at which the ultrafiltration probe takes up water. Using this system in a bigger soil sample, or even out in the field, this approach may yet be able to provide

insightful information in the short term regarding the nature of the soil matrix; the flow of nitrate to the MD probe can give an insight into the flux of nitrate around the probe, whilst the uptake from the ultrafiltration probe can give information about the motion of water through the soil, as soils with higher moisture retention will form moisture depletion zones around the probe.

3.3.3 Analysis of Nitrate in Glucose-doped Soil

To analyse the performance in the system, a week-long study was devised involving the addition of glucose to nitrate-doped soil. The presence of glucose should cause a rapid decrease in nitrate after a couple of days as the glucose leads to an increased amount of microbial activity[137, 138].

For the glucose experiments, soil columns were built up in the same manner as before, except for the glucose columns the solution added was made up of glucose (100 mM) and nitrate (Either 30 or 10 mM). This was done in line with Zagal, 1994[138], using a soil mass of 6.70 g and a solution volume of 3.34 mL, affording a glucose concentration around 2500 µg C g^{-1} soil. The test was first run continuously over 5 days and then intermittently for 12 days.

Continuous monitoring was attempted for MD, in which the probe was run over a 5-day period (Figure 30). From previous studies[137, 138] we would expect a sharp drop in nitrate after a few days, yet a significant drop appeared to happen after day 1, after which a gradual decrease was observed. Whilst it still showed there was a significant decrease in nitrate when glucose was added, the continuous drop from the control showed that there were other forces at play. This drop may have been due to the sampling rate; if the flux of the nitrate was slightly higher through the membrane of the probe than it was from the bulk of the soil to the area around the probe, the nitrate would slowly appear to deplete. Whilst useful information about the flux of nitrate in the soil can be picked up from this in

the short term, this would not be very helpful for a long-term sampling study as the absorbance may continue to decrease, reducing the sensitivity of the results gathered.

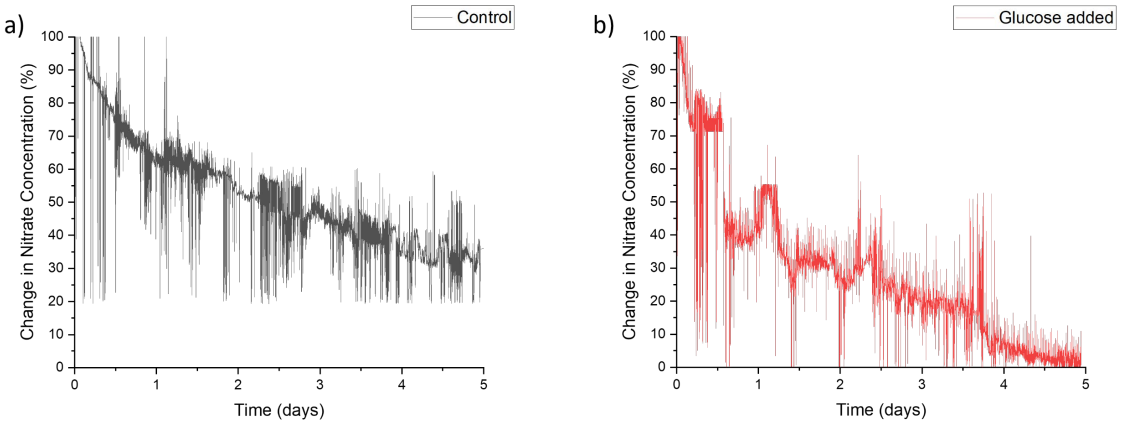

Figure 30 Continuous monitoring of the glucose experiment using microdialysis

Ultrafiltration wasn't used for continuous sampling in-column as the moisture content would change too rapidly. At 4 µLmin^{-1} the ultrafiltration probe would take up 240 µL per hour; at 100% WHC there would only be 3.5 mL and so over the course of a day the probe would deplete the soil of all moisture. If ultrafiltration were to be used for in-field soil sampling, it should be done intermittently to allow the soil to replenish its moisture levels. A much larger sample of soil will need to be used than we use currently if ultrafiltration was to be tested, to prevent a complete depletion of moisture.

To rectify the drop seen from the continuous MD sampling, an intermittent sampling technique was attempted. This would include sampling for a set period of time (e.g. 30 minutes) followed by a stoppage of the pump (e.g. 2 hours) (Figure 26). This was first tested on a soil spiked with 5 mM NO_3^- solution over various stopping times. As expected, the relative recovery increased and the absorbance was more consistent over time than the continuous sampling method, so this was adapted going forward.

3.3.3.1 Redesign of Glucose Test with Intermittent sampling

The glucose test was then repeated with the intermittent sampling technique (Figure 31), which gave a much clearer picture of the trends than the continuous sampling. A gap of 6 hours was chosen to give 4 measurements per day, with a reagent consumption per measurement of only 0.198 mL.

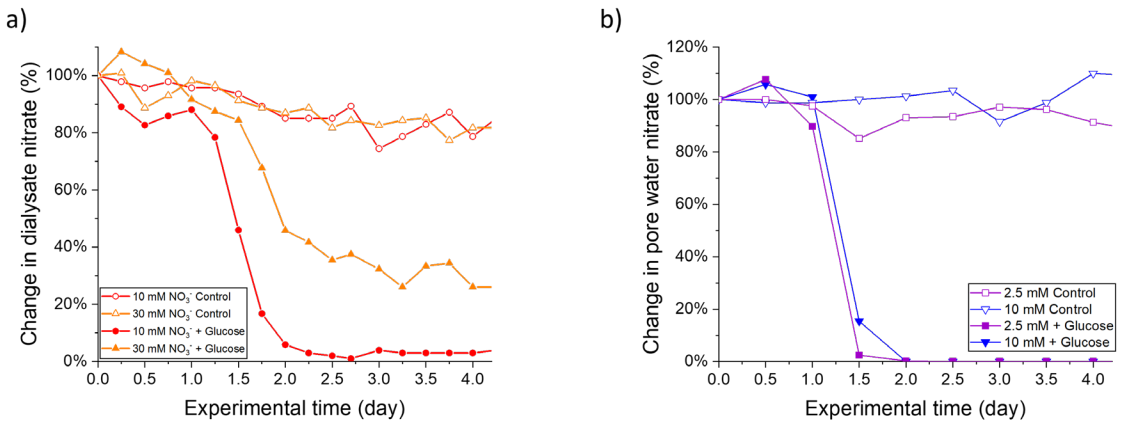

Figure 31 Intermittent sampling of nitrate from soils spiked with glucose using the two different sampling types; a) Microdialysis (Using higher nitrate due to the lower recovery), b) Ultrafiltration.

From the start point of the test, the nitrate level initially increases. This is believed to be caused by nitrate previously bound to the air-dried soil releasing due to the increase moisture. After day 2 there was a sharp decrease in nitrate from both samples, following the trends outlined by previous studies. The 10 mM-spiked sample seemed to deplete of nitrate almost completely after day 2, as the level was not sufficient for the microbes to process before the glucose had been consumed fully, leading to a complete drop in nitrate level. Meanwhile the 30 mM-spiked sample depleted to 25% of its original value, suggesting that the glucose had been consumed fully leading to a decrease in microbial activity.

After this drop in nitrate, previous studies have shown that the nitrate level slowly starts to increase. This increase would be due to "nitrate turnover", in which the biomass formed starts to get mineralised back into inorganic N and nitrate that was previously immobilised in the soil gets released[137]. This didn't seem to occur in this test, and it may be due to the moisture content we used. The previous studies used 70% WHC whilst this study used 100% WHC. Azam et al[137] suggests that at higher moisture contents the nitrate mineralisation rate may be slowed due to a drop in aerobic activity, meaning that when the organic source is added less of the nitrate is immobilised, making it more available to be converted into biomass. As it takes longer for biomass to be remineralised than it does for it to be released from the soil, it may take far longer for an increase in nitrate to be observed. This test could be repeated at lower moisture contents to ascertain whether this is the cause of the apparent lack of nitrate turnover or if it is an issue with the setup of the system itself.

The overall downward trend in the soil control tests could have been attributed to the degradation of the Griess+ Reagent. With time the VCl_3 in the reagent will slowly decompose, leading to slower

reaction kinetics. In the river sensor[95], the reaction was performed at 65 ^{o}C for 7 minutes, whilst the reaction takes place at 40 ^{o}C for 3 minutes in this study. These conditions were chosen to increase the measurable range at the expense of sensitivity as the previous sensor would only be able to analyse up to ~2 mM, whilst the range of concentrations in the Writtle forest soil can go from below 100 uM to 20 mM. An end-point calibration was done to take the degradation into account, in which the value of a particular concentration is measured at the start and end of the experiment. However, due to the short timescale of the experiment it is unlikely to be due to degradation in reagent, which has shown very little drift over 3-day periods. This drop at higher concentrations could be more attributed to a slight microbial uptake by the soil, given that it happened on the same timescale as the drop for the glucose experiments, and could have been due to organic matter already present in the soil..

Measuring this large range of concentrations may require the development of a dilution system, possibly incorporating a second pump to allow for dilution of the sample before it enters the droplet. This pre-droplet dilution would prevent the decrease in signal with the degradation of VCl_3 but will require careful construction to keep flow rates consistent during the running of the system.

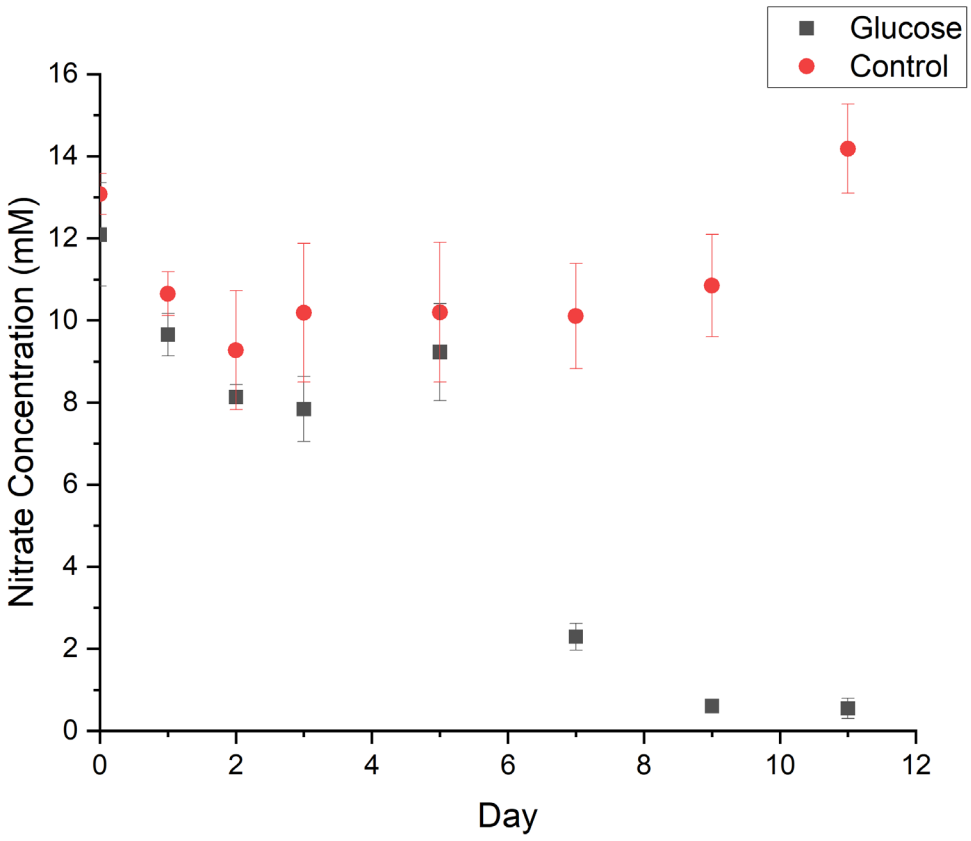

Figure 32 Plate reader analysis of 10 mM Glucose test. High points at beginning and end (Day 0, Day 11) are believed to be caused by uneven heating of the well plate during analysis as these wells were situated around the edge of the well plate.

Destructive sampling performed alongside the MD test was analysed via a plate reader (Heated at 65 ^{o}C, 7 minutes). This showed a trend in the control that was suggested to be due to uneven heating of the well plate (Figure 32), suggesting that the well plate needs to be heated before the reagent is added. Outside of the results at the beginning and end of the test (caused by this uneven heating), the trends found via the well plate method seemed to agree with that found in the MD method, with a sharp decline in nitrate between days 3 and 6. This was later than the MD results showed, which could be due to the greater aerobic activity as the destructive sampling was performed on the top of the column whereas the probes were installed below the surface.

3.3.4 Nitrate Analyser Field Deployments

The nitrate analyser deployments were carried out at two different locations. The first deployment was carried out next to a river on the Highfield campus of the University of Southampton. This site was chosen as the water content of the soil was likely to remain more consistent, being close to or over the water holding capacity. The sensor deployed here was equipped with an ultrafiltration probe (due to the constant high water content) and a microdialysis probe. The analyser ran for 30 minutes 4 times a day, with a 6 hour gap inbetween for a period of 12 days. Each measurement consumed approx. 96 µL of reagent and consumed 16.2 kJ, giving an intermittent running time of 15 days at 4 measurements per day or 30 days at 2 measurements per day.

3.3.4.1 Highfield Campus Deployment

As a preliminary test an analyser was deployed on Highfield Campus (Southampton, UK) with manual nitrate spikes to observe change. The site was next to a river to ensure a high moisture content throughout the sampling period. As expected, the attached soil moisture sensor plateaued at its maximum value and did not change throughout this deployment. The analyser was programmed to run with a 6 hour interval, giving 4 measurements per day. Spiking was performed by adding standard nitrate solutions (1 mM on day 2 and 2 mM on day 7) over the area monitored by the probe, used to mimic fast-release mineral nitrate fertilisation.

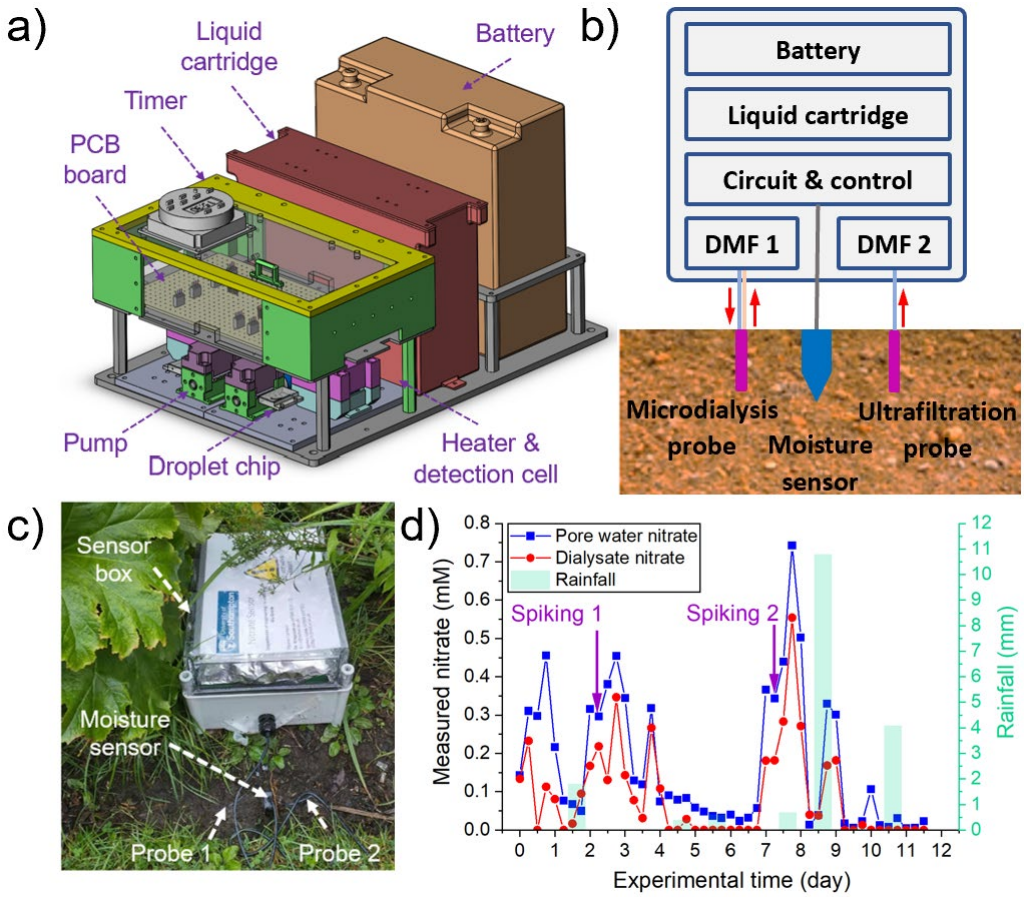

Figure 33 Initial campus deployment of nitrate analyser. a) 3D schematic of the analyser. b) Overall schematic of the system, outlining the insertion of the probes and moisture sensor into the soil. c) Photo of the deployed sensor next to the campus stream. d) Graph displaying the change in pore water nitrate (Ultrafiltration, blue squares) and dialysate nitrate (Microdialysis, red circles) over the sampling period. Rainfall data (green columns) was obtained from a local weather station. This figure has been directly adapted from (Lu et al, 2024)[133] with permission from ACS, Copyright January 2024.

Both modes of sampling were able to capture similar trends, showing good responses to spiking. Initial levels of nitrate were found to be low in the soil (0.15 mM for pore water nitrate, 0.13 mM for dialysate nitrate). The spiking events (1 mM nitrate on day 2, 2 mM nitrate on day 7) were observed in the analyser data, showing concentrations of 0.45 mM and 0.35 mM for ultrafiltration and microdialysis respectively on day 2 and 0.74 mM and 0.55 mM on day 7. After each spiking event, the measured nitrate dropped significantly, indicating nitrate leaching (potentially due to the very high moisture content) alongside potential uptake from the nearby plants or denitrification.

Over the 12 day deployment period, 47 measurements were collected with no maintenance required. The analyser worked well in showing trends in line with both spiking and rainfall events. No air bubbles were seen in the ultrafiltration data and no depletion between measurements was observed for the microdialysis sensor, yet these were probably helped by the high moisture content of the analysed soil. Still, this test was an important first step in testing the analyser's field deployment capabilities in being robust enough to monitor spikes in soil nitrate with high rainfall events.

3.3.4.2 Writtle Forest Deployment

Following the campus deployment, two analysers were deployed in Stoneymore Wood, situated in the Writtle Forest in Essex. This location was chosen as it had trees with various levels of oak decline, ranging from healthy trees to those with acute oak decline (AOD) and chronic oak decline (COD). The analysers were placed approximately 1.5 m from the base of each tree and were fitted with 2 microdialysis probes per analyser. The analysers were set to run twice per day, at 8 am and 8 pm. Due to the dry summer period of July-August 2022, ultrafiltration probes were not used as the lack of soil moisture could have led to less meaningful data.

A comparison was done to observe the difference of installation methods of the microdialysis probes into the soil. For each probe, the top surface of soil (approx.. 10 cm) was cleared away before installation. For each analyser, one microdialysis probe was then making a rectangular groove on the soil big enough for the end of the probe to fit into (10x3x3 cm). The probe was then placed into the groove and the topsoil was then replaced and lightly compressed to improve probe-soil contact. The other probe was installed by punching a hole in the soil with a needle and then placing the tip of the probe into the hole using a plastic sheath (provided with the CMA microdialysis probes) to prevent damaging the probe. The plastic sheath is designed to split and be removed after insertion, after which the surrounding soil was lightly compressed to improve soil-probe contact. Probes from the same unit were placed approximately 10 cm from each other to prevent interaction between each other through depletion zone formation (Figure 34).

Figure 34 Installation of the microdialysis probes into the soil at Writtle using the two different methods.

The analysers were calibrated on-site each month through the connection of a PTFE tube filled with a standard of a known nitrate concentration between the inlet and outlet holes used for the microdialysis probe. Maintenance was carried out each month in which the battery and liquid bags containing Griess+ reagent, FC-40, and waste were replaced. The analysers were calibrated before and after this maintenance to account for any degradation in Griess reagent over the sampling period, yet these calibrations were normally similar (maximum 4.7% variation in calibrations over the deployment), showing the robustness of droplet generation and heating.

The lab analysis samples at Writtle were collected and analysed by Selva Dandaphani (University of Reading) through collecting soil around the same tree at the depth of the probes (50-100 g). 40 g of this soil was mixed with KCl solution(1 M, 200 mL). This was then shaken for an hour and gravity filtered through GF/A filter paper. The filtrate was then analysed using a Skalar wet chemistry analyser (Skalar Analytical B.V., Netherlands). Nitrate present was first reduced to nitrite through reduction by hydrazinium sulfate before being analysed together with nitrite through the Griess assay, measured at 540 nm.

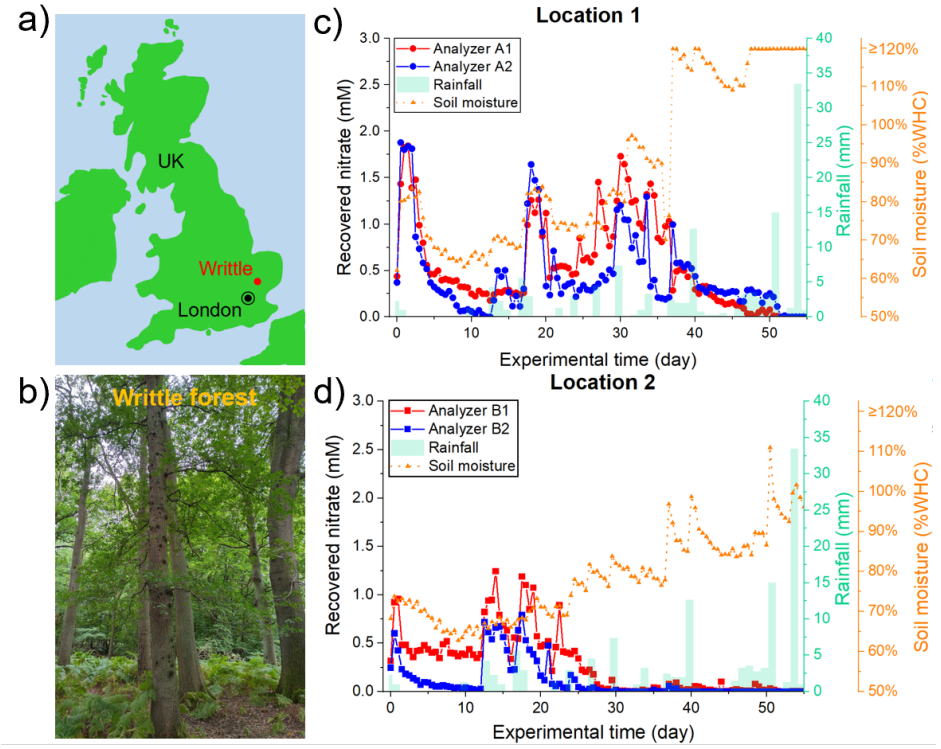

Figure 35 Field deployment in Writtle Forest. a) UK map showing the deployment location, in Essex. b) Photogrqaph of the deployment location, with oak trees with varying levels of oak decline. c,d) Recorded dialysate nitrate over the deployment, with soil moisture obtained from an on-board moisture sensor and rainfall data recorded by a local weather station. Deployment duration was from 14/09/2022 to 15/11/2022. This figure has been directly adapted from (Lu et al, 2024)[133] with permission from ACS, Copyright January 2024.

Over the deployment period, the data from both units from each of the analysers was quantitatively consistent. At location 1, Analyser A1 and A2 both showed peaks of nitrate in line with rainfall events (Figure 35c). Slight differences in values between the two probes would be due to soil-probe contact, due to their different installation methods. At both locations the soil moisture level increased over the sampling period. Towards the end of the deployment, both units gave very low nitrate levels, which could be due to dilution and leaching of nitrate out of the soil with the high level of rainfall.

Using the soil moisture data and the moisture calibration study earlier (Figure 27c), recovered nitrate ($C_{dialysate}$, mM) was converted to absolute soil nitrate (C_{soil}, µg NO_3^-/g dried soil, Figure 36) using the following equation[45]:

$$C_{soil} = \frac{(C_{dialysate}\ or\ C_{pore})}{R_{soil}} \times M_r \times W_{soil} \quad (9)$$

Where R_{soil} is the soil moisture dependent recovery, representing the proportion of nitrate to the external nitrate in the soil pore water, M_r is the molecular weight of nitrate (62.0049 g/mol) and W_{soil} is the moisture content (%WHC).

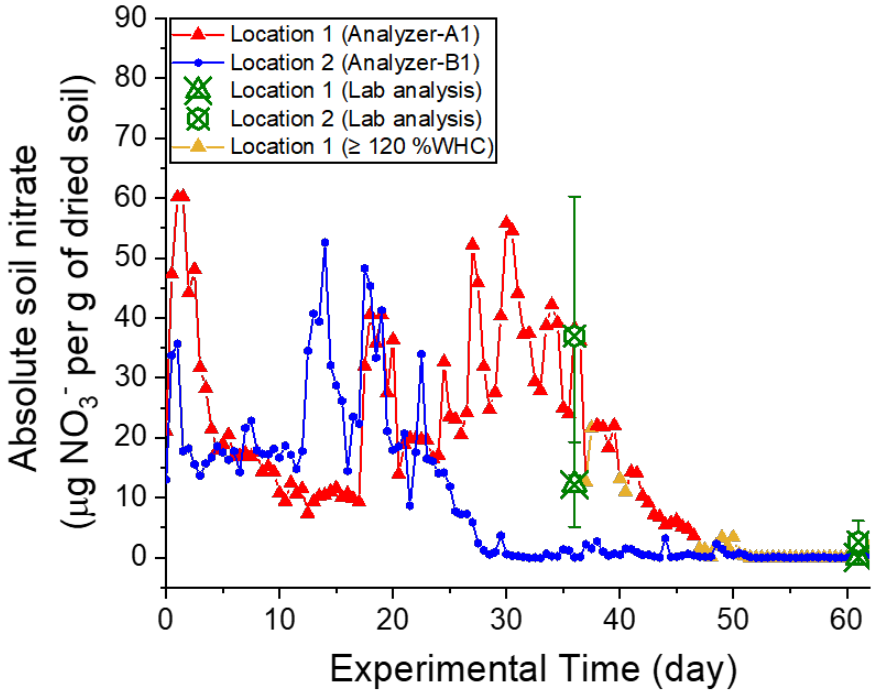

Figure 36 Estimation of absolute soil nitrate at the probe, calculated from corresponding soil moisture-dependent recovery and dialysate nitrate, compared to grab samples over an extended period, from September 2022 to November 2022. This figure has been directly adapted from (Lu et al, 2024)[133] with permission from ACS, Copyright January 2024.

The data collected from the analysers shows a highly dynamic change in nitrate from both locations, with similar reduction is soil nitrate being found by other studies from September to November[139]. The deployment was continued past this period, yet soil nitrate was very low over the winter period in both lab analysis and analyser data. Location 1 had a higher moisture level, with the soil moisture plateauing at its maximum value until April (Figure 37). This high moisture level and low nitrate suggests that significant leaching took place over these months.

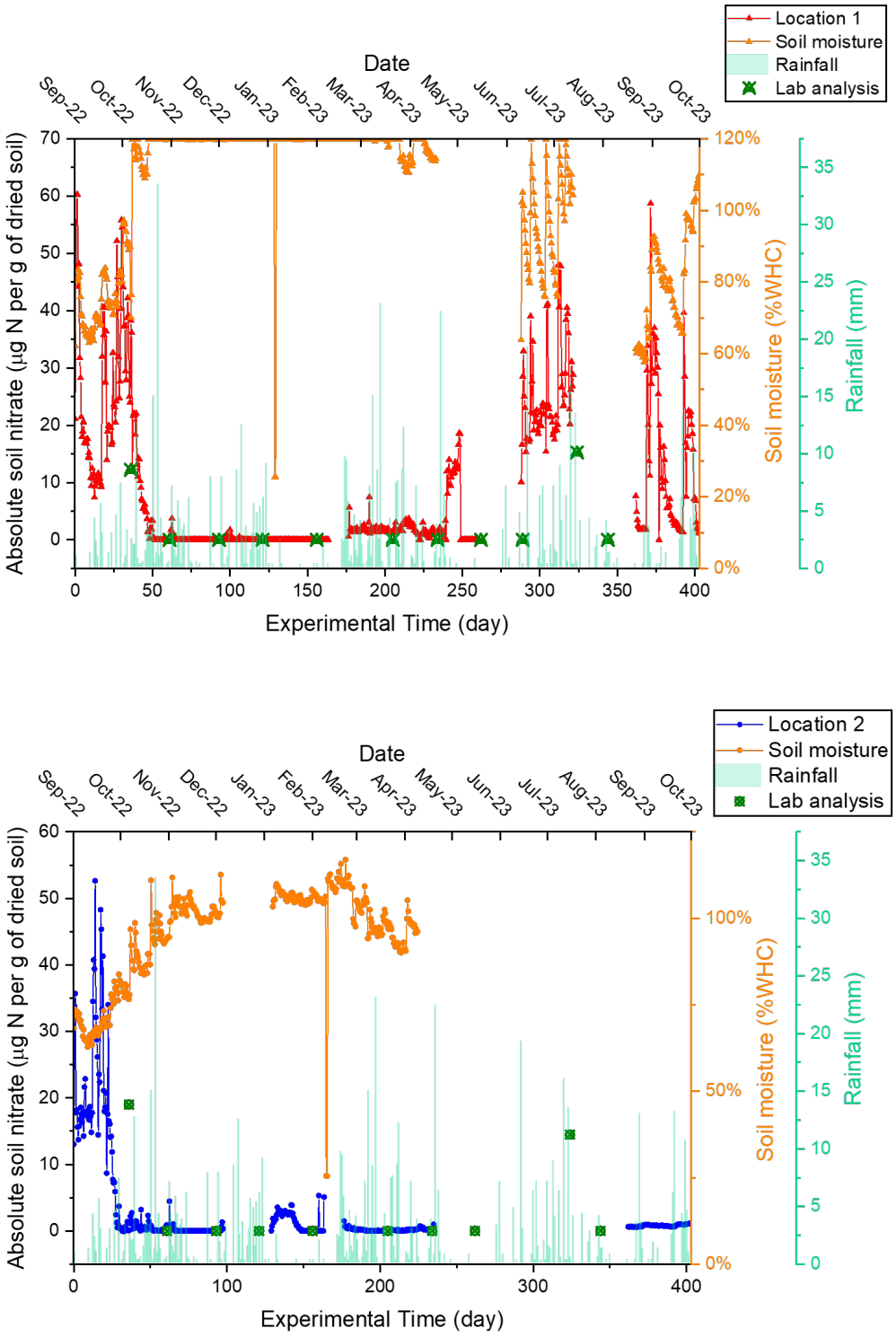

Figure 37 Extended deployment period for Writtle, showing the low nitrate level from November 2022 to June 2023. Data from day 240 was missing due to the sensor being taken away for maintenance.

3.4 Conclusion

In conclusion, a nitrate analyser for use in soil environments was developed, using microdialysis or ultrafiltration probes to give stable and accurate data, with the ability to monitor changes in soil nitrate with either sampling method. For both sampling methods, calibrations were performed in both water and soil and calibration curves were obtained at a range of soil moistures, showing good linearity. For water, an LOD of 2 µM was achieved, whilst LODs of 0.07 µg NO_3^- per g dried soil for microdialysis (at 100% WHC) and 0.06 µg NO_3^- per g dried soil for ultrafiltration were achieved. Using organic material (Glucose) to increase microbial activity, dynamic changes in soil were captured using both methods, whilst showing capability for the addition of dilution lines to capture high concentration (up to 20 mM when using the dilution line), showing good prospects for field deployment.The soil analyser was then packaged into a waterproof container with an on-board power source and was deployed in two locations; first on campus for a two week deployment then a second in the Writtle forest for a year-long deployment. Overall, the two deployments showed the analyser was able to respond to dynamic changes in soil nitrate, in line with grab samples. Both probes had their benefits, with microdialysis providing good data at a wider range of moisture contents (50 to 100 %WHC compared to 70 to 100 %WHC) whilst ultrafiltration gave more consistent data at higher moisture contents. The data was able to be converted from mM to µg NO_3^-/g dried soil through consistent recording of soil moisture around the probe, allowing microdialysis to be used in-situ for an extended period. However, due to the heterogeneous nature of soil and the small sample area analysed by the probe one analyser alone won't be enough to analyse an area; a network of these analysers or using this in conjunction with other sensors will provide a more accurate picture of a larger area's soil nitrate.

Chapter 4 Long Pathlength Detection of Phosphate

In this chapter, improvements in the analysis of phosphate by droplet microfluidic analysers will be improved through a process of oil extraction and long path length detection, combining the mixing benefits of droplet microfluidics and the path length manipulation of continuous microfluidics.

Information in this chapter was published in (Lu et al, 2024)[140] , of which I was a co-author. My contribution was in the fabrication of the paired oil extraction and flow cell units, preparation of reagents and experimental running for calibration for the flow cell units of different path lengths and helping with data analysis of these calibrations.

4.1 Introduction

In comparison to the detection of ammonium and nitrate, the lower levels of phosphate ions present in riverine environments causes a major issue in implementing this into the small path length detectors that we have previously used. When analysing such small levels it is difficult to produce good data with very low absorbance values that come close to the limit of detection.

Many microfluidic colorimetric phosphate sensors incorporate methods to improve the sensitivity to circumvent this, allowing for good sensitivity, such as by using cells with a long geometry (10 to 30 mm in length) or using multi-pass flow cells, in which mirrors placed along the flow channel allow for light to pass through the fluid in the cell multiple times before reaching the detector. These sensitivity increasing methods are difficult to incorporate into droplet microfluidics; with two distinct phases present in the droplet channel (aqueous droplet and carrier fluid), lensing effects due to the different refractive indexes of these fluids prevent many path lengthening techniques.

Z-shaped geometries have been used to good effect in elongating droplets. Yang et al (2017)[141] integrated waveguides in PDMS to focus a laser along very thin tubing which elongated droplets inside it. By only measuring one droplet at a time using this technique, droplets of only 460 pL in size with a path length of 700 µm were able to be analysed. Our group attempted to elongate µL-sized droplets using Z-channels in transparent fluoropolymer chips made of Dyneon[124], showing good success with path lengths of up to 10 mm, as long as the volume of the flow channel was smaller than the droplet to avoid additional lensing effects. The fluorous nature of the chip allowed for the carrier fluid to wet the channel walls without use of surface treatments typically used for typical

microfluidic chips made of PDMS, giving the chips a much longer lifetime (16 weeks with no droplet breakup). However, using this form of droplet elongation would eventually lead to droplet breakup using higher pathlengths due to Rayleigh-Plateau instability[142].

In this experiment, we explore the potential for oil extraction techniques to increase absorbance sensitivity for a droplet microfluidic device. By removing the carrier oil and returning the system to a continuous flow we can combine the long path lengths possible of a continuous microfluidic system with the lack of Taylor dispersion and uniform mixing of droplet microfluidics. To achieve this, path lengths of 5, 10, 15 and 20 mm were tested and the flow cells were used to analyse river samples containing low concentrations of phosphate using a modified phosphomolybdenum blue assay[143], showing the potential for this to be applied to an environmental sensing device.

Oil extraction techniques have been successfully used in the past for MALDI-MS (Pereira, 2013) capillary electrophoresis (Niu, 2013), through using an oleophilic membrane on top of a bed of cotton wool. The carrier oil passes through the membrane and into the wool to take the oil away from the membrane to allow more oil to pass through. This same technique will be used in this device.

Objectives:

1. Develop a paired oil extraction and long path length flow cell to allow for droplet microfluidic devices to use longer path lengths
2. Use the phosphomolybdate blue assay with this platform to analyse real samples for PO_4^{3-} and compare this with lab-based colorimetric analysis

4.2 Materials and Methods

Unless stated otherwise, all chemicals were purchased from Sigma-Aldrich (now Merck), UK. Ultrapure water was obtained from a Milli-Q Direct Water Purification System, with a resistance of 18.2 MΩ (Millipore, Merck). IR-820 Dye was used to characterise the pathlengths of the prepared flow cells by comparison with a UV-Vis spectrophotometer. Solutions of potassium phosphate monobasic (2.5 to 10 µM) were used for calibration with the colorimetric assay. As with previous experiments, the carrier fluid was Fluorinert FC-40 (3M). River water samples were taken from the River Itchen (Southampton, UK) and were analysed on the same day of sampling.

The oil extraction and long path length flow cell was designed and printed by Bingyuan Lu, fabrication and experimental work was done by both myself and Bingyuan Lu.

In the modified phosphomolybdenum blue assay, two reagents were used. Reagent A was a mixture of ammonium molybdate tetrahydrate (4 wt%, 1.042 mL), potassium antimony tartrate hydrate (0.5 wt%, 0.395 mL), sulfuric acid (2.5 M, 3 mL) and ultrapure water (5.564 mL). Reagent B was an ascorbic acid solution (0.1 wt%). The assay ratio was 3:1:1 (Sample to Reagent A to Reagent B). With addition of phosphate sample, phosphomolybdyic acid is formed which is then reduced to a blue product of phosphomolybdenum is produced with a maximum wavelength of 876 nm.

4.2.1 Fabrication of Oil Extraction and Flow Cell

The detection flow cells and T-junction microfluidic chips were designed by Bingyuan Lu and printed using an Elegoo Mars 3. The two halves of the system were printed as shown in Figure 38. To the open channel in a), a PTFE membrane (Whatman) was glued using a thin layer of epoxy (Araldite 2012). Acrylic optical fibres were polished to give flat end surfaces and inserted into the two optical fibre holes in part a), with the end surface in contact with the optical channel. By having the optical channel in contact with the optical fibre instead of slightly set back we were able to better prevent air pockets or pockets of oil that could get past the oil extraction step to build up in the corners. Printing the two pieces in a more transparent material would allow for the optical fibres to be recessed from the flow channel and further prevent this buildup but would also increase the amount of stray light that didn't travel through the flow cell to hit the detector. An IR LED (860 nm, OSRAM) and a photodiode (TSL257-LF, RS Components) were then coupled to the two optical fibres. The oil absorption pad (Cotton wool) was inserted into its groove on part b and the parts A and B were glued together using epoxy. Tubing was then glued to the inlet and outlets (UT7 for the inlet for connection to the droplet microfluidic chip, 0.38 mm PEEK for the outlets).

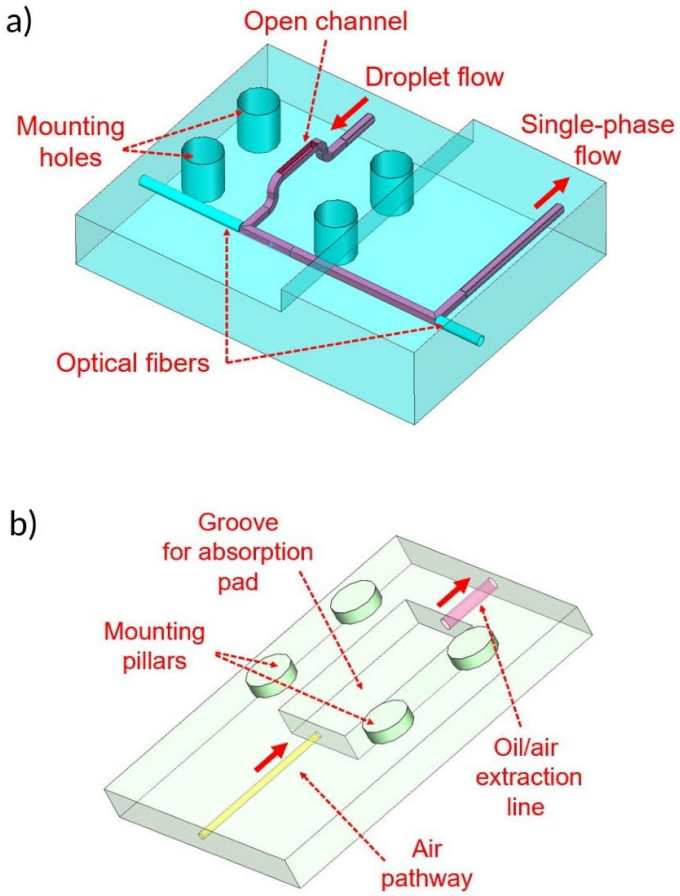

Figure 38 Both 3D-printed halves of the oil extraction and long path length system, which are then glued together by matching the mounting holes and pillars. This figure was directly adapted from (Lu et al, 2024)[140], Copyright Lu, Lunn, Nightingale and Niu, 2024 (CC BY 4.0).

The droplet generation method was the same used in the nitrate analyser (Section 3.2.1.2), except with three aqueous lines instead of two. Before passing into the oil extraction chamber, the absorbance of the droplets was recorded using a UT7 flow cell described earlier (Section 3.2.1.3). A total schematic for the system is shown in Figure 39c.

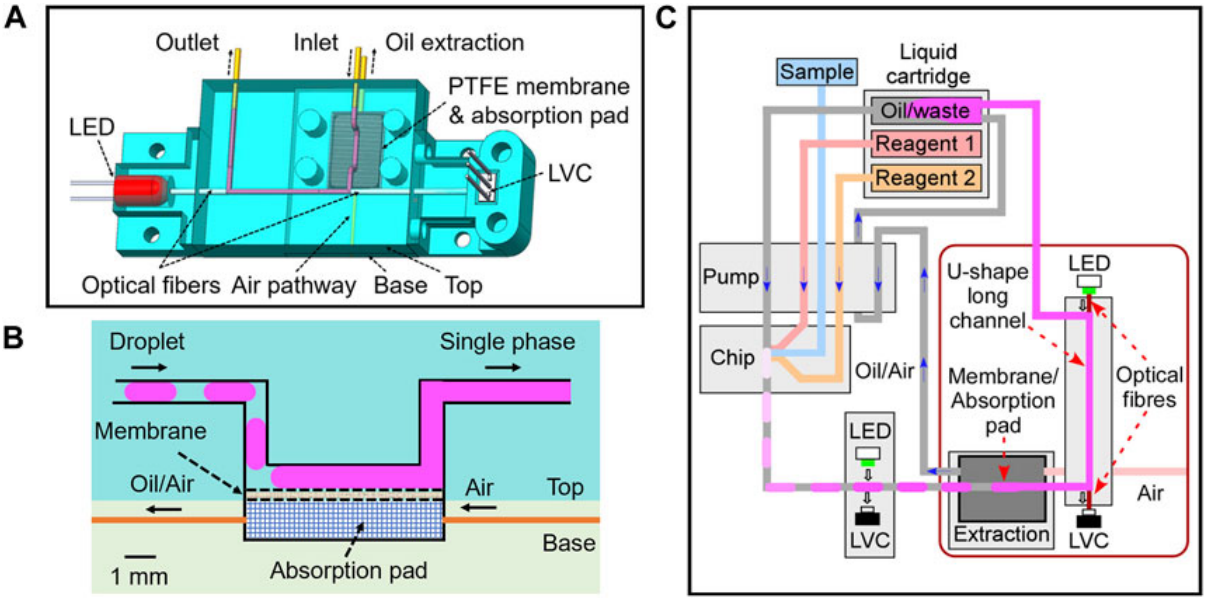

Figure 39 A) 3D design of the oil extraction and long path length detector. B) Schematic of the droplet extraction system, using a PTFE membrane and a cotton wool absorption pad. C) Schematic of the full system. This figure was directly adapted from (Lu et al, 2024)[140] with permission from Frontiers, Copyright May 2024.

4.2.2 Fluid Control

Fluid control was performed using the same peristaltic pump method with 5 lines; the three aqueous phases were 3:1:1 (Sample to Reagent A to Reagent B) whilst the oil inlet and oil extraction lines were in a ratio of 1.5:1.65 to prevent oil from accumulating in the oil extraction pad. A speed of 10 RPM was chosen for the droplet measurements, giving flow rates of 7.2 µL/min for sample, 2.4 µL/min for each reagent, 3.6 µL/min for the oil and 3.85 µL/min for oil extraction. For the continuous phase experiment (in which no carrier oil was used) the aqueous flow rates were increased by increasing the motor speed to 13 RPM to give a similar total flow rate.

4.2.3 Lab-Based Analysis

For comparison with the microfluidic system, a UV-Vis spectrophotometer (Lambda 35, PerkinElmer) was used to analyse the IR-820 dye solutions, phosphate standards and the river samples. The optical pathlength of the spectrophotometer (10 mm) was used as a baseline to evaluate the path lengths of the flow cells using IR Dye, through comparison of the absorbances between the two. To perform the spectrophotometric analysis of phosphate in the standards and river samples, the

sample and reagents were mixed in a 3:1:1 ratio (600 µL of sample and 200 µL of each reagent) in a 1.5 mL Eppendorf and were left at RT for 10 minutes before analysis.

4.3 Results and Discussion

4.3.1 Testing and Calibration

The oil removal system was stress-tested through doubling the flow rate (Pump speed of 20 RPM) and trying to reduce the section exposed to the PTFE membrane from 5 to 2 mm and in both cases the oil extraction performed well, with no FC-40 being detected, which would have caused a significant decrease in intensity through lensing effects or a lower absorbance through the artificially reduced path length. No aqueous solution was observed passing through the oil extraction system, which would have led to droplets of water being observed in the tubing coming out of the oil extraction system. The oil extraction system was continuously run at 10 RPM for 4 days, with no degradation in performance.

The effective path length of the flow cells was evaluated by manually injecting an IR dye solution into each flow cell, comparing the absorbance to that recorded by the UV-Vis spectrophotometer (Figure 40a). The effective path length for the longer flow cells was very close to the expected value with the 20 mm flow cell having an effective path length of 18 mm, with a slight deviation in the 5 mm path length cell in which the effective path length was higher than expected. These could be due to a fabrication error in either the 3D-printing or the placement of the optical fibre.

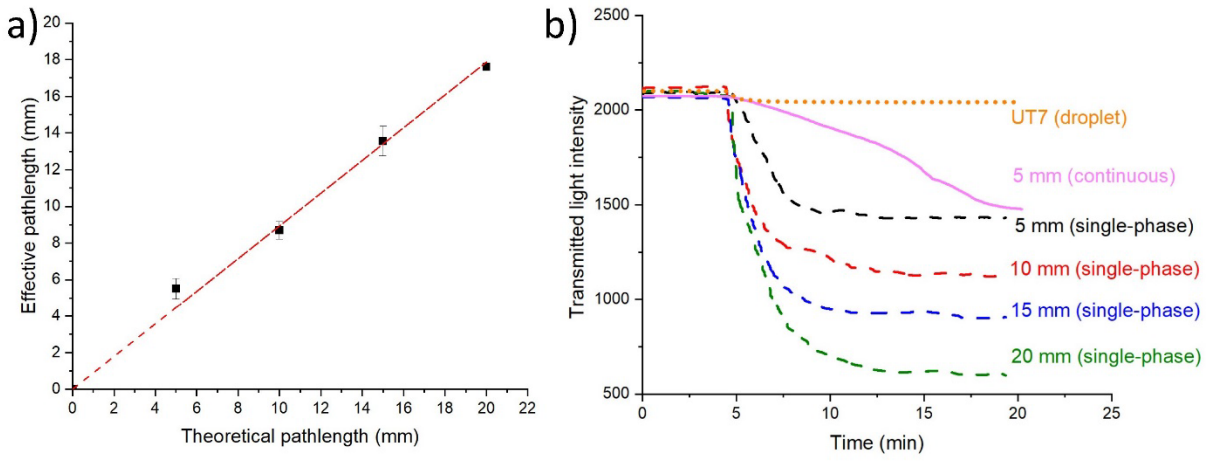

Figure 40 a) Effective pathlength study of the different flow cells, with absorbances compared to that of a spectrophotometer (10 mm pathlength). b) View of the change of intensity from a

blank measurement to an IR dye solution using each flow cell using the oil extraction procedure, compared to that of the UT7 flow cell and just pumping the aqueous phase. This figure was directly adapted from (Lu et al, 2024)[140] with permission from Frontiers, Copyright May 2024.

Each flow cell was then tested through seeing how quickly the different detection cells reached a plateau (Figure 40b). As expected, the shorter flow cells took a shorter time to plateau than the longer ones, with the 5mm flow cell stabilising within 5 minutes whilst the 20 mm flow cell took closer to 10 minutes. This is due to the increased distance in the flow cell, with the blank taking longer to exit the flow cell.

To evaluate the effectiveness of a droplet flow with an oil extraction technique to a continuous microfluidic flow, the 5 mm flow cell was run using both methods. The continuous phase did not reach the same intensity as the droplet extraction cell until after 15 minutes, showing the much greater effect Taylor dispersion has in the continuous flow regime, which can hinder the responsiveness of the flow cell when used in-situ compared to the droplet flow regime. The large extent of the difference is due to the line of UT7 after the flow cell, which takes 10 minutes for the droplets to traverse (to match the timings of the spectrophotometer reading), in which the droplet flow does not undergo Taylor dispersion whilst the continuous flow does. Through having this lower transition time between samples, less sample and reagent can be used per measurement and sample to signal times are significantly lower using this droplet regime.

The flow cells were then tested using phosphate standards, in which standards were combined with the PMB assay reagents in the microfluidic chip to create droplets which then flowed through UT7 tubing for 10 minutes. These droplets were made using the same peristaltic pumping method used before yet using a different roller, creating aqueous droplets with a ratio of 3:1:1 (sample to Reagent A to Reagent B), with a section of carrier oil in-between each droplet as mentioned in 4.2. These droplets passed through the droplet flow cell (Figure 41a. b) then these droplets were merged to create a single-phase flow using the oil extraction section. Figure 41c shows the detection of the single-phase detection in the long path length flow cell, with Figure 41d showing the calibrations for all flow cells, UT7 and the UV spectrometer, which gave a very similar calibration line to the 10 mm flow cell. Using the 3-sigma method described earlier (Chapter 3.3.1.1) LODs were calculated for each flow cell, giving 3.87 µM for the UT7 droplet flow cell, 2.83 µM for 5 mm, 1.37 µM for 10 mm,

0.89 µM for 15 mm and 0.66 µM for 20 mm. The 20 mm flow cell was chosen to be used for river sample analysis due to this lower LOD.

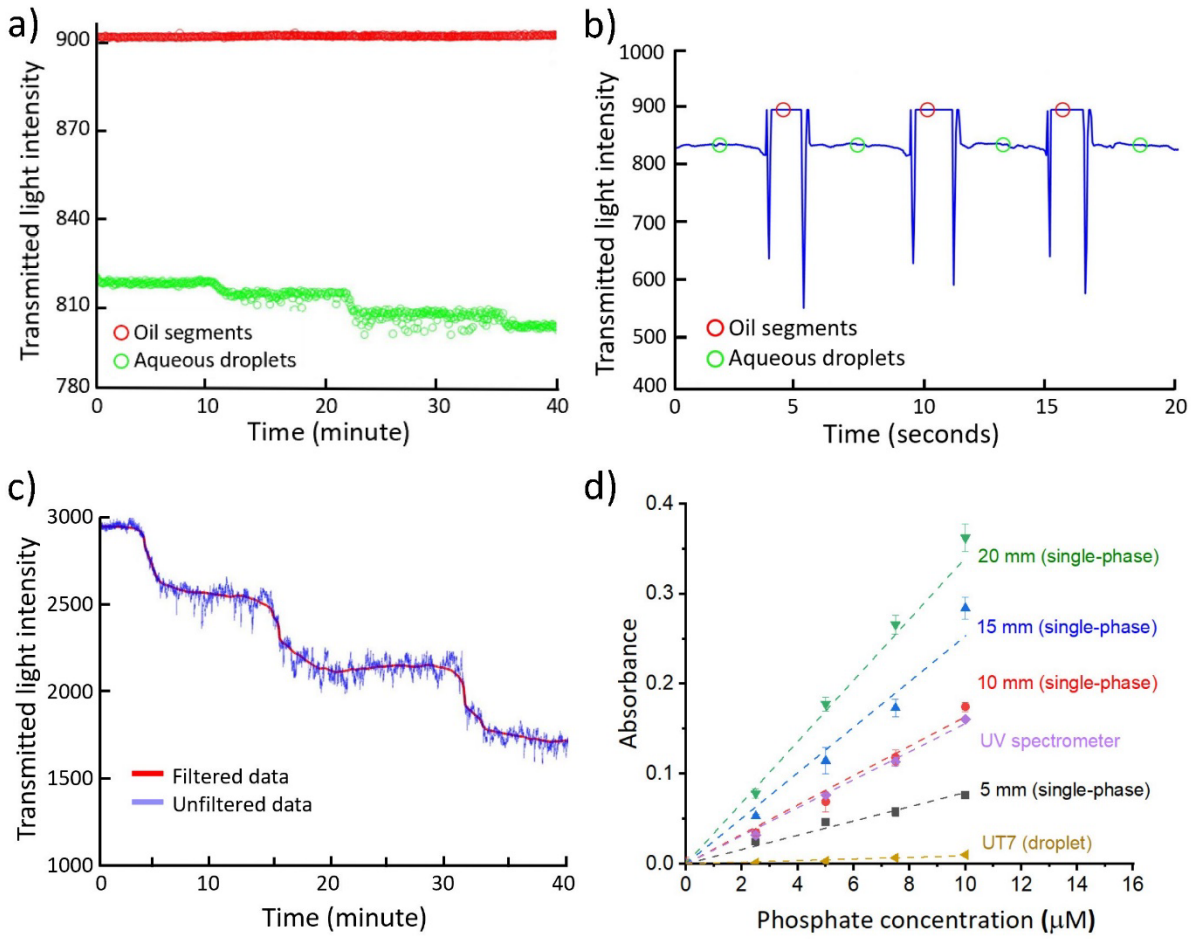

Figure 41 a) Oil and droplets picked up during calibration. b) Zoomed in view, showing the oil and aqueous segments of the raw data, in which the code finds and reports the mean value of the centre of each. c) Filtering of the droplet data through averaging of droplet values to give a smoother plateau. d) Calibrations for each flow cell and the spectrophotometer using the modified PMB assay. This figure was directly adapted from (Lu et al, 2024)[140] with permission from Frontiers, Copyright May 2024.

4.3.2 River Sample Analysis

Samples were obtained from points along the river Itchen (Sample points shown in Figure 42a). This tidal chalk river has had areas designated as Sites of Special Scientific Interest, Special Areas of

Conservation and Special Protection Areas thanks to its mudflat and saltmarsh habitats, being the home of protected species including brent geese and terns, as well as the breeding ground of migratory fish, including salmon and trout. This stretch of river provides useful sampling sites due to the presence of these zones alongside the presence of urban development in the form of a sewage treatment works and maritime industries, as well as fish farming and watercress growing. The river also has the presence of salt water where it meets with Southampton Water, a tidal estuary, giving a wide range of testing sites along a small stretch of river. Samples were collected (50 mL volume) and were passed through a syringe filter before analysis. The filtered samples were pumped in to the system in the same regime used for the calibrations. Using the calibration curve for the 20 mm flow cell in Figure 41d, average values for each sample were collected and plotted against the concentration derived from using the UT7 flow cell and the spectrophotometer (Figure 42b).

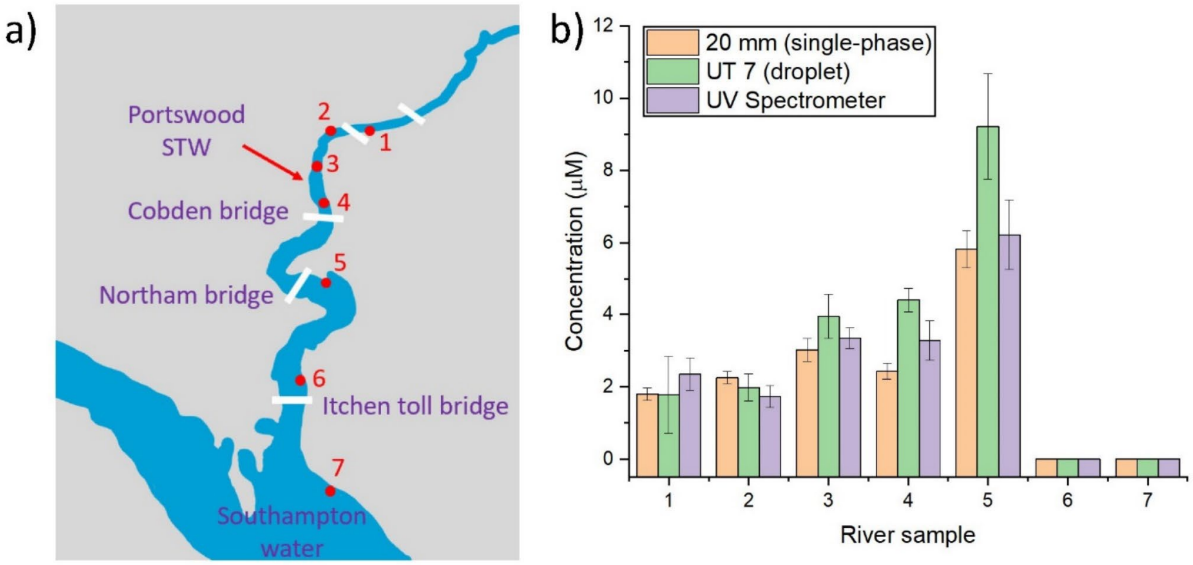

Figure 42 a) Map illustration of where sampling took place. b) Bar chart comparison of 20 mm flow cell, UT7 flow cell (0.7 mm) and UV-Vis spectrophotometer. Each measurement performed in triplicate. This figure was directly adapted from (Lu et al, 2024)[140] with permission from Frontiers, Copyright May 2024.

From sample point 1 to sample point 5, phosphate was detected and gradually increased when going downstream. At points 1 and 2, a level of 2 µM was detected. At points 3 and 4 this increased to 3 µM followed by a significant increase to 6 µM at point 5, placing the final stretch of river as moderate agricultural status (Between 4.5 and 6.9 µM P for a high alkalinity, lowland river[144]). After point 5 no phosphate was detected, which is due to the significant dilution from the saltwater

Southampton Water. An increase in phosphate downstream along this river has been previously observed[145] and has been attributed to anthropogenic input from the STW at Portswood, from which phosphate can migrate downstream and collect around site 5. The UT7 flow cell absorbance deviated significantly at point 5 from both the UV spectrophotometer and 20 mm flow cell whilst the 20 mm one was in good agreement with the spectrophotometer (<1 μM deviation) throughout the experiment, with less error than the UT7 flow cell.

4.4 Conclusion

In conclusion, we developed an oil extraction and long path length flow cell for monitoring UV-Vis absorbance, allowing for droplet microfluidic systems to take advantage of the higher sensitivity afforded by longer path length, significantly reducing the limit of detection to sub-micromolar levels. This system is robust enough to allow for extended monitoring periods (4 days continuous running), producing high quality data in line with that of a benchtop UV-Vis Spectrophotometer, allowing for future in-situ deployments in both wastewater and riverine studies. As with the previous system, this can be used with other colorimetric assays and will have the ability to be retrofitted into other droplet microfluidic absorbance analysers through the addition of one pump line to perform oil extraction. In future experiments, this extraction cell will be used to develop an in-situ phosphate analyser with the ability to monitor low levels of phosphate over significant periods of time.

However, this phosphate analysis technique was not incorporated into further work done in this thesis as the flow cell had significant noise, which was probably caused by the vibrations of the two stepper motors used for pumping, which would require either signal noise processing or damping effects to mitigate. The stability of the oil extraction cell would also need to be tested for longer periods of time before it can be deployed in the field.

Chapter 5 Development of Multinutrient System

In this chapter, a combined flow cell and heater system will be developed for the monitoring of 3 nutrients, ammonium, nitrate, and nitrite simultaneously, allowing for short-term inter-nutrient fluxes to be analysed.

5.1 Introduction

With the successes of measuring a single analyte robustly using our nitrate analyser, we thought to further expand this to multiple analytes through multiplexing. By combining two or three analysers into one system we can greatly increase the utility of the output data. Through analysing multiple nutrients from a single source we greatly reduce the variance in sample to signal delay, which will aid the processing of the data, whilst also reducing the total power consumption and the amount of space needed for deployment. Through analysing multiple forms of N simultaneously, we can investigate how inorganic N is processed from one form to another, which is key in both aquaponic and bioreactor settings. This multinutrient analyser system, once further developed, has the potential to be implemented with control systems to provide autonomous feedback loops.

Objectives:

1. Develop a combined heater/flow cell system allowing for the measurement of 3 colorimetric reactions simultaneously (Griess+ Assay for NO_3^-, Griess Assay for NO_2^-, Salicylate Assay for NH_4^+)
2. Fabricate of a 2-pump system to allow for 10 lines of pumping
3. Create pumping regimes to allow for either continuous or intermittent sampling
4. Benchmark performance of all three assays in both continuous or intermittent sampling modes against standard laboratory assays using water standards

5.2 Materials and Methods

5.2.1 Development of Combined Flow Cell and Heater

Adapting the original flow cell design, a second 540 nm flow cell and a 660 nm flow cell was introduced to allow for nitrate, nitrite, and ammonium to be measured simultaneously. The LEDs were purchased

from RS (660 nm wavelength LED from Kingbright, L-53SRC-C) and the photodiode was from Farnell (Part no.TSL257) . I redesigned the flow cell/heater 3D printed piece used in the nitrate analyser to incorporate 3 flow cells in a single device to allow for the use on only one heater (Figure 43). A recess was made for an aluminium rod (16 mm diameter) which was placed in contact with the existing heater plate to conduct heat. This rod was friction fit into the flow cell through a groove in its base. The UT7 tubing lines were coiled around the aluminium rod to ensure full contact between the heater and the tubing at all points. This unit was then surrounded by thermal insulation and placed in a 3D-printed housing (Tough PLA, Bambu Lab) that was printed on a Bambu X1C. Conditions were chosen to allow for the flow cells to only use one heater to increase efficiency and a temperature of 58 °C was used. With consistent pumping, the NH_4^+ reaction should go to completion with this temperature whilst the NO_3^- will not fully go to completion but will give a consistent result in calibration. The nitrite line would not be affected by temperature as the colour, produced in seconds at room temperature, is stable at this elevated temperature.

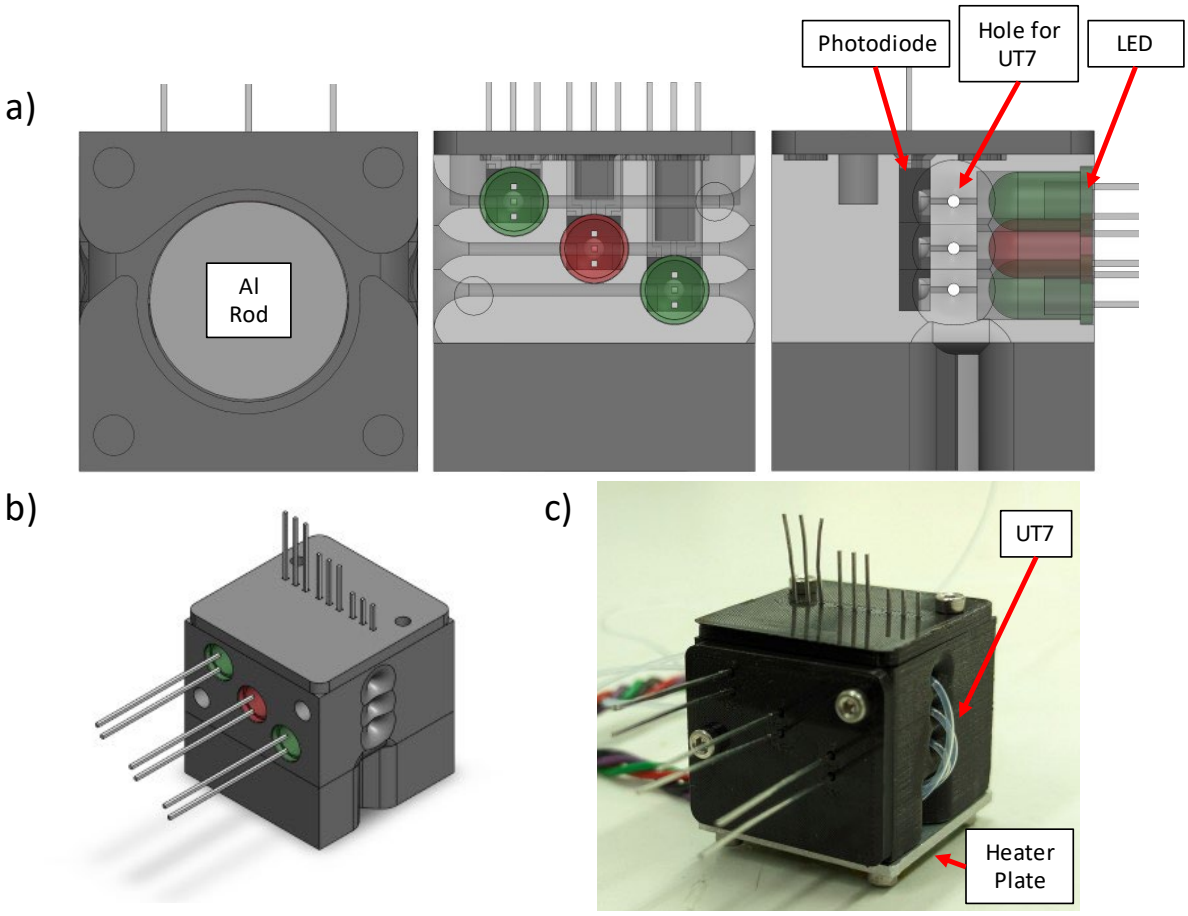

Figure 43 a) Orthographic and b) 3D representation of combined flow cells. Left: view of the metal rod of the heater, which the UT7 tubing from the chips wraps around before looping into

the flow cell. The middle view shows the positioning of the three LEDs and photodiodes and the right view shows the holes through which the UT7 passes through; The green LEDs are for NO_2^- and NO_3^- measurement whilst the red LED is for NH_4^+. c) Mid-fabrication photograph of the flow cell-heater, with cover plated for LED and photodiodes.

5.2.2 Ammonium Procedure

Two reagents are required for the ammonium assay. Salicylate reagent was made by dissolving Sodium Salicylate (13 g), trisodium citrate dihydrate (13 g) and sodium nitroprusside (0.097 g) in 100 mL of Milli-Q water (18.2 MΩ). Sodium dichloroisocyanurate (DIC) reagent was made by dissolving sodium dichloroisocyanurate (0.2 g) and sodium hydroxide (3.2 g) in 100 mL of Milli-Q. both of these reagents were stored in aluminium-lined foil bags and were refrigerated (4 °C) until use.

Griess Reagent for Nitrite quantification was prepared by adding HCl (15 mL, 37%), Sulfanilamide (1.25 g) and NEDD (0.125 g) to Milli-Q. For spectrophotometric detection, a ratio of 10.5:1:1 (Sample:Salicylate:DIC) was used for ammonium detection, whilst a ratio of 1:1 (Sample:Griess) was used for Nitrite detection.

The procedure for ammonium was adapted from our group's previous drybox sensor work[146], using a modified Berthelot assay[147] producing a blue indophenol product. In this reaction () hypochlorite ions are first generated through sodium dichloroisocyanurate in a basic solution (1). These hypochlorite ions then react with ammonia, formed in basic conditions with ammonium present, to form monochloramine (NH_2Cl) (2), which then reacts with salicylate to form 5-aminosalicylate (3). This chemical then can form a resonance structure stabilised by the presence of sodium nitroprusside (4), which can then react with another molecule of 5-amino salicylate to form an indophenol dye (5).

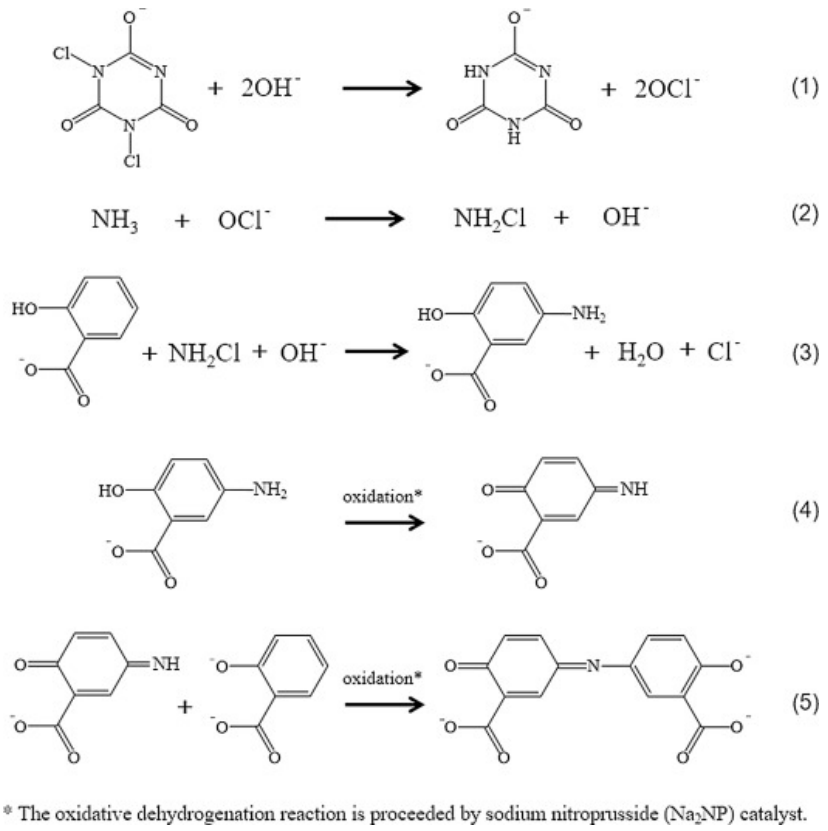

Figure 44 Reaction scheme of the modified Berthelot assay. This figure has been adapted from ref. 147 with permission from Elsevier, copyright March 2018.

For the soil study, a 2-pump system was made; one using 3 lines for nitrate and one using 4 for ammonium. Previously used metal rollers were used for the nitrate system whilst ammonium rollers were fabricated from Tough PLA using an Ultimaker 3. The notches in this roller were sufficient to make a 3:1:1 Sample:Salicylate:DIC droplet. To facilitate the difference in ratio, the ammonium reagents were diluted with Milli-Q to compensate.

Both pumps fed into separate microfluidic chips and after droplet formation both UT7 lines were fed into the single heater-flow cell unit, with the UT7 threading around the aluminium rod several times (depending on RPM of the pump, length of the droplet and reaction time with each turn of UT7 around the 18 mm rod having approx. 50 mm in circumference) before being threaded into two of the three flow cells. With a pump speed of 10 RPM, 2 full turns are needed for the nitrate line and 5 full turns are needed for ammonium for a reaction time of 4 and 5 minutes respectively.

5.2.3 Development of Ammonium, Nitrate and Nitrite Analyser

Design for the stainless steel frame and the acrylic base was done by José Fabelo Morales, electronics were made by Ken Yeung, microfluidic components (Pump, Chips) were designed by Bingyuan Lu and Liam Carter, with modifications by myself and José Fabelo Morales to modify the pump design (pump head and roller) to accommodate 5 lines.

Capturing the three micronutrients at once led to a change in pump configuration; instead of each nutrient and chip being connected to a separate pump, the number of lines for each pump was increased from 4 to 5. This allowed for two pumps to run the three nutrients, with one chip straddling both pumps (). This pump system also had a change in how pressure was applied to the pump bed. Earlier systems used 4 screws to fix the pump bed in place, but this new technique used a hinge-based approach with a lock to fix the pump beds in place (a). This allowed for much easier removal of pump beds to allow for much quicker maintenance of the system and will later be used to develop a liquid cartridge-style system where either the liquid bags can be easily removed and quickly replaced or for the potential to easily swap the microfluidic system for another one during maintenance without having to move the sampling line. With two 5-line pumps, stable droplet generation was able to be achieved.

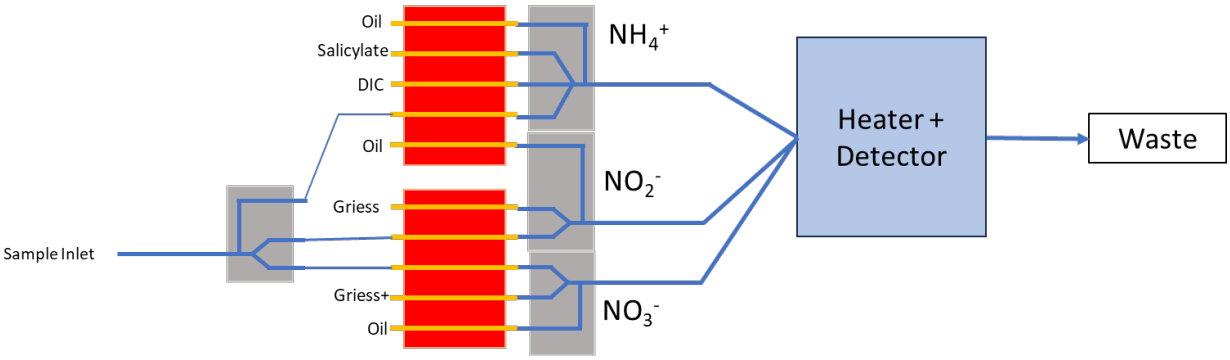

Figure 45 Microfluidic schematic of the pumping regime for the multinutrient analyser, using two 5-line peristaltic pumps run in tandem.

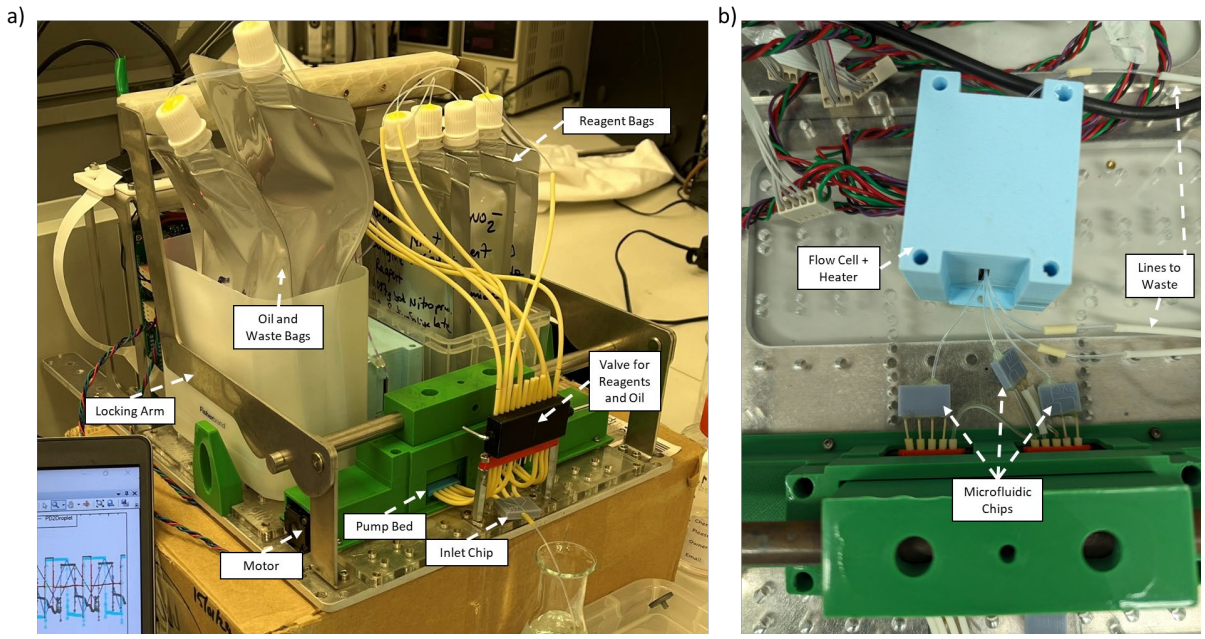

Figure 46 Images of the multinutrient analyser without its enclosure. a) A view of the whole analyser, showing its locking arm mechanism to hold down a stainless-steel bar in place to hold down the pump beds. b) A close-up of the microfluidic chip layout post-pump, showing the resin-printed microfluidic chips connected to the pump

5.3 Results and Discussion

The LEDs were tested through changing their intensity to see if there was any cross-LED interference (Figure 47). Each LED was turned on separately and then the intensity of each LED was changed again to look for any changes in other LEDs, which would be visible in shifts of more than one photodiode at a time. Over the testing window, the flow cells gave consistent signals with no interference between them.

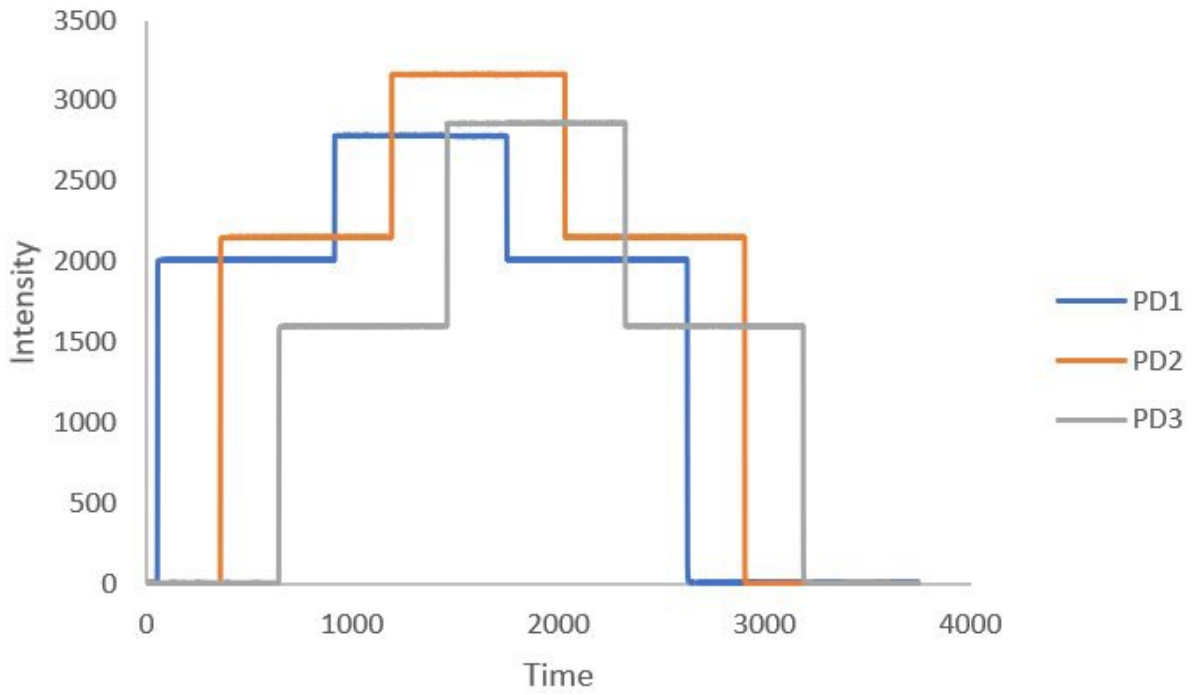

Figure 47 Interference study of the flow cells in the multinutrient flow cell array, showing good stability of all three LED-photodiode pairs.

The heater was tested to see how much of an effect the aluminium rod had on heater stabilisation time (Figure 48). With the aluminium rod sitting on top as a heat sink, it was suspected that the heater would take a much longer time to stabilise than the previous system. However, the NTC in the heater showed a very similar heating curve to that of the previous heater configuration, taking approximately 5 minutes to stabilise.

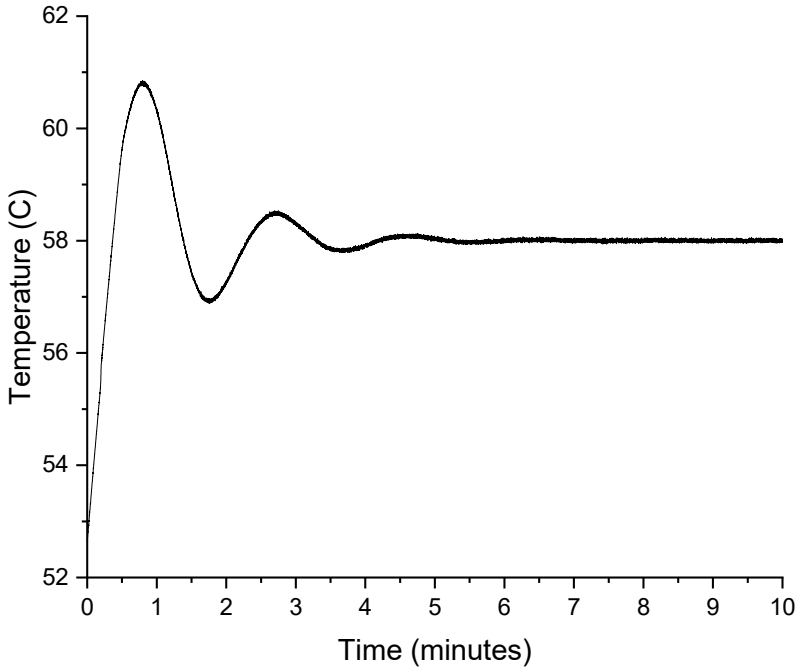

Figure 48 Stabilisation of the multinutrient flow cell temperature after starting up. Whilst the starting temperature is not shown, the change seen in heater temperature compared to that of the previous heater system was negligible, showing it stabilise within 5 minutes.

There were two use cases tried for this analyser. One was in collaboration with the University of Reading to analyse the effects of different organic sources of carbon in the levels of ammonium and nitrate around baby spinach. The other was to analyse ammonium, nitrate and nitrite in a bioreactor to help monitor the rate of change of inorganic nitrogen forms using nitrifying bacteria. These two environments would have significantly different nutrient levels and the mixing ratios needed to be changed between them. They also have different measurement requirements, with the wastewater treatment setup needing to have continuous measurement whilst the spinach test only requires daily measurement.

Using a 10.5:1:1 Sample:Salicylate:DIC ratio, the well plate assay gave a linear result until approx. 0.15 mM (Figure 49). This was higher than the 3:1:1 result using the droplet assay (Figure 49). The droplet assay plateaus at a lower concentration as the concentration of sample is lower in each droplet than in the well plate assay.

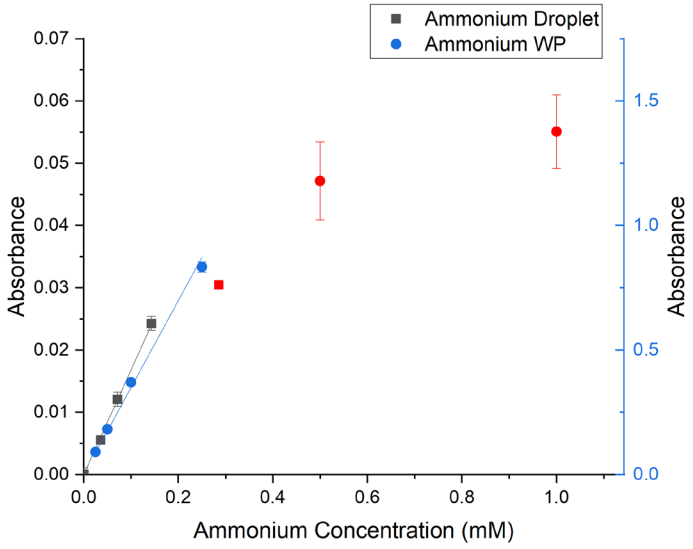

Figure 49 Calibration of Ammonium Analyser for use in the soil study, compared to that of a Well-Plate analyser. Points in red were omitted from making the linear fit.

Unlike with the baby spinach experiment, which only had to measure on a per-day basis, the bioreactor experiment would see a change in N composition over a much quicker scale, with bacteria being able to consume ammonium on a millimolar level over a period of hours. Due to the increased sampling rate required, the system was modified to run continuously at a lower flow rate (2 RPM instead of 10 RPM). The length of the heater tubing was modified to account for this change in speed and the change in mixing ratios.

Whilst the ammonium levels in soil range from 0 to 400 µM, wastewater treatment plants deal with much larger ammonium levels (30 to 150 mM)[148]. To incorporate such large levels would require a significant dilution of sample before addition to the bioreactor system. The 3:1:1 ratio (Sample:Salicylate reagent:DIC reagent) was changed to a 1:7:7 ratio in line with previous experiments done by the group[146], going from 60% of the droplet to 6.6%, theoretically raising the upper limit for ammonium by an order of magnitude, allowing the potential changes to be better captured. This wouldn't be a significant enough dilution to be used in wastewater treatment plants due to the upper limit being approximately 4 mM for ammonium but would be enough for researching bacterial culture. The NO_3^- and NO_2^- ratios also had to be changed to adapt to this, going from a 1:1 ratio (Sample:Reagent) to 1:6, going from 50% to 14.3% sample in droplet, giving a theoretical upper limit of around 2.8 mM. Further modification would be required to observe higher

concentrations, such as those typically seen in wastewater treatment plants, which could be achieved through addition of dilution lines or by lowering the temperature of the heater as done in the previous nitrate sensor work. The nitrate absorbance for PD2 was less than the nitrite absorbance, signifying that the reduction reaction had not gone to completion, yet the consistency of the pumping method ensures that the heater time remains consistent.

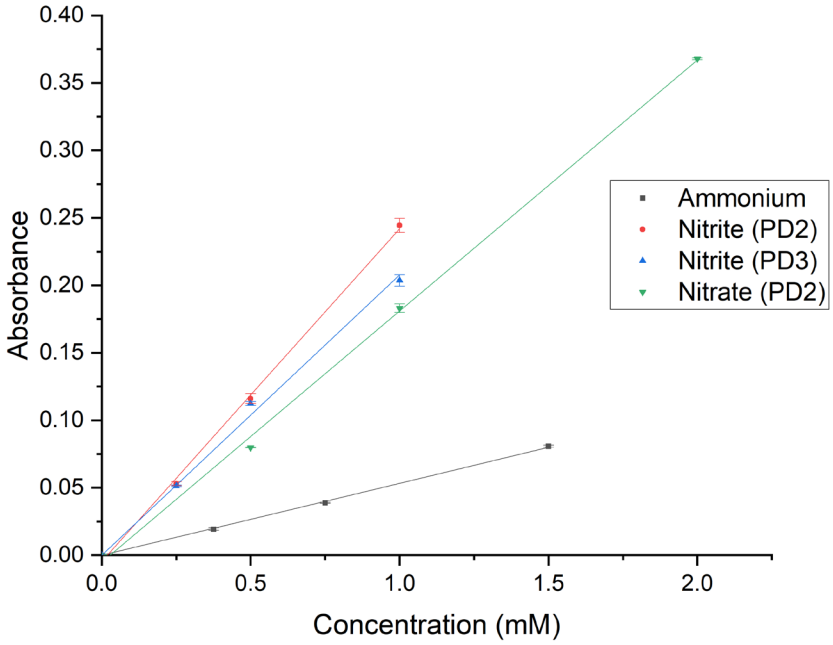

Figure 50 Calibration of multinutrient analyser, showing good calibration curves for all three analytes. Nitrite was measure in multiple photodiodes to allow for conversion between PD3 (which only measures nitrite) and PD2 (which measures nitrate and nitrite simultaneously) to extract nitrate concentration in the sample.

Sampling nitrate, nitrite and ammonium with this system simultaneously consumes approx. 1.73 µL of sample per pump revolution; at 2 RPM, 103 µL is taken up every hour. Over a 3-day deployment period, only 7.5 mL of water will be sampled. 10 mL of both Griess and Griess+ reagent and 11.6 mL of Salicylate and DIC reagent are consumed every day. Including oil, 246 mL of waste is generated in a 3-day deployment. After each deployment, the FC-40 was separated out from the waste and reused, as was done in the river sensor work previously.

5.4 Conclusion

Through development of combining 3 flow cells and a heater into a single unit, a multinutrient analysis platform was developed. This allows for the concurrent analysis of 3 colorimetric assays, showing good calibration for Nitrite, Nitrate and Ammonium. This development allows for different nutrients to be tracked as they change from one form to the other, which is typically seen in environments like wastewater treatment or aquaponic scenarios with interplay of different forms of inorganic N, which can potentially allow for the development of control systems in future. The combined heater and flow cells can be used for various colorimetric reactions, allowing for easier multiplexing of droplet microfluidic absorbance devices in future.

Chapter 6 Multinutrient Analyser Deployments

In this chapter, two deployment scenarios for versions of the multinutrient system will be discussed. First, a 2-month organic amendment experiment analysing how inorganic nitrogen is fixed in soil by different forms of organic carbon. Then, a bioreactor system aiming to observe nitrification will be built and observed.

The processes through which inorganic nitrogen changes from one species to another in soil have been well studied, typically through collection of soil by hand. When this process occurs, changes take place in the sample resulting in certain species being overpredicted. This, having only been found recently with increasing use of in-situ techniques, could potentially have led us to implement fertilisation schemes which do not fully benefit the soil. Through measurement of different forms of inorganic N in soil *in situ*, the interplay between these forms can give light to potential changes in fertilisation regime.

6.1 Organic Amendment Experiment

6.1.1 Introduction

Analysers for nitrate and ammonium were used in a study in collaboration with University of Reading, analysing the effects of the application of high carbon organic amendments on N losses from soil during the production of babyleaf spinach. Organic amendments of C to soil have been shown to prevent N loss through leaching of NO_3^- and volatilisation of nitrogen oxides[149], and current spinach production methods often do not incorporate such amendments. This experiment was used to test how different organic amendments could be applied to spinach production and how the soil is affected post-harvest through use of these different treatments.

Objectives:

- Deploy the intermittent multinutrient analyser in an experiment to analyse the effect of different organic amendments (Glycerol or Straw) on the level of nitrate and ammonium present in soil during production and post-harvest phases
- Verify the results from the multinutrient analyser through comparison with grab samples taken from Rhizon pore water samplers

6.1.2 Materials and Methods

This experiment was prepared by Ellie Barbrook (University of Reading). 186.68 g of dried soil was added to each pot and was then rehydrated to 85% maximum WHC (0.4 g H_2O / g dry soil with ultrapure water (18.2 MΩ·cm). For the Straw experiment, air-dried barley straw cut to lengths of 50 mm were added to the soil at a rate of 960 kg C ha^{-1}. For the Glycerol experiment, glycerol was incorporated in the form of a 50% v/v solution at the same rate of 960 kg C ha^{-1}.

Non-N fertilisers were added when the soil was being rehydrated: 200 kg P ha^{-1} superphosphate (P_2O_5, Miracle-Gro®); 225 K Kg ha^{-1} Sulphate of potash (K_2O, Westland) and 100 Mg Kg ha^{-1} Kieserite heptahydrate ($MgO_4S·7H_2O$, Fischer Scientific).

Five spinach seeds (Spinicia oleracea variety Kodak) were sown into the pots (depth of 2 cm, equidistant apart) 24 hours after the soil was rehydrated. After one week, the spinach plants were thinned to leave 3 plants in each pot. A week after sowing Calcium ammonium nitrate (CAN) fertiliser was added in 5x100 µL aliquots at a concentration of 143.03 mg mL^{-1}, giving an application rate of 60 kg N ha^{-1}. Throughout the experiment the soil was kept at 85% soil moisture content.

The analysers were connected to one pot each (Figure 51, one control, one glycerol amended, and one straw amended), with each analyser collecting soil pore water from two ultrafiltration probes. Each ultrafiltration probe was placed at opposite sides of the pot to avoid interaction of the depletion zones that would form. The analyser ran once a day at 10:00 with a half an hour run time.

Figure 51 Pictures of the Organic Amendment experiment. Left: Overall experiment of pots with different amendments. Right: Analysers connected to three pots.

The experiment was split into a production phase and a post-harvest phase. After a month of growing, at which point the spinach leaves were at a length of 8-10 cm, the spinach was harvested and approximately half of the spinach was reincorporated with the soil in each pot to simulate cultivation residue after commercial harvesting.

6.1.3 Results and Discussion

During the production phase, nitrate levels for the control were significantly higher than those with organic amendments but were also much more variable. In the glycerol-amended soil, the level of nitrate was constant throughout but the ammonium level dropped over production. This was probably due to microbial processes converting ammonium into organic amino acids, as well as the spinach taking up ammonium via N-fixing.

The take up of both nitrate and ammonium was captured smoothly for the straw amendment pot, showing a longer time before the nitrogen species were taken up. This is due to the straw having to be broken down before the microbes can process the sugars present in the straw, leading to lower initial levels in activity. Unfortunately the ammonium level above 0.8 µg N/ g dried soil (0.14 mM, calculated using equation (9)) would have fallen outside the calibration range, so the signal above that level would be unreliable, yet would still be a signifier of high ammonium. When repeating this test, the sample:reagent ratio would need to be changed by increasing the amount of reagent in each droplet, as was done in the bioreactor project, to capture a wider range.

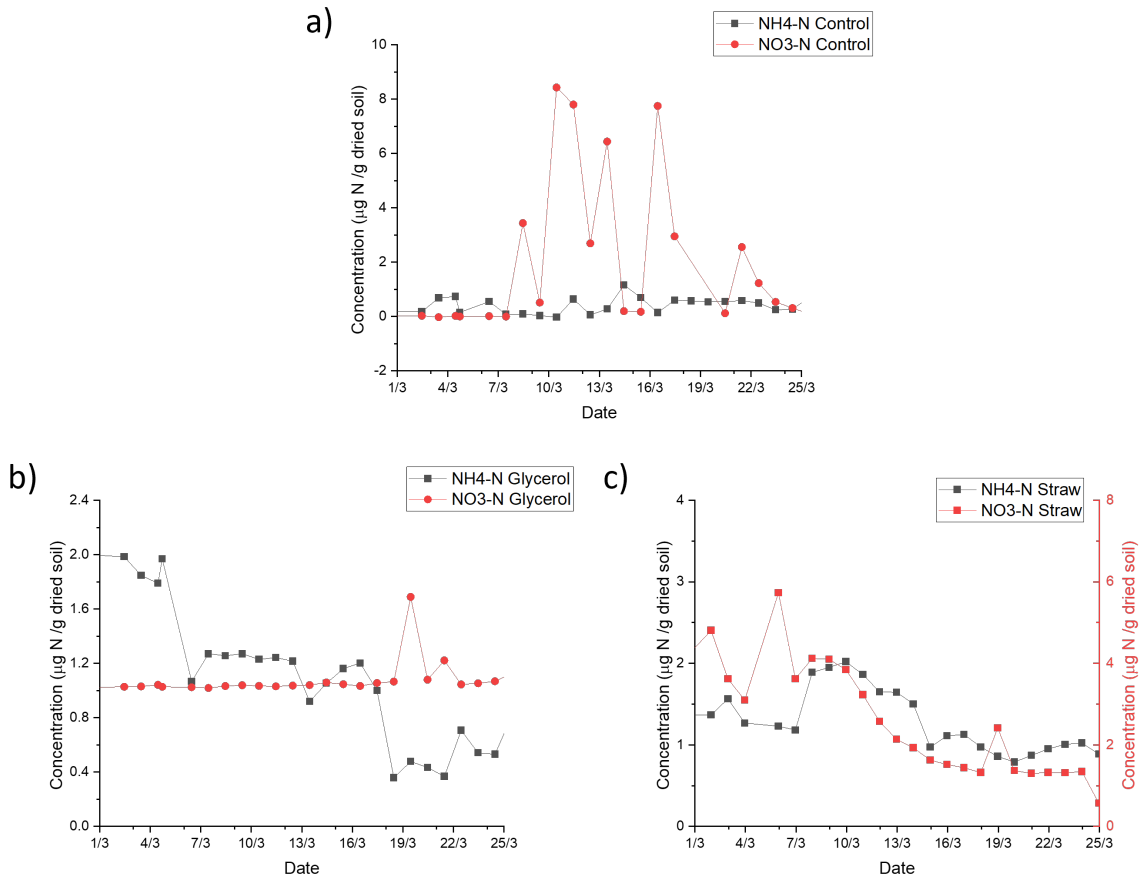

Figure 52 Production phase analysis of nitrate and ammonium with amendment with different sources of carbon (a) No addition, b) Glycerol, c) Straw); Glycerol should provide a quicker release of C into the soil, given that the straw amendment has to be broken down first.

After the production phase, the spinach was harvested. The harvested spinach was then split into two batches. Any leaves that were not healthy were recombined with the soil to mimic harvesting. The analysers were connected to three pots and the soil was monitored for a 6-week period.

In the control, after the first week the nitrate spiked to 6 µg N /g dried soil. This is indicative of when the spinach leaves would have started to release nitrate into the soil upon decomposition. Then, with some C present as well, mineralisation takes place over the next weeks. In the two organic amendment plots the immobilisation of ammonium is apparent over the sample period, but the rate is significantly slower than that seen in the production phase, which is due to the lack of presence of the spinach plant as a nutrient sink.

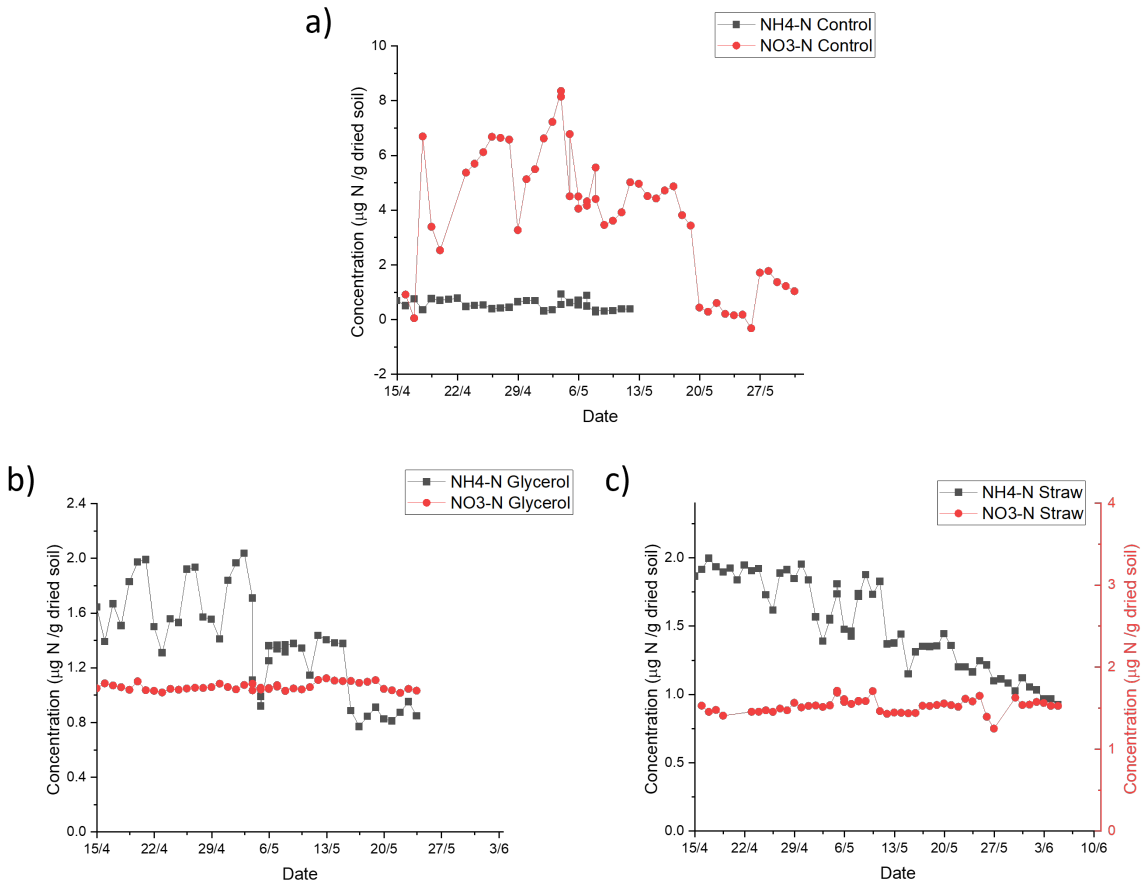

Figure 53 Post-harvest phase of organic amendment test, in which discarded spinach leaves were recombined with soil (a) No addition, b) Glycerol, c) Straw. In glycerol and straw, nitrate levels remained consistent whilst ammonium drops whilst in the Control only nitrate was present

Whilst this data shows explainable trends, the grab samples taken through collection of leachate from other pots showed different trends. The nitrate level from all three treatments were significantly higher, yet this could be due to how the samples were collected; with each run. In all experimental scenarios the nitrate was significantly higher than ammonium when looking at the grab samples; it could be that the sample extraction process causes a significant change in soil nitrogen composition[38].

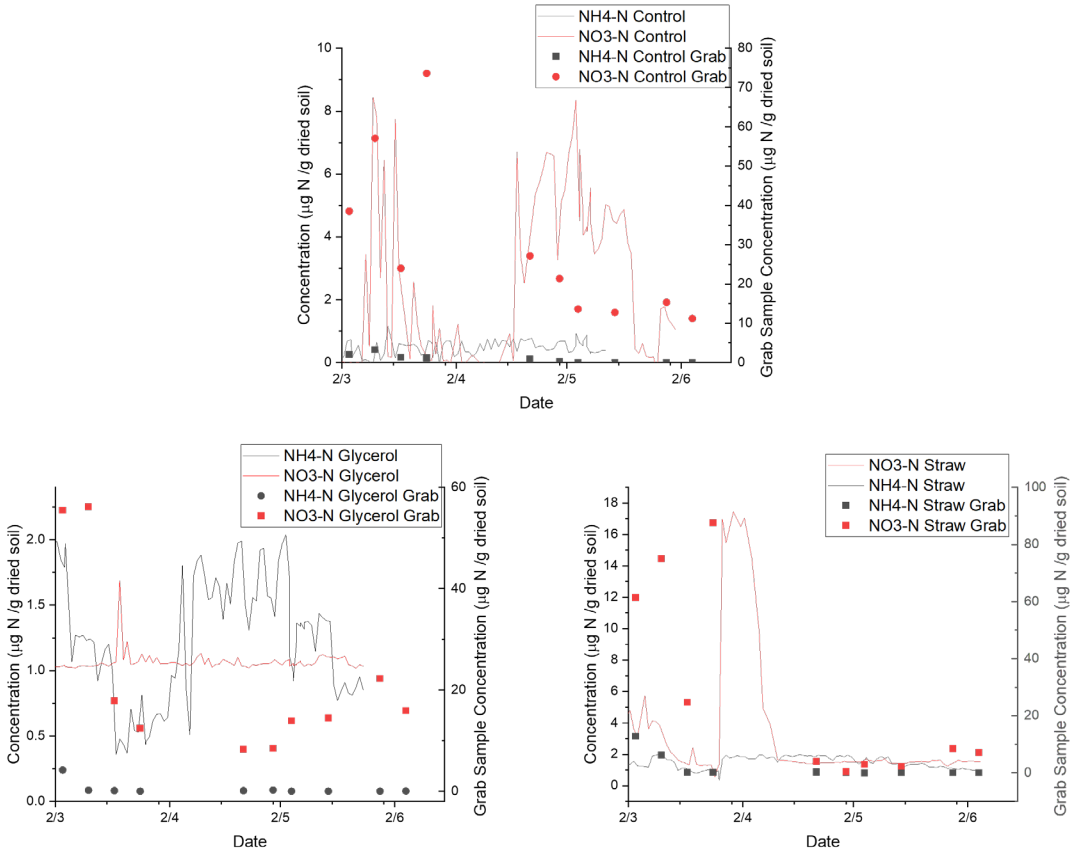

Figure 54 Overall views of the organic amendment deployment (Top: Control, Bottom left: Glycerol, Bottom right: Straw), showing the mismatching between the sampler and grab samples

Overall, the analysers were able to capture significant changes in both nitrate and ammonium simultaneously, showing qualitative trends observing nutrient consumption by both the spinach plant and the microbes in the soil. However, there were significant limitations in the collection of data for ammonium due to the low upper range captured by the analyser. For nitrate measurement, the data collected fell well into the range that the sensor was able to record. However, this did not line up well with the grab sample data collected, which showed significantly higher nitrate throughout the deployment period (Figure 54). This suggests that the method of collection may be affecting the result; both systems collect pore water yet one is refrigerated before analysis, and one is analysed immediately. It could be that different forms of both inorganic and organic N are being oxidised to NO_3^- before the sample is analysed. Such phenomena has been found to occur for water extraction solutions[150] but not to the same extent for pore water. In this agricultural soil the majority of extractable N should be in the form of nitrate, as observed in the grab samples acquired, yet the direct analysis of pore water by the analyser contradicts this, at least for the organic amendment pots. It

could be that the lower flow rate used for the analyser extraction induces less stress on the soil matrix than the Rhizon sampling used for the grab samples.

Another potential reason for the disparity between the grab samples and that taken from the analyser were that the pore water samplers were only measuring from one pot from each treatment. The small volume of water taken up from each UF probe may also contribute to the difference, in which the heterogenous nature of soil means that the collection of pore water from one area may not be representative of the entire pot. In future studies, more analysers will need to be deployed to give a more accurate look into the effect of organic amendments in plant growth.

6.2 Bioreactor Experiment

6.2.1 Introduction

In wastewater and bioreactor processes, nitrifying bacteria are used for processing forms of inorganic N, such as ammonium and nitrite, into less harmful forms like nitrite or nitrogen gas before release into waterways. These bacteria have been implemented into granules and have very high removal efficiencies over long periods of time[151] and their growth is currently monitored using grab sampling techniques, analysing granular size and turnover of ammonium to nitrate over the cycling period. Automation in this sector would help to prevent external factors from affecting growth or measurement and could also allow for automated control of the system based on ammonium consumption, allowing for more efficient bacterial growth.

6.2.2 Materials and Methods

Return Activated Sludge (RAS) was obtained from Millbrook Wastewater Treatment and Recycling Centre (Southampton, UK). A sequencing batch reactor system was fabricated to allow for autonomous, consistent feeding of the sludge. The reactor was made from a plastic bottle, with luer fittings glued on the side using epoxy onto the side of the bottle for inflow of feedstock, outflow of waste and for an air supply. Figure 55 shows an overview of the bioreactor setup. Inflow and outflow of artificial wastewater from the bioreactor was controlled using a multi-channel peristaltic pump (Masterflex Ismatec REGLO ICC, VWR). An air pump (PYP370) supplied air at a regulated rate of 0.2 L/min, using a flow meter (VFA-21-BV, Dwyer), via an aquarium air stone diffuser. Code for the air pump and peristaltic pump was developed by Sherif Attia.

a)

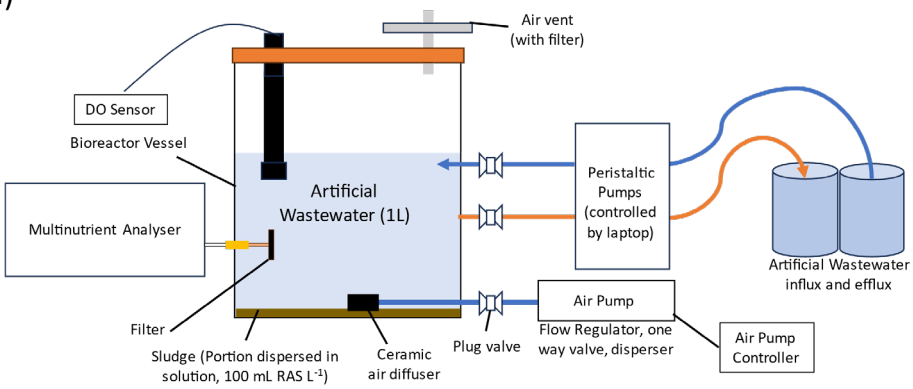

b)

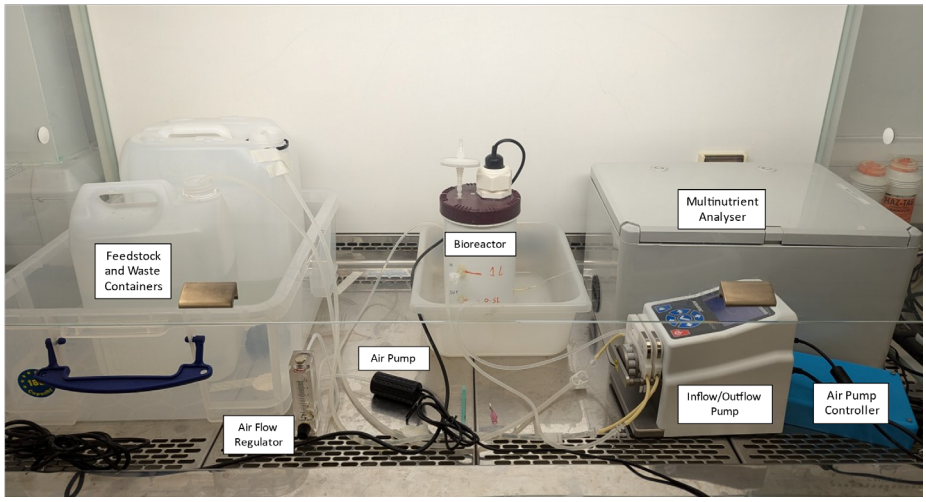

Figure 55 Overview of Bioreactor experiment. a) Schematic overview, b) Annotated view of the system in a biological safety cabinet.

The sequence batch reactor method, outlined in Chen et al, 2015[151], was operated by the manner shown in Figure 56. To start with, 100 mL of RAS was added to 1 L of artificial wastewater (Per L: 25 mg NH_4-N, 15 mg PO_4-P, 270 mg $NaHCO_3$). Each cycle consisted of four steps, with a total cycle time of 12 hours. The first step involves aerating the sludge, which also allows for water to be stirred and the sludge to be dispersed through the solution to improve the activity of the bacteria. The air pump is then shut off, allowing for the sludge to settle at the bottom of the tank. Processed artificial wastewater is then pumped out until the total volume of the mixture is 500 mL, dictated by the height of the total solution, then fresh feedstock is pumped in to 1 L total volume to restart the cycle. The sludge was incubated in this system for 3 days (6 cycles) using this pumping cycle before the multinutrient device was turned on and measurements were taken.

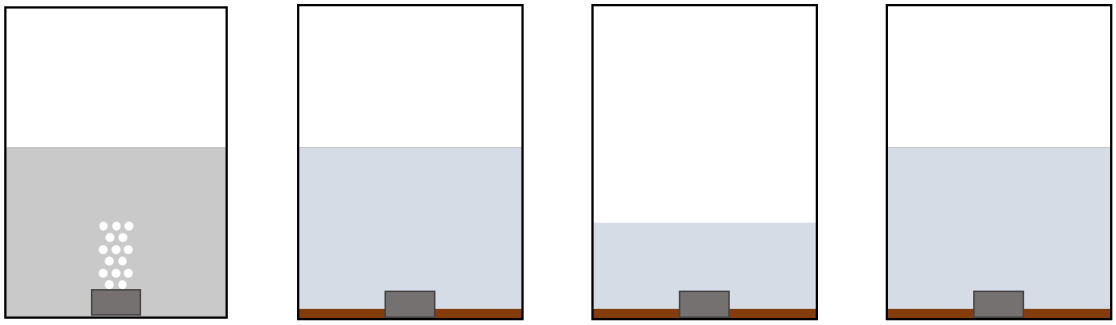

Figure 56 Sequencing Batch Reactor setup used in the bioreactor experiment, along with approximately how long each section took – The extended time for inflow and outflow was due to the low flow rate of the pump, this will be replaced with high flow rate centrifuge pumps in future versions.

A filter with a small internal volume was prepared to decrease the sample to signal time of the system, in which a 0.22 µm filter membrane was fitted and glued using an epoxy (Araldite 2012, RS) onto a 3D-printed housing.

6.2.3 Results and Discussion

In the first test run, grab samples were collected by briefly disconnecting the sample line to the sensor and collecting 1 mL of the fluid into a syringe. This was then transferred to an Eppendorf tube and centrifuged at 3000 RPM for 5 minutes. The supernatant was then removed and passed through a filter and was then diluted in a 1:4 ratio (sample:MQ) and refrigerated until processing. In future runs, a second filter was added to allow for grab samples to be taken without interfering with the sensor results. Results from the first bioreactor run were shown in Figure 57.

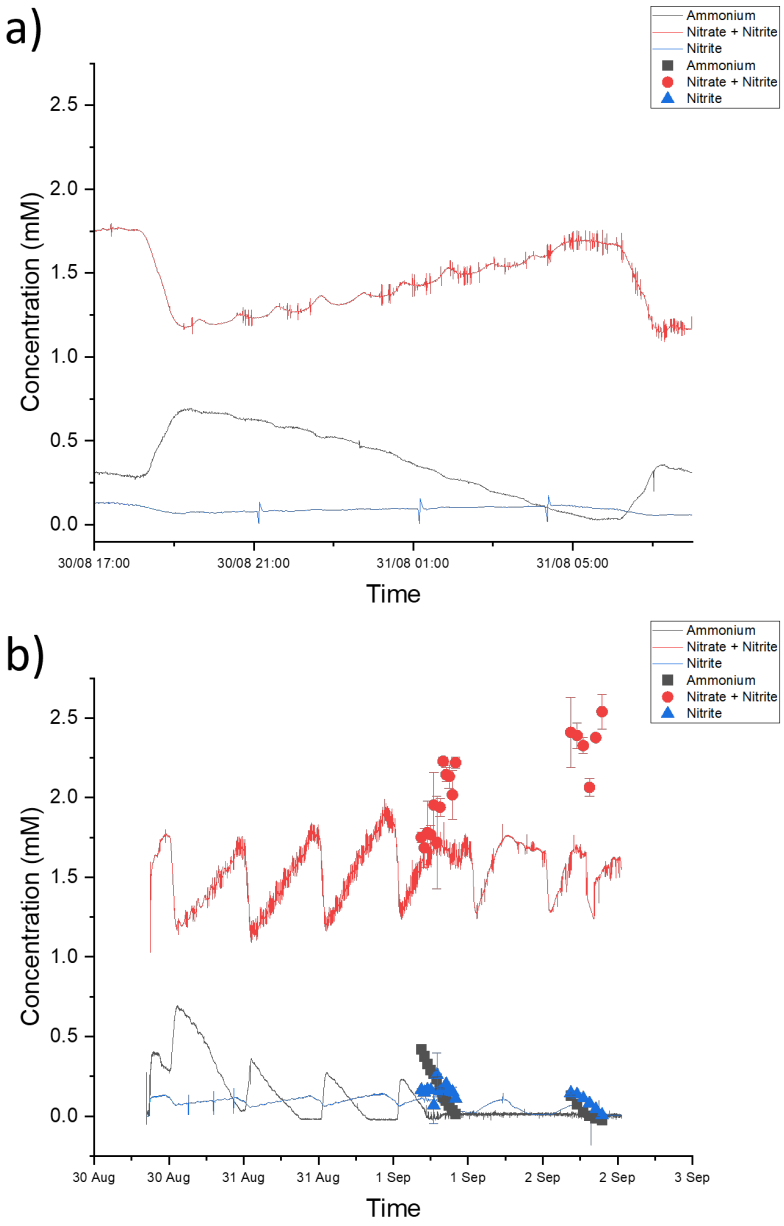

Figure 57 Bioreactor run in which the ammonium level differed significantly from the grab sample analysis. a) First cycle, showing the conversion of ammonium into nitrate over the 12-hour period, with very little intermediate nitrite throughout. b) Full 3-day experiment in which the ammonium level recorded by the analyser significantly decreases at the start of each run before flatlining after day 2, signifying an issue of either backpressure or blockage

In a fully cultivated bioreactor system, we would expect a high starting concentration of ammonium that would consistently decrease over the cycle period, with a small increase in nitrite as the

intermediate species followed by a decrease as the nitrifying bacteria then convert this nitrite into nitrate and a consistent increase in nitrate over the sample period, as monitored in Chen et al[151]. The trends exhibited in the first test showed that the ammonium uptake by the nitrifying bacteria was much slower, with a much more gradual decrease over a 12-hour period, which is to be expected due to the much shorter cultivation time of the sludge (3 days). This lower ammonium processing rate led to a much lower nitrite level throughout the deployment, as the small amount of nitrite produced was quickly converted into nitrate.

After the first recorded cycle (Figure 57a), the analyser recorded much lower ammonium levels than expected. The nitrate level trends were consistent through the 3-day deployment, showing that this was not an issue with the bacteria. This decrease in recorded ammonium may have been due to filter bypass, with the bacteria being able to get past the bioreactor filter and make its way to the inlet chip. This would have led to a buildup of sediment around the Santoprene-PVC connection in the ammonium inlet line, leading to a blockage forming over time. In the other lines, where wider bore tubing was used from the inlet chip to the pump, no visible degradation in signal was seen over the same timeframe. This was affirmed by the presence of an accumulation of solids at the bottom of the waste pouch of the analyser.

This first experiment was successful in showing the ability of the analyser to monitor all three nutrients simultaneously, yet more work needed to be done to make the system more robust. The membrane filter used was changed to a 13 mm 0.2 µm membrane (Supor 60298, Pall Corporation) glued using a thin layer of epoxy into a resin 3D-printed housing (printed using an Elegoo Mars 3 Pro), with one face of the membrane open to the bioreactor. These were then tested for leaks by inserting the filter into water and applying air pressure using a syringe. No bubbles were seen up to a pressure of 3.5 bar which aligned with the minimum bubble point for 0.2 µm pore size.

Calibrations were performed with and without this filter attached to see the difference in how quickly the signal plateaued (Figure 58); with the filter attached the time taken to plateau went from 15 minutes to approximately 1 hour, which will lead to a slight underestimation in concentration when going from low to high concentration and an overestimation when going from high to low concentrations.

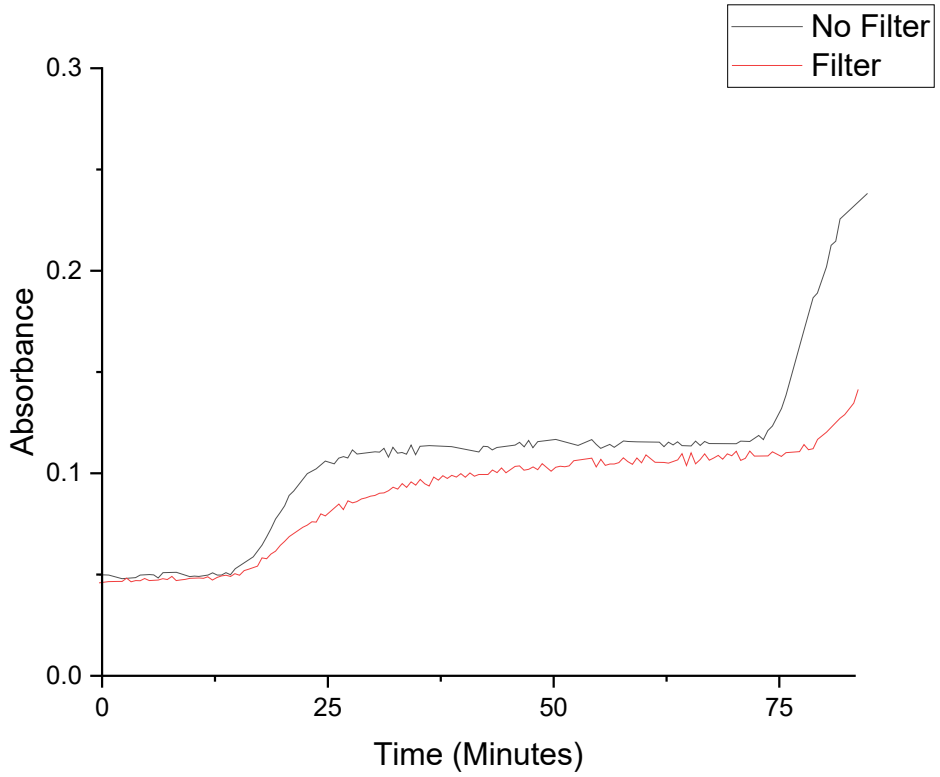

Figure 58 Comparison for the NO_2^- line with and without the addition of an external filter, showing the large increase of plateauing time induced with the added filter

The prefilter sample to signal time was calculated for each line to be 15 minutes for Nitrite and 30 minutes for Nitrate and Ammonium, which was then increased to approximately 1 hour when the filter was added. During processing, the absorbance value for nitrite (PD3) was subtracted from the absorbance value for Nitrite and Nitrate (PD2) 15 minutes later to calculate the Nitrate absorbance, given the similar absorbance values for a given nitrite concentration between PD2 and PD3.

With the new filter, the bioreactor experiment was rerun (Figure 59). The cycle time was kept at 12 hours, given the rate of ammonium consumption from the last experiment this seemed appropriate. The rate of ammonium consumption observed was much quicker than in the previous run, being consumed in several hours instead of 12 hours seen in the previous experiment.

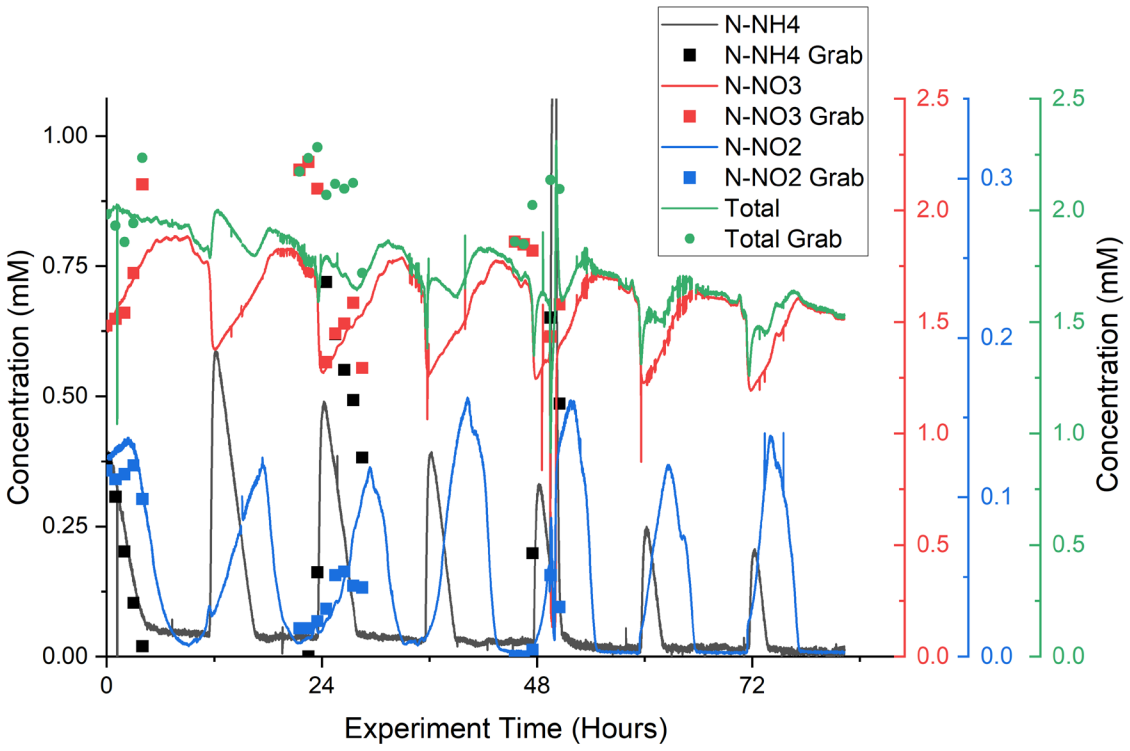

Figure 59 Bioreactor run after the switch to a resin filter, showing a similar trend in Ammonium response to the previous test, with total N declining over time in comparison to the grab sample measurements.

In this run, the same conversion from ammonium to nitrite to nitrate over the course of each cycle. The rate at which the ammonium converted to nitrite was much quicker in this experiment, signifying a much greater microbial activity than the previous run. With the first cycle, the ammonium grab samples matched very closely to the level recorded by the analyser. The nitrate grab samples appear to deviate at higher concentrations, which indicates that the nitrate level in the sample is saturated above 2 mM, which will need to be corrected by either lowering the amount of ammonium in the feedstock to 1 mM or to increase the dilution factor beyond 1:6 sample:Griess+ in future experiments. The nitrite samples matched well with the analyser in each grab sample period. Over time, the total level of N recorded by the analyser decreases over time to a greater rate than that shown by the grab samples, indicating it is a fault of the analyser.

During this run, the peak ammonium signal decreased with each cycle. The filter was disconnected and 1.5 mM ammonium standard was added just after the 48 hour mark and the ammonium signal

gave 1.4 mM, meaning that the signal drop was not mainly due to reagent degradation. The sample line was reconnected afterwards to continue the experiment.

Compared to the previous run the decline in ammonium signal was more gradual, which could signify it being a slow buildup of contaminant on the filter. This would lead to increased backpressure in the inlet line, inducing a drop in the amount of sample picked up by the peristaltic pump with each droplet. As a similar drop in signal is also seen in the nitrate line, this is a probable cause. To ameliorate this, a shorter inlet line can be used. This would slow the signal decay by reducing the overall backpressure but would not completely solve the issue; further tests needed to be done to ascertain the cause of this signal decay.

In this group's previous running of the drybox ammonium sensor[146], a similar drop over time had been observed. This system had a recirculating pump and a shorter connection between the pump and a filter. In this case the drop was thought to be caused by matrix interference by the presence of thiourea, yet it could be that this degradation in pumping was the case.

The system was run without sludge for several days, to help determine whether the signal decay was due to the presence of the sludge. Considering that the system performed well consistently during calibration, it would either be found to be due to the sludge or the makeup of the feedstock.

The first experiment was run without a filter to provide a baseline, with very little signal drop over the three day period (Figure 60). Over the same period, the signal in the bioreactor experiment for ammonium dropped by approximately 30% but in this experiment the change was within the standard deviation of samples, signifying very little change.

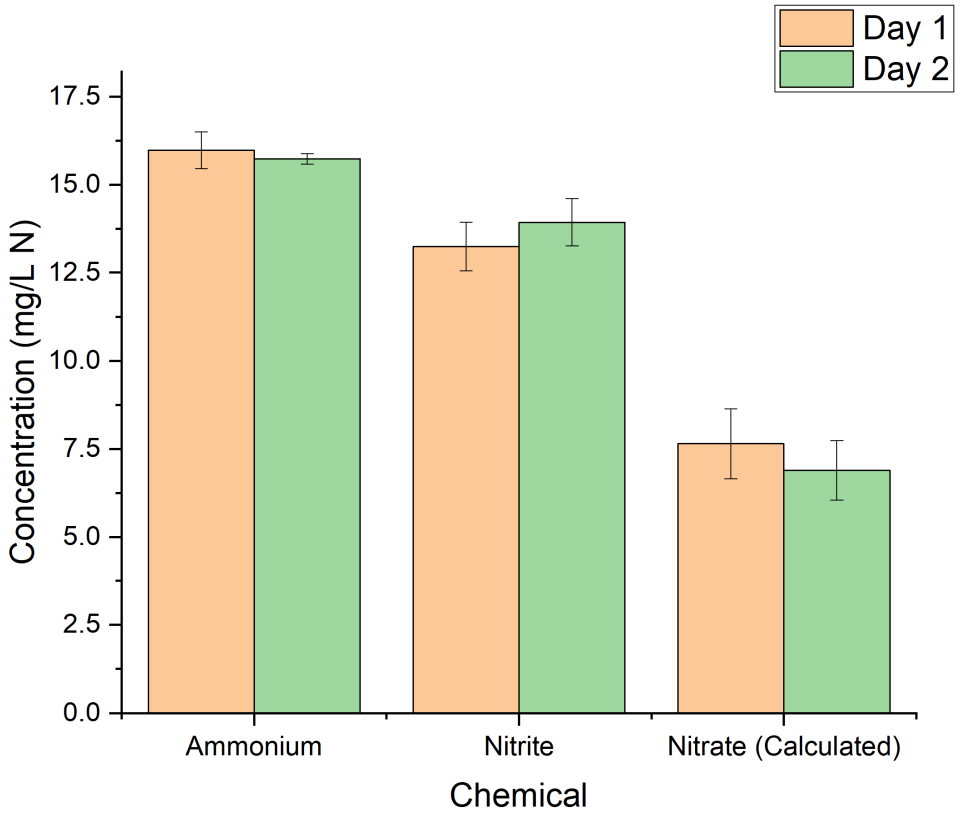

Figure 60: Two day experiment in which ammonium and nitrate were doped into feedstock solution and run continuously, to rule out that the composition of the feedstock was degrading or blocking the system over time.

In the non-filter experiment, no appreciable drop was seen over the two day period, showing the issue was not due to degradation of the feedstock and was at least partly due to the filter system. This signified that the issue would be due to the filter system or interaction with the sludge. More work will be performed in future work to find the root cause of this issue.

Overall, the bioreactor system shows promise for multinutrient analysis in-situ, being able to see the transition of ammonium to nitrite and then nitrate over a 3-day window. This incorporated system was able to show good calibration curves for all three analytes and was able to qualitatively track the trends in N present in the bioreactor yet had significant issues in monitoring the system over a 3 day experiment. More work will need to be done to analyse the root cause of the issue in signal degradation for both ammonium and nitrate but it is probably due to a buildup of backpressure in the inlet section from the filter to the pump due to filter blockage.

More work will need to be done to extend the lifetime of the filter system; this can be done through reducing the backpressure in the inlet part by making the length of small-bore tubing shorter between the bioreactor and the inlet chip. Alternatively, this can be reduced through the use of a recirculating pump to continuously provide sample, as was done in the ammonium drybox sensor work previously, and can be combined with some way of dislodging contaminants from the filter if that is the cause of the signal degradation.

Even with the theoretical maximum limit of around 2.8 mM, the system struggled to give a reading of more than 2 mM, which was probably due to the overpresence of nitrite as the two compounds are measured simultaneously. More work will need to be done to extend the range of the system for nitrate, which could consist of adapting the dilution technique used for the soil analysis work in which a fourth line could introduce Milli-Q, which would require an increase in pumping lines of the sensor. The range can also be extended through separating out the heater systems and lowering the temperature for nitrate; this will increase the power consumption of the system but will allow for better range control for each of the analytes.

6.3 Conclusion

In both experiments, the multinutrient analyser was able to track fluxes in multiple forms of organic N. In the organic amendment experiment, decreases in both ammonium and nitrate were captured after the introduction of organic matter, in line with previous studies, yet there was a significant mismatching of data between the grab samples taken and the data from the multinutrient analyser, which could be due to the small sample area monitored by the probe, changes in the grab sample post-collection.

The bioreactor experiment showed the potential for the multinutrient analyser to collect continuous data over several days, recording fluxes between ammonium, nitrite and nitrate through the nitrification process. However, whilst it performed well in calibration, signal degradation occurred after the first cycle in two separate tests, meaning that the system still has some way to go before it can monitor real samples.

Chapter 7 Conclusions and Further Work

In the first half of this project, we developed an integrated system for monitoring nitrate capable of using two different probes (MD and UF) for the monitoring of nutrients in soil. This first foray into nitrate monitoring has allowed us to prove the potential of the system, being able to detect trends over long time periods, with two successful deployments.

Firstly, the system was calibrated through solution-based testing, giving a baseline from which relative recovery can be measured. The system was then tested in soil at a range of moisture contents, giving good linearity across moisture contents (100 to 70% with UF, 100 to 50% with MD), showing how the MD system could be used at potentially lower moisture contents to analyse bioavailable nitrate whilst ultrafiltration can be used at higher moisture contents to analyse pore water nitrate.

The system was then used to measure trends in nitrate after addition of glucose into soil over the course of 2 weeks. The system was able to autonomously measure changes in nitrate, with low reagent consumption (96 µL per measurement, 4 measurements per day), giving trends similar to that in literature. From these results, we then developed this into a packaged system for field deployment to allow for in-situ monitoring, which allows for a much greater insight into real-time soil nitrogen dynamics with low maintenance requirements (once per month) and low reagent usage. This system is the first use of microdialysis as part of an in-situ analyser for soil, which has the potential to be a large player in soil analysis in the future.

From the two deployments, the soil analyser produced data in line with grab samples over periods of 12 days and 60 days, with the second deployment continuing for another 10 months after that. The longer deployment was able to study quantitative changes in soil nitrate, with data that was found to be in line with conventional methods (KCl extraction). This was a testament to the robustness of the system, highlighting the benefits of droplet microfluidics from the lack of biofouling seen over the course of the deployment. This showed the potential for microdialysis to be used as part of an in-situ monitoring system and should be further explored, with its major benefits over other sampling methods, such as ultrafiltration, due to its diffusion-based approach having less effect on the soil matrix over time, allowing for significantly longer deployments. I expect microdialysis to be used further in future with microfluidic analysers due to its low impact sampling method, which could give new insights into nutrient dynamics which previous collection methods have been unable to capture.

With the UT7 flow cell regime we had developed, phosphate was still difficult to measure due to its low level in river water. A long path length phosphate device was fabricated to counter this, including an oil extraction part for removing the oil flow and a long U-shaped detection channel, combining the benefits of mixing in droplet microfluidics with the detection limits available to continuous microfluidic techniques. Multiple lengths were tested between 5 and 20 mm, with the 20 mm channel giving the lowest LOD (0.66 µM for 20 mm path length, 3.87 µM for UT7). This oil extraction section also gives the added benefit of easily cycling oil in the system, with only one extra line needed to pump per analyte, preventing time-consuming processing of waste and reducing the potential for the oils to be released into the environment upon disposal of the waste. However, further work needs to be performed in testing the long-term performance of the oil extraction system before it should be deployed, which could be hampered by deterioration of the membrane material or cotton wool pad over time.

A multi-nutrient analyser was then developed to measure ammonium, nitrate, and nitrite simultaneously which was then used to monitor two different scenarios; one more long-term (2 months intermittent running) in the form of monitoring soil dynamics using ultrafiltration and one short-term (3 days continuous running) used to track the activity of denitrifying bacteria. The measurement of these three analytes at once using a droplet microfluidic sensor has clear benefits to using a continuous microfluidic sensor, with the decreased risk of biofouling over time and the decrease in smearing from one concentration to the next, with each droplet acting as a discrete reaction vessel. With further development, this system has the capability to be used in many environmental scenarios, from aquaponics and wastewater treatment to soil management and agriculture. The analyser design could also be adapted to fit other colorimetric reactions through a change in roller design, LED change and reagent usage, allowing for different analytes to be collected in tandem. However, further development needs to be done on the inlet of the system before it can be used to monitor systems with a high risk of biofouling such as wastewater as the signal quickly degraded over the 3-day continuous running period. It is suspected that this is due to the filter system, which needs to be further developed before it can be used to run continuously. This analyser has potential to be used in conjunction with control systems if this issue is resolved, which could be a great help to growing denitrifying bacteria as the analyser was able to qualitatively track trends in the different forms of N over the sampling period.

7.1 Further Work

7.1.1 Future Applications

Inorganic N sensing is critical in several sectors. In the new frontier of aquaponics, in which fish are cultivated alongside crops in a symbiotic manner, high spikes of certain forms of N can lead to both crop failure or fish death. Control systems are essential for this type of production, needing high precision with small response times. Integration of the multinutrient analyser with an automated control system, activating different systems based on the concentration analysed by the system, will provide a nutrient feedback loop to prevent toxic conditions. Such control systems will be invaluable in both aquaponics and other research scenarios, like bacterial growth.

Further work will be done in the multinutrient analyser to find the root cause of the issue behind the signal degradation, with experiments varying parameters like $NaHCO_3$ quantity or sludge level to find what is contributing to this. After those tests are done and the cause has been found and the system has been adapted to account for it, the bioreactor experiment will be repeated and future work can be done to improve the range of each nutrient to increase its utility.

Further soil monitoring can be performed to analyse the potential of microdialysis to study microbial and root uptake of nutrients, yet more needs to be understood regarding the makeup of samples taken using microdialysis and ultrafiltration techniques. With different sampling techniques giving preferential treatment to analytes in different studies, such as inorganic N being more prevalent with ultrafiltration techniques[111] whilst organic positively charged amino acids are better captured with microdialysis, more work needs to be done to observe different N forms in-situ.

7.1.2 Challenges for Future Users

Further work will need to be done to reduce the sample to signal time of the continuous running system; the integration of a recirculating pump close to the inlet of the multinutrient system will facilitate this, allowing the multinutrient analyser to be deployed much farther away from the source being analysed, increasing its utility for application in closed, indoor systems like bioreactors.

The filter system used in the bioreactor project also needs improvement, showing clogging after several days. Having a way to remove particulate matter from the surface of the filter may help with this and will be valuable for small fluid volume sampling in-situ. A small stream of water directed at

the filter during the cycle turnover could perform this but could be challenging due to the current thin membranes used.

For the soil sensors, the addition of an external power source, such as a solar array, will allow for much longer deployment times without maintenance. This will increase its utility in remote agricultural areas without the ability to easily connect to mains and if on-board calibrations can take place then a much longer deployment window can be achieved without maintenance.

One issue with the soil analyser is the variability of its results, due to the heterogeneity of the soil environment. Using multiple analysers, perhaps connected to an IoT environment, will allow for much more accurate data to be collected for a given sample period. Giving these analysers the capability to be used alongside other analysers seamlessly will greatly improve its potential for field application.

Through further development of the multinutrient sensor, such as incorporation of microdialysis probes for each line, deployments in soil would also become possible. Incorporation of a phosphate sensor will allow for both N and P forms to be studied, both of which are of great importance to plant growth and overall soil health. This could be in the form of a Nitrate, Ammonium and Phosphate sensor, yet would require the microdialysis probes to be separate otherwise the peaks given through intermittent sensing using microdialysis will be split up between the three analytes and would also require many more lines to facilitate a push-pull system with microdialysis.

References

1. Bank, W. Arable Land (% of land area). https://data.worldbank.org/indicator/AG.LND.ARBL.ZS (accessed 31/03/2021).

2. Tan, Z. X.; Lal, R.; Wiebe, K. D., Global Soil Nutrient Depletion and Yield Reduction. *Journal of Sustainable Agriculture* **2005,** *26* (1), 123-146.

3. Rezaei Rashti, M.; Wang, W.; Moody, P.; Chen, C.; Ghadiri, H., Fertiliser-induced nitrous oxide emissions from vegetable production in the world and the regulating factors: A review. *Atmospheric Environment* **2015,** *112*, 225-233.

4. Behrenfeld, M. J.; Halsey, K. H.; Milligan, A. J., Evolved physiological responses of phytoplankton to their integrated growth environment. *Philosophical Transactions of the Royal Society B: Biological Sciences* **2008,** *363* (1504), 2687-2703.

5. VOLLENWEIDER, R. In *COASTAL MARINE EUTROPHICATION - PRINCIPLES AND CONTROL*, SCIENCE OF THE TOTAL ENVIRONMENT, SUPPLEMENT 1992, 1992-01-01; **1992**; pp 1-20.

6. Beusen, A.; Doelman, J.; Van Beek, L.; Van Puijenbroek, P.; Mogollón, J.; Van Grinsven, H.; Stehfest, E.; Van Vuuren, D.; Bouwman, A., Exploring river nitrogen and phosphorus loading and export to global coastal waters in the Shared Socio-economic pathways. *GLOBAL ENVIRONMENTAL CHANGE-HUMAN AND POLICY DIMENSIONS* **2022,** *72*.

7. Kuypers, M. M. M.; Marchant, H. K.; Kartal, B., The microbial nitrogen-cycling network. *Nature Reviews Microbiology* **2018,** *16* (5), 263-276.

8. Stitt, M.; Krapp, A., The interaction between elevated carbon dioxide and nitrogen nutrition: the physiological and molecular background. *PLANT CELL AND ENVIRONMENT* **1999,** *22* (6), 583-621.

9. Hodge, A.; Robinson, D.; Fitter, A., Are microorganisms more effective than plants at competing for nitrogen? *Trends in Plant Science* **2000,** *5* (7), 304-308.

10. Thompson, R. B.; Incrocci, L.; Van Ruijven, J.; Massa, D., Reducing contamination of water bodies from European vegetable production systems. *Agricultural Water Management* **2020,** *240*, 106258.

11. Green, P. A.; Vörösmarty, C. J.; Meybeck, M.; Galloway, J. N.; Peterson, B. J.; Boyer, E. W., Pre-industrial and contemporary fluxes of nitrogen through rivers: a global assessment based on typology. *Biogeochemistry* **2004,** *68* (1), 71-105.

12. Fan, A. M.; Steinberg, V. E., Health Implications of Nitrate and Nitrite in Drinking Water: An Update on Methemoglobinemia Occurrence and Reproductive and Developmental Toxicity. *Regulatory Toxicology and Pharmacology* **1996,** *23* (1), 35-43.

13. Schlesinger, W. H., On the fate of anthropogenic nitrogen. *Proceedings of the National Academy of Sciences* **2009,** *106* (1), 203-208.

14. Tegeder, M.; Masclaux-Daubresse, C., Source and sink mechanisms of nitrogen transport and use. *New Phytologist* **2018,** *217* (1), 35-53.

15. Pi, H.-W.; Lin, J.-J.; Chen, C.-A.; Wang, P.-H.; Chiang, Y.-R.; Huang, C.-C.; Young, C.-C.; Li, W.-H., Origin and Evolution of Nitrogen Fixation in Prokaryotes. *Molecular Biology and Evolution* **2022,** *39* (9).

16. Setubal, J. O. C.; Dos Santos, P.; Goldman, B. S.; ErtesvåG, H.; Espin, G.; Rubio, L. M.; Valla, S.; Almeida, N. F.; Balasubramanian, D.; Cromes, L.; Curatti, L.; Du, Z.; Godsy, E.; Goodner, B.; Hellner-Burris, K.; Hernandez, J. A.; Houmiel, K.; Imperial, J.; Kennedy, C.; Larson, T. J.; Latreille, P.; Ligon, L. S.; Lu, J.; Mærk, M.; Miller, N. M.; Norton, S.; O'Carroll, I. P.; Paulsen, I.; Raulfs, E. C.; Roemer, R.; Rosser, J.; Segura, D.; Slater, S.; Stricklin, S. L.; Studholme, D. J.; Sun, J.; Viana, C. J.; Wallin, E.; Wang, B.; Wheeler, C.; Zhu, H.; Dean, D. R.; Dixon, R.; Wood, D., Genome Sequence ofAzotobacter vinelandii, an Obligate Aerobe Specialized To Support Diverse Anaerobic Metabolic Processes. *Journal of Bacteriology* **2009,** *191* (14), 4534-4545.

17. Li, Q.; Liu, X.; Zhang, H.; Chen, S., Evolution and Functional Analysis of orf1 Within nif Gene Cluster from Paenibacillus graminis RSA19. *International Journal of Molecular Sciences* **2019,** *20* (5), 1145.

18. Nitzse, L. K.; Emtsev, V. T.; Shelley, S. I., Ecological Aspects of Nitrogen-Fixing Activity of Anaerobic Bacteria Genus Clostridium. In *Advances in Nitrogen Fixation Research: Proceedings of the 5th International Symposium on Nitrogen Fixation, Noordwijkerhout, The Netherlands, August 28 – September 3, 1983*, Veeger, C.; Newton, W. E., Eds. Springer Netherlands: Dordrecht, **1984**; pp 267-267.

19. Scott, E., Lightning-fixed nitrogen. *Nature Reviews Earth & Environment* **2023,** *4* (9), 601-601.

20. Jan, M.; Roberts, P.; Tonheim, S.; Jones, D., Protein breakdown represents a major bottleneck in nitrogen cycling in grassland soils. *Soil Biol. Biochem.* **2009,** *41* (11), 2272-2282.

21. Coker, H. R.; Lin, H.-A.; Shackelford, C. E. B.; Tfaily, M. M.; Smith, A. P.; Howe, J. A., Drought stimulates root exudation of organic nitrogen in cotton (Gossypium hirsutem). *Frontiers in Plant Science* **2024,** *15*.

22. Aerts, R.; Bakker, C.; De Caluwe, H., Root turnover as determinant of the cycling of C, N, and P in a dry heathland ecosystem. *Biogeochemistry* **1992,** *15* (3), 175-190.

23. Farzadfar, S.; Knight, J. D.; Congreves, K. A., Soil organic nitrogen: an overlooked but potentially significant contribution to crop nutrition. *Plant and Soil* **2021,** *462* (1-2), 7-23.

24. Kuzyakov, Y.; Xu, X., Competition between roots and microorganisms for nitrogen: mechanisms and ecological relevance. *New Phytologist* **2013,** *198* (3), 656-669.

25. Pandey, C.; Kumar, U.; Kaviraj, M.; Minick, K.; Mishra, A.; Singh, J., DNRA: A short-circuit in biological N-cycling to conserve nitrogen in terrestrial. *SCIENCE OF THE TOTAL ENVIRONMENT* **2020,** *738*.

26. Xia, X.; Zhang, S.; Li, S.; Zhang, L.; Wang, G.; Zhang, L.; Wang, J.; Li, Z., The cycle of nitrogen in river systems: sources, transformation, and flux. *ENVIRONMENTAL SCIENCE-PROCESSES & IMPACTS* **2018,** *20* (6), 863-891.

27. Mosier, A.; Doran, J.; Freney, J., Managing soil denitrification. *JOURNAL OF SOIL AND WATER CONSERVATION* **2002,** *57* (6), 505-513.

28. Galloway, J.; Dentener, F.; Capone, D.; Boyer, E.; Howarth, R.; Seitzinger, S.; Asner, G.; Cleveland, C.; Green, P.; Holland, E.; Karl, D.; Michaels, A.; Porter, J.; Townsend, A.; Vörösmarty, C., Nitrogen cycles:: past, present, and future. *BIOGEOCHEMISTRY* **2004,** *70* (2), 153-226.

29. Mulder, A., Anaerobic ammonium oxidation discovered in a denitrifying fluidized bed reactor. *FEMS Microbiology Ecology* **1995,** *16* (3), 177-183.

30. Hou, L.; Zheng, Y.; Liu, M.; Li, X.; Lin, X.; Yin, G.; Gao, J.; Deng, F.; Chen, F.; Jiang, X., Anaerobic ammonium oxidation and its contribution to nitrogen removal in China's coastal wetlands. *Scientific Reports* **2015,** *5* (1), 15621.

31. Kim, H.; Bae, H.; Reddy, K.; Ogram, A., Distributions, abundances and activities of microbes associated with the nitrogen cycle in riparian and stream sediments of a river tributary. *WATER RESEARCH* **2016,** *106*, 51-61.

32. Environment Agency, Phosphorus: challenges for the water environment. **2021**.

33. Childers, D.; Corman, J.; Edwards, M.; Elser, J., Sustainability Challenges of Phosphorus and Food: Solutions from Closing the Human Phosphorus Cycle. *BIOSCIENCE* **2011,** *61* (2), 117-124.

34. HOLTAN, H.; KAMPNIELSEN, L.; STUANES, A., PHOSPHORUS IN SOIL, WATER AND SEDIMENT - AN OVERVIEW. *HYDROBIOLOGIA* **1988,** *170*, 19-34.

35. Nislow, K.; Armstrong, J.; McKelvey, S., Phosphorus flux due to Atlantic salmon (Salmo salar) in an oligotrophic upland stream:: effects of management and demography. *CANADIAN JOURNAL OF FISHERIES AND AQUATIC SCIENCES* **2004,** *61* (12), 2401-2410.

36. SHARPLEY, A.; CHAPRA, S.; WEDEPOHL, R.; SIMS, J.; DANIEL, T.; REDDY, K., MANAGING AGRICULTURAL PHOSPHORUS FOR PROTECTION OF SURFACE WATERS - ISSUES AND OPTIONS. *JOURNAL OF ENVIRONMENTAL QUALITY* **1994,** *23* (3), 437-451.

37. Sharpley, A.; Jarvie, H. P.; Buda, A.; May, L.; Spears, B.; Kleinman, P., Phosphorus Legacy: Overcoming the Effects of Past Management Practices to Mitigate Future Water Quality Impairment. *Journal of Environmental Quality* **2013,** *42* (5), 1308-1326.

38. Bailey, T.; Robinson, N.; Farrell, M.; Macdonald, B.; Weaver, T.; Antille, D. L.; Chin, A.; Brackin, R., Storage of soil samples leads to over-representation of the contribution of nitrate to plant-available nitrogen. *Soil Research* **2022,** *60* (1), 22.

39. Inselsbacher, E.; Ohlund, J.; Jamtgard, S.; Huss-Danell, K.; Nasholm, T., The potential of microdialysis to monitor organic and inorganic nitrogen compounds in soil. *Soil Biol. Biochem.* **2011,** *43* (6), 1321-1332.

40. Kjeldahl, J., Neue Methode zur Bestimmung des Stickstoffs in organischen Körpern. *Fresenius' Zeitschrift für analytische Chemie* **1883,** *22* (1), 366-382.

41. Lima, J.; Delerue-Matos, C.; Vaz, M., Flow-injection analysis of Kjeldahl nitrogen in milk and dairy products by potentiometric detection. *Anal. Chim. Acta* **1999,** *385* (1-3), 437-441.

42. Sáez-Plaza, P.; Navas, M.; Wybraniec, S.; Michalowski, T.; Asuero, A., An Overview of the Kjeldahl Method of Nitrogen Determination. Part II. Sample Preparation, Working Scale, Instrumental Finish, and Quality Control. *CRITICAL REVIEWS IN ANALYTICAL CHEMISTRY* **2013,** *43* (4), 224-272.

43. MEHLICH, A., MEHLICH-3 SOIL TEST EXTRACTANT - A MODIFICATION OF MEHLICH-2 EXTRACTANT. *COMMUNICATIONS IN SOIL SCIENCE AND PLANT ANALYSIS* **1984,** *15* (12), 1409-1416.

44. Tinker, P. B.; Nye, P. H., *Solute movement in the rhizosphere*. Oxford University Press: **2000**.

45. Bungay, P. M.; Morrison, P. F.; Dedrick, R. L., STEADY-STATE THEORY FOR QUANTITATIVE MICRODIALYSIS OF SOLUTES AND WATER INVIVO AND INVITRO. *Life Sci.* **1990,** *46* (2), 105-119.

46. Rogers, M. L.; Feuerstein, D.; Leong, C. L.; Takagaki, M.; Niu, X.; Graf, R.; Boutelle, M. G., Continuous Online Microdialysis Using Microfluidic Sensors: Dynamic Neurometabolic Changes during Spreading Depolarization. *ACS Chemical Neuroscience* **2013,** *4* (5), 799-807.

47. Buckley, S.; Brackin, R.; Jamtgard, S.; Nasholm, T.; Schmidt, S., Microdialysis in soil environments: Current practice and future perspectives. *Soil Biol. Biochem.* **2020,** *143*, 13.

48. Brackin, R.; Näsholm, T.; Robinson, N.; Guillou, S.; Vinall, K.; Lakshmanan, P.; Schmidt, S.; Inselsbacher, E., Nitrogen fluxes at the root-soil interface show a mismatch of nitrogen fertilizer supply and sugarcane root uptake capacity. *Scientific Reports* **2015,** *5* (1), 15727.

49. Demand, D.; Schack-Kirchner, H.; Lang, F., Assessment of diffusive phosphate supply in soils by microdialysis. *Journal of Plant Nutrition and Soil Science* **2017,** *180* (2), 220-230.

50. Mckay Fletcher, D. M.; Shaw, R.; Sánchez-Rodríguez, A. R.; Daly, K. R.; Van Veelen, A.; Jones, D. L.; Roose, T., Quantifying citrate-enhanced phosphate root uptake using microdialysis. *Plant and Soil* **2019**.

51. Deltedesco, E.; Inselsbacher, E.; Gorfer, M.; Zechmeister-Boltenstern, S.; Keiblinger, K.; Potsch, E. M., High-resolution dynamics of available N in a grassland ecosystem under a multiple climate manipulation experiment. *Applied Soil Ecology* **2023,** *185*, 6.

52. Gao, W.; Blaser, S. R. G. A.; Schlüter, S.; Shen, J.; Vetterlein, D., Effect of localised phosphorus application on root growth and soil nutrient dynamics in situ – comparison of maize (Zea mays) and faba bean (Vicia faba) at the seedling stage. *Plant and Soil* **2019,** *441* (1-2), 469-483.

53. Torres, N. T.; Hauser, P. C.; Furrer, G.; Brandl, H.; Müller, B., Sediment porewater extraction and analysis combining filter tube samplers and capillary electrophoresis. *Environmental Science: Processes & Impacts* **2013,** *15* (4), 715.

54. Kuang, J.; Wen, J.; Cai, X.; Zhou, L.; Yuan, Y., In situ and on-line monitoring of cadmium in soil pore water using an automatic sampling integrated electrochemical sensor. *Science China Technological Sciences* **2024,** *67* (9), 2894-2904.

55. Taylor, A. C.; Mills, G. A.; Gravell, A.; Kerwick, M.; Fones, G. R., Passive sampling with suspect screening of polar pesticides and multivariate analysis in river catchments: Informing environmental risk assessments and designing future monitoring programmes. *Science of The Total Environment* **2021,** *787*, 147519.

56. Gravell, A.; Fones, G. R.; Greenwood, R.; Mills, G. A., Detection of pharmaceuticals in wastewater effluents—a comparison of the performance of Chemcatcher® and polar organic compound integrative sampler. *Environmental Science and Pollution Research* **2020,** *27* (22), 27995-28005.

57. Zhang, H.; Davison, W., Diffusional characteristics of hydrogels used in DGT and DET techniques. *Anal. Chim. Acta* **1999,** *398* (2-3), 329-340.

58. Kodithuwakku, K.; Huang, J.; Doolette, C. L.; Mason, S.; Boland, J.; Lombi, E.; Lehto, N. J.; Teasdale, P. R., Evaluation of the diffusive gradients in thin-films (DGT) technique for measuring nitrate and ammonium in soil. *Environmental Chemistry* **2023,** *19* (8), 483-494.

59. Huang, J.; Bennett, W.; Teasdale, P.; Gardiner, S.; Welsh, D., Development and evaluation of the diffusive gradients in thin films technique for measuring nitrate in freshwaters. *Anal. Chim. Acta* **2016,** *923*, 74-81.

60. Huang, J.; Bennett, W.; Welsh, D.; Li, T.; Teasdale, P., Development and evaluation of a diffusive gradients in a thin film technique for measuring ammonium in freshwaters. *Anal. Chim. Acta* **2016,** *904*, 83-91.

61. Österlund, H.; Chlot, S.; Faarinen, M.; Widerlund, A.; Rodushkin, I.; Ingri, J.; Baxter, D., Simultaneous measurements of As, Mo, Sb, V and W using a ferrihydrite diffusive gradients in thin films (DGT) device. *Anal. Chim. Acta* **2010,** *682* (1-2), 59-65.

62. Zhang, S.; Williams, P.; Zhou, C.; Ma, L.; Luo, J., Extending the functionality of the slurry ferrihydrite-DGT method: Performance evaluation for the measurement of vanadate, arsenate, antimonate and molybdate in water. *CHEMOSPHERE* **2017,** *184*, 812-819.

63. You, N.; Chen, S.; Wang, Y.; Fan, H.; Sun, L.; Sun, T., In situ sampling of tetracycline antibiotics in culture wastewater using diffusive gradients in thin films equipped with graphene nanoplatelets. *ENVIRONMENTAL RESEARCH* **2020,** *191*.

64. Cao, H.; Bu, Q.; Li, Q.; Yang, L.; Tang, J.; Yu, G., Evaluation of the DGT passive samplers for integrating fluctuating concentrations of pharmaceuticals in surface water. *SCIENCE OF THE TOTAL ENVIRONMENT* **2024,** *926*.

65. Pelcová, P.; Docekalová, H.; Kleckerova, A., Development of the diffusive gradient in thin films technique for the measurement of labile mercury species in waters. *Anal. Chim. Acta* **2014,** *819*, 42-48.

66. Lu, Y.; Li, C.; Wang, Y.; Wang, Z.; Liu, C.; Fan, H.; Sun, T., A SERS Responsive DGT Sensing Device for On-Site Determination of Organic Contaminants Underwater. *ACS SENSORS* **2023,** *8* (10), 3762-3771.

67. Shen, X.; Zheng, H.; Pang, R.; Liu, G.; Wu, D.; Tian, Z., Experimental and Theoretical Study of Surface-Enhanced Raman Spectra of Sulfadiazine Adsorbed on Nanoscale Gold Colloids. *JOURNAL OF PHYSICAL CHEMISTRY A* **2019,** *123* (42), 9199-9208.

68. Birrell, S. J.; Hummel, J. W., Real-time multi ISFET/FIA soil analysis system with automatic sample extraction. *Computers and Electronics in Agriculture* **2001,** *32* (1), 45-67.

69. Garland, N. T.; Mclamore, E. S.; Cavallaro, N. D.; Mendivelso-Perez, D.; Smith, E. A.; Jing, D.; Claussen, J. C., Flexible Laser-Induced Graphene for Nitrogen Sensing in Soil. *ACS Applied Materials & Interfaces* **2018,** *10* (45), 39124-39133.

70. Dhamu, V. N.; Somenahally, A. C.; Paul, A.; Muthukumar, S.; Prasad, S., Characterization of an In-Situ Soil Organic Carbon (SOC) via a Smart-Electrochemical Sensing Approach. *Sensors* **2024,** *24* (4), 1153.

71. Petry, R.; Schmitt, M.; Popp, J., Raman Spectroscopy - A prospective tool in the life sciences. *CHEMPHYSCHEM* **2003,** *4* (1), 14-30.

72. Wang, C.; Weng, G.; Li, J.; Zhu, J.; Zhao, J., A review of SERS coupled microfluidic platforms: From configurations to applications. *Anal. Chim. Acta* **2024,** *1296*.

73. Morgan, S.; Luy, E.; Miller, L.; Pittman, M.; Phelan, K.; Wright, M.; Furlong, A.; Sieben, V.; IEEE In *An In Situ Phosphate Analyzer for Marine Environments Using Inlaid Microfluidics*, OCEANS 2021: SAN DIEGO - PORTO, 345 E 47TH ST, NEW YORK, NY 10017 USA, 2021-01-01; IEEE: 345 E 47TH ST, NEW YORK, NY 10017 USA, **2021**.

74. Rushworth, C. M.; Davies, J.; Cabral, J. T.; Dolan, P. R.; Smith, J. M.; Vallance, C., Cavity-enhanced optical methods for online microfluidic analysis. *Chemical Physics Letters* **2012,** *554*, 1-14.

75. Rushworth, C. M.; Jones, G.; Fischlechner, M.; Walton, E.; Morgan, H., On-chip cavity-enhanced absorption spectroscopy using a white light-emitting diode and polymer mirrors. *Lab on a Chip* **2015,** *15* (3), 711-717.

76. James, D.; Oag, B.; Rushworth, C. M.; Lee, J. W. L.; Davies, J.; Cabral, J. T.; Vallance, C., High-sensitivity online detection for microfluidics via cavity ringdown spectroscopy. *RSC Advances* **2012,** *2* (12), 5376.

77. Rushworth, C. M.; Yogarajah, Y.; Zhao, Y.; Morgan, H.; Vallance, C., Sensitive analysis of trace water analytes using colourimetric cavity ringdown spectroscopy. *Anal. Methods* **2013,** *5* (1), 239-247.

78. Medcalf, E.; Gantz, M.; Kaminski, T.; Hollfelder, F., Ultra-High-Throughput Absorbance-Activated Droplet Sorting for Enzyme Screening at Kilohertz Frequencies. *ANALYTICAL CHEMISTRY* **2023,** *95* (10), 4597-4604.

79. Ellis, G.; Adatia, I.; Yazdanpanah, M.; Makela, S., Nitrite and nitrate analyses: A clinical biochemistry perspective. *CLINICAL BIOCHEMISTRY* **1998,** *31* (4), 195-220.

80. Kodamatani, H.; Yamazaki, S.; Saito, K.; Tomiyasu, T.; Komatsu, Y., Selective determination method for measurement of nitrite and nitrate in water samples using high-performance liquid chromatography with post-column photochemical reaction and chemiluminescence detection. *Journal of Chromatography A* **2009,** *1216* (15), 3163-3167.

81. Beaton, A. D.; Cardwell, C. L.; Thomas, R. S.; Sieben, V. J.; Legiret, F.-E.; Waugh, E. M.; Statham, P. J.; Mowlem, M. C.; Morgan, H., Lab-on-Chip Measurement of Nitrate and Nitrite for In Situ Analysis of Natural Waters. *Environmental Science & Technology* **2012,** *46* (17), 9548-9556.

82. Amali, R. K. A.; Lim, H. N.; Ibrahim, I.; Huang, N. M.; Zainal, Z.; Ahmad, S. A. A., Significance of nanomaterials in electrochemical sensors for nitrate detection: A review. *Trends Environ. Anal. Chem.* **2021,** *31*, 21.

83. Shao, Y.; Ying, Y.; Ping, J., Recent advances in solid-contact ion-selective electrodes: functional materials, transduction mechanisms, and development trends. *Chemical Society Reviews* **2020,** *49* (13), 4405-4465.

84. Capella, J. V.; Bonastre, A.; Ors, R.; Peris, M., An interference-tolerant nitrate smart sensor for Wireless Sensor Network applications. *Sensors and Actuators B: Chemical* **2015,** *213*, 534-540.

85. Capella, J. V.; Bonastre, A.; Campelo, J. C.; Ors, R.; Peris, M., A New Ammonium Smart Sensor with Interference Rejection. *Sensors* **2020,** *20* (24), 7102.

86. Lin, L.; Zeng, X., Toward continuous amperometric gas sensing in ionic liquids: rationalization of signal drift nature and calibration methods. *Analytical and Bioanalytical Chemistry* **2018,** *410* (19), 4587-4596.

87. Ali, M. A.; Wang, X.; Chen, Y.; Jiao, Y.; Mahal, N. K.; Moru, S.; Castellano, M. J.; Schnable, J. C.; Schnable, P. S.; Dong, L., Continuous Monitoring of Soil Nitrate Using a Miniature Sensor with Poly(3-octyl-thiophene) and Molybdenum Disulfide Nanocomposite. *ACS Applied Materials & Interfaces* **2019,** *11* (32), 29195-29206.

88. Liu, H.; Crooks, R. M., Highly reproducible chronoamperometric analysis in microdroplets. *Lab on a Chip* **2013,** *13* (7), 1364.

89. Gu, S.; Lu, Y.; Ding, Y.; Li, L.; Song, H.; Wang, J.; Wu, Q., A droplet-based microfluidic electrochemical sensor using platinum-black microelectrode and its application in high sensitive glucose sensing. *Biosensors and Bioelectronics* **2014,** *55*, 106-112.

90. Moo, Y. C.; Matjafri, M. Z.; Lim, H. S.; Tan, C. H., New development of optical fibre sensor for determination of nitrate and nitrite in water. *Optik* **2016,** *127* (3), 1312-1319.

91. Tossanaitada, B.; Masadome, T.; Imato, T., Sequential injection analysis of nitrate ions using a microfluidic polymer chip with an embedded ion-selective electrode. *Analytical Methods* **2012,** *4* (12), 4384.

92. Thomas, D. H.; Rey, M.; Jackson, P. E., Determination of inorganic cations and ammonium in environmental waters by ion chromatography with a high-capacity cation-exchange column. *Journal of Chromatography A* **2002,** *956* (1-2), 181-186.

93. Yi, R.; Song, P.; Liu, X.; Maruo, M.; Ban, S., Differences in dissolved phosphate in shallow-lake waters as determined by spectrophotometry and ion chromatography. *Limnology* **2020,** *21* (3), 329-339.

94. Li, X.; Zou, N.; Wang, Z.; Sun, Y.; Li, H.; Gao, C.; Wang, T.; Wang, X., An electrochemical sensor for determination of nitrite based on Au nanoparticles decorated MoS2 nanosheets. *Chemical Papers* **2020,** *74* (2), 441-449.

95. Nightingale, A. M.; Hassan, S.-U.; Warren, B. M.; Makris, K.; Evans, G. W. H.; Papadopoulou, E.; Coleman, S.; Niu, X., A Droplet Microfluidic-Based Sensor for Simultaneous in Situ Monitoring of Nitrate and Nitrite in Natural Waters. *Environmental Science & Technology* **2019,** *53* (16), 9677-9685.

96. Alifragis, Y.; Volosirakis, A.; Chaniotakis, N. A.; Konstantinidis, G.; Iliopoulos, E.; Georgakilas, A., AlGaN/GaN high electron mobility transistor sensor sensitive to ammonium ions. *physica status solidi (a)* **2007,** *204* (6), 2059-2063.

97. Abbas, M. N.; Radwan, A. L. A.; Nooredeen, N. M.; El-Ghaffar, M. A. A., Selective phosphate sensing using copper monoamino-phthalocyanine functionalized acrylate polymer-based solid-state electrode for FIA of environmental waters. *Journal of Solid State Electrochemistry* **2016,** *20* (6), 1599-1612.

98. SUNA V2 UV NITRATE SENSOR User Manual. Sea-Bird Scientific: 2024.

99. Dudala, S.; Dubey, S. K.; Goel, S., Microfluidic Soil Nutrient Detection System: Integrating Nitrite, pH, and Electrical Conductivity Detection. *IEEE Sensors Journal* **2020,** *20* (8), 4504-4511.

100. Ganesh, S.; Khan, F.; Ahmed, M. K.; Velavendan, P.; Pandey, N. K.; Kamachi Mudali, U., Spectrophotometric determination of trace amounts of phosphate in water and soil. *Water Science and Technology* **2012,** *66* (12), 2653-2658.

101. Kumar, A.; Mehtab, S.; Singh, U. P.; Aggarwal, V.; Singh, J., Tripodal Cadmium Complex and Macrocyclic Ligand Based Sensors for Phosphate Ion Determination in Environmental Samples. *Electroanalysis* **2008,** *20* (11), 1186-1193.

102. D'Angelo, E.; Crutchfield, J.; Vandiviere, M., Rapid, Sensitive, Microscale Determination of Phosphate in Water and Soil. *Journal of Environmental Quality* **2001,** *30* (6), 2206-2209.

103. Gal, C.; Frenzel, W.; Müller, J., Re-Examination of the Cadmium Reduction Method and Optimisation of Conditions for the Determination of Nitrate by Flow Injection Analysis. *Microchimica Acta* **2004,** *146* (2), 155-164.

104. Miranda, K. M.; Espey, M. G.; Wink, D. A., A rapid, simple spectrophotometric method for simultaneous detection of nitrate and nitrite. *Nitric Oxide-Biol Ch* **2001,** *5* (1), 62-71.

105. Hood-Nowotny, R.; Umana, N. H.-N.; Inselbacher, E.; Oswald- Lachouani, P.; Wanek, W., Alternative Methods for Measuring Inorganic, Organic, and Total Dissolved Nitrogen in Soil. *Soil Science Society of America Journal* **2010,** *74* (3), 1018-1027.

106. Nolan, M. A.; Tan, S. H.; Kounaves, S. P., Fabrication and Characterization of a Solid State Reference Electrode for Electroanalysis of Natural Waters with Ultramicroelectrodes. *Analytical Chemistry* **1997,** *69* (6), 1244-1247.

107. Krom, M. D., Spectrophotometric determination of ammonia: a study of a modified Berthelot reaction using salicylate and dichloroisocyanurate. *The Analyst* **1980,** *105* (1249), 305.

108. Cogan, D.; Cleary, J.; Fay, C.; Rickard, A.; Jankowski, K.; Phelan, T.; Bowkett, M.; Diamond, D., The development of an autonomous sensing platform for the monitoring of ammonia in water using a simplified Berthelot method. *Anal. Methods* **2014,** *6* (19), 7606-7614.

109. Joly, M.; Marlet, M.; Durieu, C.; Bene, C.; Launay, J.; Temple-Boyer, P., Study of chemical field effect transistors for the detection of ammonium and nitrate ions in liquid and soil phases. *Sens. Actuator B-Chem.* **2022,** *351*, 12.

110. Wang, X.; Sun, L.; Shi, Y., Research on a Miniature Multiparameter Water Quality Sensor Chip and a System with a Temperature Compensation Function. *Journal of Sensors* **2020,** *2020*, 1-16.

111. Inselsbacher, E.; Wanek, W., An unexpected source of nitrogen for root uptake: positively charged amino acids dominate soil diffusive nitrogen fluxes. *New Phytologist* **2021**.

112. Inselsbacher, E.; Peticzka, R., Diffusive fluxes and water-extractable concentrations of different nitrogen forms in a temperate agricultural soil. *Soil Research* **2021**.

113. Clunes, J.; Deltedesco, E.; Pinochet, D.; Mentler, A.; Inselsbacher, E.; Keiblinger, K. M., Inorganic Nitrogen diffusion in undisturbed volcanic soils during continuous drying-rewetting cycles. *Journal of Plant Nutrition and Soil Science* **2020,** *183* (6), 648-658.

114. Leitner, S.; Minixhofer, P.; Inselsbacher, E.; Keiblinger, K. M.; Zimmermann, M.; Zechmeister-Boltenstern, S., Short-term soil mineral and organic nitrogen fluxes during moderate and severe drying–rewetting events. *Applied Soil Ecology* **2017,** *114*, 28-33.

115. Charbaji, A.; Heidari-Bafroui, H.; Anagnostopoulos, C.; Faghri, M., A New Paper-Based Microfluidic Device for Improved Detection of Nitrate in Water. *Sensors* **2020,** *21* (1), 102.

116. Yan, J. C.; Ren, J.; Ren, L. L.; Jian, J. M.; Yang, Y.; Yang, S. F.; Ren, T. L., Development of a portable setup using a miniaturized and high precision colorimeter for the estimation of phosphate in natural water. *Anal. Chim. Acta* **2019,** *1058*, 70-79.

117. Altahan, M. F.; Esposito, M.; Achterberg, E. P., Improvement of On-Site Sensor for Simultaneous Determination of Phosphate, Silicic Acid, Nitrate plus Nitrite in Seawater. *Sensors* **2022,** *22* (9), 3479.

118. WIZ PORTABLE IN-SITU PROBE FOR WATER ANALYSIS. WIZ_06E ed.; SYSTEA SpA.

119. Raabe, J.; Kurtay, G.; Fontenot, A.; Greene, S.; Martignette, A.; Milbrandt, E.; Roberts, B.; Stauffer, B., Operation and integration of a commercially available nitrate sensor in Gulf of Mexico estuarine monitoring programs. *ENVIRONMENTAL TECHNOLOGY & INNOVATION* **2024,** *35*.

120. Solvas, X. C. I.; deMello, A., Droplet microfluidics: recent developments and future applications. *Chem. Commun.* **2011,** *47* (7), 1936-1942.

121. Stroock, A. D., Chaotic Mixer for Microchannels. *Science* **2002,** *295* (5555), 647-651.

122. Song, H.; Chen, D. L.; Ismagilov, R. F., Reactions in Droplets in Microfluidic Channels. *Angewandte Chemie International Edition* **2006,** *45* (44), 7336-7356.

123. Tice, J. D.; Lyon, A. D.; Ismagilov, R. F., Effects of viscosity on droplet formation and mixing in microfluidic channels. *Anal. Chim. Acta* **2004,** *507* (1), 73-77.

124. Nightingale, A. M.; Hassan, S.-U.; Makris, K.; Bhuiyan, W. T.; Harvey, T. J.; Niu, X., Easily fabricated monolithic fluoropolymer chips for sensitive long-term absorbance measurement in droplet microfluidics. *RSC Advances* **2020,** *10* (51), 30975-30981.

125. Nightingale, A. M.; Leong, C. L.; Burnish, R. A.; Hassan, S.-U.; Zhang, Y.; Clough, G. F.; Boutelle, M. G.; Voegeli, D.; Niu, X., Monitoring biomolecule concentrations in tissue using a wearable droplet microfluidic-based sensor. *Nature Communications* **2019,** *10* (1).

126. Wells, S. S.; Bain, I. J.; Valenta, A. C.; Lenhart, A. E.; Steyer, D. J.; Kennedy, R. T., Microdialysis coupled with droplet microfluidics and mass spectrometry for determination of neurotransmitters in vivo with high temporal resolution. *The Analyst* **2024,** *149* (8), 2328-2337.

127. Song, P.; Mabrouk, O.; Hershey, N.; Kennedy, R., In Vivo Neurochemical Monitoring Using Benzoyl Chloride Derivatization and Liquid Chromatography-Mass Spectrometry. *ANALYTICAL CHEMISTRY* **2012,** *84* (1), 412-419.

128. Zestos, A.; Kennedy, R., Microdialysis Coupled with LC-MS/MS for In Vivo Neurochemical Monitoring. *AAPS JOURNAL* **2017,** *19* (5), 1284-1293.

129. Wongkiew, S.; Hu, Z.; Chandran, K.; Lee, J.; Khanal, S., Nitrogen transformations in aquaponic systems: A review. *AQUACULTURAL ENGINEERING* **2017,** *76*, 9-19.

130. Lin, B.; Xu, J.; Yu, C.; Chen, L.; Lu, M.; Xie, X., A multi-parameter in-situ water quality analyzer based on a portable document scanner and 3D printed self-sampling cells. *Anal. Chim. Acta* **2020,** *1101*, 176-183.

131. Bauer, M.; Wunderlich, L.; Weinzierl, F.; Lei, Y.; Duerkop, A.; Alshareef, H. N.; Baeumner, A. J., Electrochemical multi-analyte point-of-care perspiration sensors using on-chip three-dimensional graphene electrodes. *Analytical and Bioanalytical Chemistry* **2021,** *413* (3), 763-777.

132. Timilsina, S.; Jolly, P.; Durr, N.; Yafia, M.; Ingber, D., Enabling Multiplexed Electrochemical Detection of Biomarkers with High Sensitivity in Complex Biological Samples. *ACCOUNTS OF CHEMICAL RESEARCH* **2021,** *54*, 3529-3539.

133. Lu, B.; Lunn, J.; Yeung, K.; Dhandapani, S.; Carter, L.; Roose, T.; Shaw, L.; Nightingale, A.; Niu, X., Droplet Microfluidic-Based In Situ Analyzer for Monitoring Free Nitrate in Soil. *Environmental Science & Technology* **2024,** *58* (6), 2956-2965.

134. Warren, C. R., Development of online microdialysis-mass spectrometry for continuous minimally invasive measurement of soil solution dynamics. *Soil Biol. Biochem.* **2018,** *123*, 266-275.

135. Brackin, R.; Atkinson, B. S.; Sturrock, C. J.; Rasmussen, A., Roots-eye view: Using microdialysis and microCT to non-destructively map root nutrient depletion and accumulation zones. *Plant, Cell & Environment* **2017,** *40* (12), 3135-3142.

136. Carter, L. R. J. A droplet microfluidic redox sensor. Doctoral, University of Southampton, 2024.

137. Azam, F.; Mahmood, T.; Malik, K. A., Inmobilization-remineralization of NO3-N and total N balance during the decomposition of glucose, sucrose and cellulose in soil incubated at different moisture regimes. *Plant and Soil* **1988,** *107* (2), 159-163.

138. Zagal, E.; Persson, J., Immobilization and remineralization of nitrate during glucose decomposition at four rates of nitrogen addition. *Soil Biology and Biochemistry* **1994,** *26* (10), 1313-1321.

139. Rashid, G. H.; Schaefer, R., Seasonal rate of nitrate reduction in two temperate forest soils. *Plant and Soil* **1987,** *97* (2), 291-294.

140. Lu, B.; Lunn, J.; Nightingale, A. M.; Niu, X., Highly sensitive absorbance measurement using droplet microfluidics integrated with an oil extraction and long pathlength detection flow cell. *Frontiers in Chemistry* **2024,** *12*.

141. Yang, T.; Stavrakis, S.; deMello, A., A High-Sensitivity, Integrated Absorbance and Fluorescence Detection Scheme for Probing Picoliter-Volume Droplets in Segmented Flows. *ANALYTICAL CHEMISTRY* **2017,** *89* (23), 12880-12887.

142. Baroud, C. N.; Gallaire, F.; Dangla, R., Dynamics of microfluidic droplets. *Lab on a Chip* **2010,** *10* (16), 2032.

143. Nagul, E.; McKelvie, I.; Worsfold, P.; Kolev, S., The molybdenum blue reaction for the determination of orthophosphate revisited: Opening the black box. *Anal. Chim. Acta* **2015,** *890*, 60-82.

144. UKTAG, Updated recommendations on phosphorus standards for Rivers: river basin management (2015-21). Final report, August 2013. UK technical advisory group on the water framework directive. **2013**.

145. Veeck, L. Studies of nitrous oxide and the nitrogen cycle in a temperate river-estuarine system. Masters, University of Southampton, 2007.

146. Bhuiyan, W. T. Droplet microfluidics based platform technology for continuous chemical sensing. Doctoral, University of Southampton, 2022.

147. Cho, Y.; Jeong, S.; Chun, H.; Kim, Y., Selective colorimetric detection of dissolved ammonia in water via modified Berthelot's reaction on porous paper. *Sens. Actuator B-Chem.* **2018,** *256*, 167-175.

148. Chandrasekeran, P.; Urgun-Demirtas, M.; Pagilla, K. R., Aerobic Membrane Bioreactor for Ammonium-Rich Wastewater Treatment. *Water Environment Research* **2007,** *79* (11), 2352-2362.

149. Wang, J.; Chen, Z.; Xu, C.; Elrys, A.; Shen, F.; Cheng, Y.; Chang, S., Organic amendment enhanced microbial nitrate immobilization with negligible denitrification nitrogen loss in an upland soil. *ENVIRONMENTAL POLLUTION* **2021,** *288*.

150. Inselsbacher, E., Recovery of individual soil nitrogen forms after sieving and extraction. *Soil Biol. Biochem.* **2014,** *71*, 76-86.

151. Chen, F.-Y.; Liu, Y.-Q.; Tay, J.-H.; Ning, P., Rapid formation of nitrifying granules treating high-strength ammonium wastewater in a sequencing batch reactor. *Applied Microbiology and Biotechnology* **2015,** *99* (10), 4445-4452.